AD-A031 741 HONEYWELL INC HOPKINS MINN GOVERNMENT AND AERONAUTIC--ETC F/G 17/10
ENERGY PROPAGATION AND COUPLING STUDIES FOR LINE TRANSDUCERS.(U)
AUG 76 J B STARR F30602-75-C-0186

UNCLASSIFIED RADC-TR-76-239 NL

1 OF 2
AD A031741

RADC-TR-76-239
Final Technical Report
August 1976

# ENERGY PROPAGATION AND COUPLING STUDIES FOR LINE TRANSDUCERS

Honeywell Inc.





ROME AIR DEVELOPMENT CENTER
AIR FORCE SYSTEMS COMMAND
GRIFFISS AIR FORCE BASE, NEW YORK 13441

This report has been reviewed by the RADC Information Office (OI) and is releasable to the National Technical Information Service (NTIS). At NTIS it will be releasable to the general public, including foreign nations.

This report has been reviewed and approved for publication.

APPROVED: Robert B. Curtis

ROBERT B. CURTIS
Project Engineer

APPROVED: Rudolf C. Paltauf

RUDOLF C. PALTAUF, Lt Col, USAF
Chief, Surveillance Division

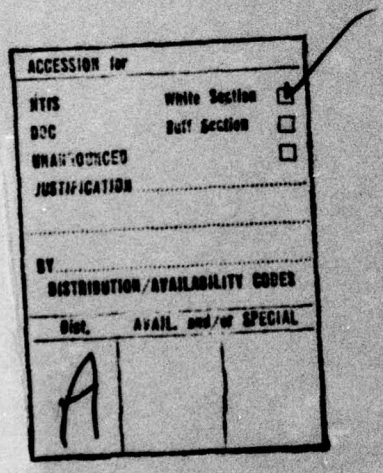


FOR THE COMMANDER: John P. Huss

JOHN P. HUSS
Acting Chief, Plans Office

Do not return this copy. Retain or destroy.

# *MISSION*
# *of*
# *Rome Air Development Center*

*RADC plans and conducts research, exploratory and advanced development programs in command, control, and communications ($C^3$) activities, and in the $C^3$ areas of information sciences and intelligence. The principal technical mission areas are communications, electromagnetic guidance and control, surveillance of ground and aerospace objects, intelligence data collection and handling, information system technology, ionospheric propagation, solid state sciences, microwave physics and electronic reliability, maintainability and compatibility.*

UNCLASSIFIED

SECURITY CLASSIFICATION OF THIS PAGE (When Data Entered)

# REPORT DOCUMENTATION PAGE

READ INSTRUCTIONS BEFORE COMPLETING FORM

| | |
|---|---|
| 1. REPORT NUMBER: RADC-TR-76-239 | 2. GOVT ACCESSION NO. |
| 3. RECIPIENT'S CATALOG NUMBER | |
| 4. TITLE (and Subtitle): ENERGY PROPAGATION AND COUPLING STUDIES FOR LINE TRANSDUCERS | 5. TYPE OF REPORT & PERIOD COVERED: Final Technical Report. 6 May 1975 — 5 May 1976 |
| 6. PERFORMING ORG. REPORT NUMBER: N/A | |
| 7. AUTHOR(s): J. B. Starr | 8. CONTRACT OR GRANT NUMBER(s): F30602-75-C-0186 |
| 9. PERFORMING ORGANIZATION NAME AND ADDRESS: Honeywell Inc./Government & Aeronautical Products Division, 600 Second Street North, Hopkins MN 55343 | 10. PROGRAM ELEMENT, PROJECT, TASK AREA & WORK UNIT NUMBERS: 62702F, 6515131C |
| 11. CONTROLLING OFFICE NAME AND ADDRESS: Rome Air Development Center (OCDS), Griffiss AFB NY 13441 | 12. REPORT DATE: August 1976 |
| | 13. NUMBER OF PAGES: 129 |
| 14. MONITORING AGENCY NAME & ADDRESS, if different from Controlling Office: Same | 15. SECURITY CLASS. (of this report): UNCLASSIFIED |
| | 15a. DECLASSIFICATION/DOWNGRADING SCHEDULE: N/A |

16. DISTRIBUTION STATEMENT (of this Report)

Approved for public release; distribution unlimited.

17. DISTRIBUTION STATEMENT (of the abstract entered in Block 20, if different from Report)

Same

18. SUPPLEMENTARY NOTES

RADC Project Engineer:
Robert B. Curtis (OCDS)

19. KEY WORDS (Continue on reverse side if necessary and identify by block number)

Security Systems, Perimeter Security, Seismics, Line Transducers, Soil Mechanics, Signal Processing

20. ABSTRACT (Continue on reverse side if necessary and identify by block number)

This program is an investigation of the effect of various soil compositions and frost conditions on performance of buried line transducers. The program encompasses theoretical modeling of transfer function of a MILES-type line transducer, controlled experiments in loam, clay, and sand soils for various frost conditions, and correlations between theory and experiment. Experiments were conducted in an indoor test facility where frost conditions could be produced. Response of transducers was measured with vertical cyclic and

DD FORM 1 JAN 73 1473 EDITION OF 1 NOV 65 IS OBSOLETE

UNCLASSIFIED

SECURITY CLASSIFICATION OF THIS PAGE (When Data Entered)

406490

impulse loads of defined magnitude applied at the soil surface.

Experimental data indicates that as long as frost does not penetrate below the burial depth of the transducer, often there is no significant attenuation of line sensitivity; such cases occur when the frozen layer above the transducer does not form a continuous shelf of frozen ground. When a continuous shelf forms, or when frost penetrates below the transducer burial depth, some upward gain adjustment is necessary for satisfactory performance.

Several approaches to minimizing performance problems in frozen ground are identified. Lines may be buried at significantly greater depths. Frost penetration may be artifically limited by insulating materials. Adaptive gain control may be introduced based on either frequency domain information or soil temperature measurements.

# ENERGY PROPAGATION AND COUPLING FOR LINE TRANSDUCERS

## REPORT SUMMARY

This investigation deals with problems that may arise when MILES transducers are buried where ground frost is encountered. Some reports have indicated that with ground freezing, significant loss of sensitivity occurs. Other reports indicate no loss of sensitivity. Apparently, in some situations there is a problem. What is therefore needed is a definition of conditions under which ground frost will degrade MILES performance, and a preventive or remedial solution to that problem.

The approach taken in this program includes rigorous theoretical analysis, controlled experiments, and correlation between analysis and theory. From these efforts has developed a thorough understanding and quantitative definition of how the MILES transducer generates signals in response to loads applied at the soil surface. This understanding provides a basis for several recommendations concerning installation techniques that will minimize situations where ground frost causes problems. Other recommendations relate to signal processing techniques that will offset detrimental effects of ground frost when they occur.

### Theoretical Analysis

Theoretical investigations have generated, in effect, a transfer function for the MILES line transducer. MILES transducers (both flat and round configurations) respond to soil motion because of stress-sensitive properties of the line's core material. The core is a ferromagnetic material in which applied stresses produce a change in magnetic flux. Such changes in flux will generate in sense windings an electrical signal which is the output signal of the transducer. Stresses are generated in the core by soil motion

in the direction of the line. The magnitude of the stress increases with rigidity of the soil and the extent of soil motion. A vertical load of 150 pounds applied at the soil surface directly above a line may provide a tension load of several pounds.

The range containment properties of the MILES transducer lead to significant simplifications in theoretical analysis of transducer response. The transducer sense winding direction is reversed every 43 inches. In effect, this produces a gradiometer configuration in which disturbances generated more than a few meters from the line are cancelled out. Current and anticipated signal processing schemes use signal information at frequencies of 10 Hz and below. These low frequencies correspond to seismic wavelengths of the order of 10 meters or more. Thus, the distance between the transducer and disturbances of interest tends to be far less than seismic wavelengths of interest. In such a case, soil displacements may be computed using steady state equations of elasticity in which no consideration of seismic wave properties is necessary.

Predictions from theoretical transducer and soil displacement models have been compared with experimental data acquired during this program. The comparisons provide a high degree of confidence that a basic understanding of transducer response has developed.

## Experimental Program

Experiments were carried out in an enclosed freeze/thaw facility where frost conditions could be produced by artificial heating and cooling. Frost conditions generated were:

(1) Thawed soil - where the soil is thawed from the surface to a level below the depth of the transducer.

(2) Frozen soil - where the soil is frozen from the surface to a level below that of the line transducer.

(3) Partially frozen soil - where the soil is frozen from the surface to a level above that of the line transducer.

(4) Frozen layered - where the soil is frozen to a level above that of the line transducer, but thawed at the surface.

The above conditions were produced in each of three soil samples: loam, clay, and sand.

Control loads were produced for both cyclic and impulse loading. Cyclic loads above 10 Hz were produced by counter-rotation of eccentric weights. Below 10 Hz, cyclic loads were generated by varying the amount of force imparted to the ground by a 100-pound lead weight. This force variation was produced by attaching a relatively stiff spring to the lead weight and using a cam-driven mechanism to vary the tension in the spring. A unique device was developed for generating controlled impulse loads to the soil. The device produces an impulse that lasts approximately 25 milliseconds, and has an amplitude of 50 pounds.

A total of five line transducers was used in the experiments. Three of the transducers were 80-turn flat MILES. One of these transducers was equipped with special coupling elements designed to produce near perfect coupling with the soil. The intent was by comparison of the output of the special line with that of the standard configuration, one could arrive at an estimate of the effectiveness of coupling between the soil and the transducer. Two flat and two round transducers were buried at depths of 9 and 18 inches, respectively. Two geophone triads were provided in order to obtain direct measurement of soil displacement. Signal acquisition was via special instrument amplifiers designed for transducers that are rate sensitive. The amplifier gain decreases with frequency at the rate of 20 dB per decade. This feature permits broadband recording of signals without encountering problems with dynamic range.

Experimental results that describe the effectiveness of coupling of the soil motion to the transducer were generated. In general, the data

indicate that coupling between the MILES transducer and the soil is near perfect. The addition of coupling elements would offer no significant improvement in performance.

Data taken at various frequencies substantiated the conclusion that at low frequencies, steady-state equations can be used to describe soil motion. It was found that the output of the line transducer for various frequencies can be quantified in terms of a single parameter which is the output signal divided by the product of signal frequency and load magnitude. The value of this parameter at a given range is essentially constant for frequencies of 20 Hz and below. At frequencies above 20 Hz, its value is modified somewhat by wave propagation phenomena.

Experiments under various frost conditions revealed that the most severe attentuation occurs when the ground is frozen to a level below the depth of the line transducer. Normally, under this condition, some adjustment in electronic gain would be required in order to achieve satisfactory performance. Where frost had penetrated to a level above the depth of the line transducer, in many cases satisfactory performance was obtained. The theoretical model predicts that for such layers some signal attenuation should occur. However, under most layered conditions tested during this program, it is probable that a continuous shelf of frozen ground did not exist. The one exception was when a layer of frozen ground was produced in the loam soil sample by rapid freezing from above with subzero air.

## Recommendations

Recommendations resulting from this study are of two categories. First, there are several actions that can be taken immediately to reduce the probability of performance degradation in frozen ground. Deeper burial, the use of an insulating material to minimize frost penetration, and

the use of a sandy media in the vicinity of the line should improve performance under frozen ground conditions. Other actions that may be taken in the future require further study and analysis. These actions include burial of the line to depths as great as 45 inches and the use of adaptive gain adjustment techniques based on either frequency domain information or temperature measurements to offset the effects of frost.

## EVALUATION

This investigation provides valuable insight into the behavior of a buried line seismic transducer, MILES, in three types of soils under four frost conditions. This is the first time such data has been generated under carefully controlled experimental conditions and correlated with the theoretical model of the transfer function of the MILES line transducer. This work was conducted under TPO-7 to provide a continuing technology base for the development and improvement of sensors for base and installation security systems. The results of this specific study will be embodied in recommendation for modification of current installation techniques to, one, improve performance of these devices in frost, and, two, lower false alarm rates under all environmental conditions.

Robert B. Curtis

ROBERT B. CURTIS
Project Engineer

TABLE OF CONTENTS

## LIST OF ILLUSTRATIONS

LIST OF ILLUSTRATIONS (CONTINUED)

## LIST OF TABLES

## SECTION I
## SUMMARY

This is a report of a theoretical and experimental investigation of the response of MILES transducers to controlled loads under various soil conditions. Soil conditions encompass various compositions and degrees of frost penetration. The intent of the program is to provide a basis for correlation between theoretical descriptions of the transducers and experimental results. From a validated understanding of transducer response, recommendations can be made for improving performance under conditions of frost penetration into soil.

The theoretical model for response of the line transducer centers around the magnetostrictive properties of the core material. Transducer response follows from a change in magnetic induction within the coil in response to changes in pure tension or compression stresses. These stresses are generated by motion of the soil in the direction of the line. The load produced per unit length of line is proportional to the shear modulus of soil and the difference between displacement of the soil and the stretching of the line. Soil motion is described by use of the equations of the elasticity with soil properties permitted to vary in a vertical direction. Property variations admittable in the analysis may be continuous as produced by soil overpressure or discontinuous as produced by soil strata either naturally occurring or caused by frost penetration. Numerical solutions to the equations are carried out by relaxation techniques.

An experimental design is presented whereby line transducers are subjected to controlled loads under controlled environmental conditions. Experiments center around the use of a freeze/thaw facility in which frost conditions can be produced at will for a given soil sample. Control loads are produced for both cyclic loading and impulse loading. Cyclic loads above 10 Hz are produced by counter-rotation of eccentric weights. Below 10 Hz cyclic loads are generated by varying the amount of force imparted to the ground by

a 100-pound lead weight. This force variation is produced by attaching a relatively stiff spring to the lead weight and using a cam-driven mechanism to vary the tension in the spring. A unique device is presented for generating controlled impulse loads to the soil. The device produces an impulse that lasts approximately 25 milliseconds and has an amplitude of 50 pounds.

Five line transducers are used in the experiments. Three of the line transducers are 80-turn flat MILES. One of these transducers is equipped with special coupling elements designed to produce near perfect coupling with the soil. The intent is that by comparison of the output of the special line with that of the standard configuration, one can arrive at an estimate of the effectiveness of coupling between the soil and the transducer. Two flat and two round transducers are buried at depths of 9 and 18 inches respectively. Two geophone triads are provided in order to obtain direct measurement of soil displacement. Signal acquisition is via special instrument amplifiers designed for transducers that are rate sensitive. The amplifier gain decreases with frequency at the rate of 20 dB per decade. This feature permits broadband recording of signals without encountering problems with dynamic range.

Experimental results presented describe the effectiveness of coupling of the soil motion to the transducer, effects of frequency, and response to control loading under various frost conditions. In general, the data indicate that coupling between the MILES transducer and the soil is near perfect; the addition of coupling elements would offer no significant improvement in performance. Output of the line transducer for various frequencies can be quantified in terms of a single parameter which is the output signal divided by the product of signal frequency and load magnitude. The value of this parameter at a given range is essentially constant for frequencies of 20 Hz and below. At frequencies above 20 Hz, its value is modified somewhat by wave propagation phenomena. Experiments under various frost conditions reveal that the most severe attenuation occurs when the ground is frozen to a level below the depth of the line transducer. Normally under this condition, some adjustment in electronic gain would be required in order to achieve satisfactory performance. Where frost has penetrated to a level above the depth

of the line transducer, in many cases satisfactory performance will result. The theoretical model predicts that for such layers some signal attenuation should occur. However, under most layer conditions tested during this program, it is probable that a continuous shelf of frozen ground did not exist. The one exception was when a layer of frozen ground was produced in the loam soil sample by rapid freezing from above with sub-zero air.

These experimental results have been compared with the theoretical model, and in general, good correlation results were obtained. By far the best correlation is obtained for sensitivity in sand. This is because the properties of sand more closely match the elastic model used in the theory. For clay and loam soil samples, the soils are somewhat plastic and do not match as well the assumptions used in the theory.

Recommendations presented at the conclusion of this study are of two categories. First there are several actions that can be taken immediately to reduce the probability of performance degradation in frozen ground. Deeper burial, the use of an insulating material to minimize frost penetration, and use of a sandy media in the vicinity of the line should improve performance under frozen ground conditions. Other actions that may be taken in the future require further studying and analysis. These actions include burial of the line to depths as great as 45 inches and the use of adaptive gain adjustment techniques, based on either frequency domain information or temperature measurements, to offset the effects of frost.

## SECTION II
## INTRODUCTION

The presence of frost in soil in the vicinity of a MILES transducer has been shown according to some reports to affect its output. In general, the reported extent of frost effects is inconsistent. In certain environments, no apparent degradation of performance occurs. Other reports indicate that the transducer response is greatly attenuated. Because of these inconsistencies it is impossible to define with any degree of confidence the remedial action that must be taken in order to circumvent this apparent problem.

To obtain a meaningful and general solution for the frost problem, a thorough understanding of the MILES transducer and how it responds under various soil conditions is required. Such an understanding should encompass the mechanics of the soil, the nature of the frost conditions existing there and the mechanism whereby the MILES transducer responds to soil displacements. Having acquired this information, it is then probable that one can proceed to develop solutions to the frost problem that will provide a high degree of confidence of satisfactory transducer operation under all environmental conditions.

This study has taken the approach of obtaining a basic understanding of MILES transducer response under various soil conditions. The program has involved an extensive amount of data acquisition under controlled test conditions both in terms of soil composition and frost penetration. These experimental results have been correlated with the theory of transducer response to soil motion in order to arrive at a basic understanding of overall transducer response in soils of various types and compositions. The discussion which follows in this report begins with a description of the theoretical basis for MILES transducer response to soil motion. This is followed by a description of the design of experiments to gather data under controlled conditions. The discussion encompasses a description of the various load-producing devices and procedures used in generating the desired soil

conditions. Experimental results are presented for numerous tests conducted over a broad range of experimental parameters, and these results are subsequently correlated with the theoretical description. There follows from this process basic conclusions regarding the operation of a MILES transducer and recommendations whereby performance can be improved under conditions where frost has penetrated into the soil.

## SECTION III
## THEORETICAL BACKGROUND

The study of energy propagation and coupling of the line transducer reported here is based on certain key theoretical considerations. Some of these considerations follow from well-founded physical principles, whereas others are recently derived semi-empirical relationships that have not been subjected to extensive validation through experiment. Overall, the intent is to make use of the best available theoretical information in the design of a meaningful experimental program and in analysis of the data. It will be shown in subsequent sections of this report that in large measure the theoretical approach presented here has been validated by the experimental results.

A meaningful theoretical model will indicate how loads generated at the surface of the soil are translated into signals at the output of the transducer. Development of such relationship requires consideration of both soil mechanics and transducer response mechanisms. In the discussion which follows relationships for soil motion will be derived that draw extensively on existing literature. The translation of soil motion into transducer response will be presented in terms of coupling equations and the magnetostrictive properties of the core of the MILES line transducer.

### Soil Motion

The approach to be taken in deriving equations for soil motion are dictated by basic characteristics of the MILES line transducer and associated signal processors. In general, electronic detection schemes and classification algorithms are based on the processing of low frequency signals of 10 Hz or less. This means that the soil motion detected is characterized by relatively large seismic wavelengths. Seismic velocities in thawed soil are of the order of several hundred feet per second. This means that at frequencies of 10 Hz and below, wavelengths will be in excess of 10 feet.

Typically at 10 Hz, wavelengths of approximately 50 feet will exist. In addition, the configuration of the MILES transducer (winding reversals every 43 inches) ensures that disturbances detected are within a few feet of the transducer.

The net result is that the distance between the transducer and signal sources of interest tends to be much less than the wavelength of the seismic signals of interest. All relevant soil motions thus tend to move in phase. This type of soil motion can be computed using equations that describe the elastic properties of soil in which inertial terms are ignored. Soil motion corresponding to a time-dependent load can be computed by assuming at each point in time that the instantaneous load is a steady state load.

The equations of elasticity for soil motion have been solved for the case of uniform soil properties under various load conditions. Closed-form solutions for soil displacement have been derived. For example, in reference (1) are presented the following equations which provide a convenient means for calculating the radial and vertical soil displacement due to a vertical load W at a point:

$$w = \frac{W}{4\pi G}\left[z^2(r^2+z^2)^{-\frac{3}{2}} + 2(1-\nu)(r^2+z^2)^{-\frac{1}{2}}\right] \quad (1)$$

$$u = \frac{W}{4\pi G}\left[(1-2\nu)\, z\,(r^2+z^2)^{-\frac{1}{2}} - 1 + r^2z^2\,(r^2+z^2)^{-\frac{3}{2}}\right] \quad (2)$$

Although closed-form solutions are convenient to use, they are limited in terms of flexibility of boundary conditions and variations in soil properties. In general, significant soil properties variations are found because of variations in over-pressure due to soil weight and because of the existence of soil strata either naturally occurring or caused by freezing and thawing. The limitations of the closed form solution can be circumvented by using a numerical finite difference approach.

The basic equations of elasticity that describe soil motion can be found in numerous references for the case of fixed soil properties. Where soil

properties are nonuniform, equations are easily derived by simply paralleling derivations existing in the literature. Consider the case of a soil sample where a vertical load , W, is applied uniformly over a circular disk of radius $r_o$ as illustrated in Figure 1. Axisymmetry is assumed so that all circumferential derivatives are zero. For the case where soil properties are allowed to vary in the z direction, the governing equations for soil displacement are:

$$(\lambda+2G)\left[\frac{\partial^2 u}{\partial r^2}+\frac{1}{r}\left(\frac{\partial u}{\partial r}-\frac{u}{r}\right)\right]+G\frac{\partial^2 u}{\partial r^2}+(\lambda+G)\frac{\partial^2 w}{\partial r\partial z} \tag{3}$$

$$+\frac{\partial G}{\partial z}\left(\frac{\partial u}{\partial z}+\frac{\partial w}{\partial r}\right)=0 \tag{3}$$

$$(\lambda+2G)\frac{\partial^2 w}{\partial z^2}+G\left(\frac{\partial^2 w}{\partial r^2}+\frac{1}{r}\frac{\partial w}{\partial r}\right)+(\lambda+G)\left(\frac{\partial^2 u}{\partial r\partial z}+\frac{1}{r}\frac{\partial u}{\partial z}\right)$$

$$+\frac{\partial\lambda}{\partial z}\left(\frac{\partial u}{\partial r}+\frac{u}{r}\right)+\frac{\partial(\lambda+2G)}{\partial z}\left(\frac{\partial w}{\partial z}\right)=0 \tag{4}$$

In the above equations, the parameter $\lambda$ is a Lame' constant and the parameter G is the soil shear modulus. These parameters are related by the equation

$$G=\frac{\nu\lambda}{2(1-2\nu)} \tag{5}$$

wherein $\nu$ is Poisson's ratio. Equations (3) and (4) are similar to the basic equations of elasticity found in the literature with the exception of the last term in equation (3) and the last two terms in equation (4) which account for variations in soil property in the z direction. These equations assume that soil properties are a continuous function of z. In cases where discontinuities in properties exist, as with strata or frozen layers, boundary conditions must be introduced that equate normal stress in the z direction and shear stress at the interface. The equations that impose these conditions are

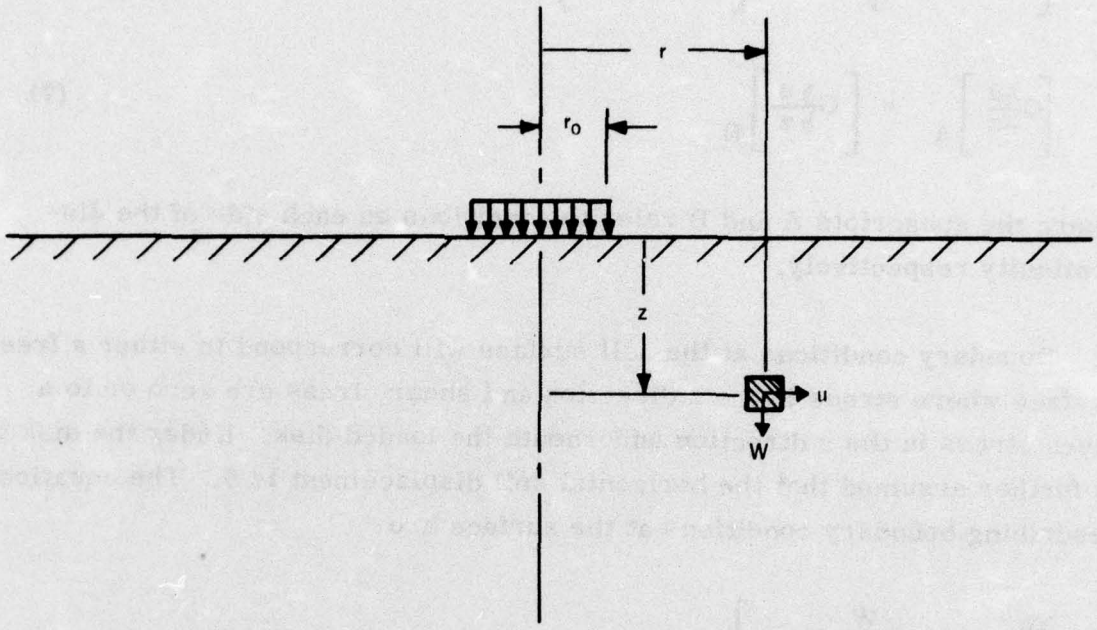


Figure 1. Coordinate notation for analytical model of soil displacement

$$\left[(\lambda+2G)\frac{\partial w}{\partial z}\right]_A = \left[(\lambda+2G)\frac{\partial w}{\partial z}\right]_B \tag{6}$$

$$\left[G\frac{\partial u}{\partial z}\right]_A = \left[G\frac{\partial u}{\partial z}\right]_B \tag{7}$$

where the subscripts A and B refer to conditions on each side of the discontinuity respectively.

Boundary conditions at the soil surface will correspond to either a free surface where stress in the z direction and shear stress are zero or to a given stress in the z direction underneath the loaded disk. Under the disk it is further assumed that the horizontal soil displacement is 0. The equations describing boundary conditions at the surface are

$$\left.\begin{aligned} \frac{\partial w}{\partial z} &= \frac{W}{\pi r_o^{\,2}(\lambda+2G)} \\ u &= 0 \end{aligned}\right\} \quad r < r_o \tag{8}$$

$$\left.\begin{aligned} \lambda\frac{\partial u}{\partial r} + \lambda\frac{u}{r} + (\lambda+2G)\frac{\partial w}{\partial z} &= 0 \\ \frac{\partial u}{\partial z} + \frac{\partial w}{\partial r} &= 0 \end{aligned}\right\} \quad r \geq r_o \tag{9}$$

In the absence of strata within the soil, vertical variations in soil properties will exist because of overpressure effects. Expressions for variations in soil shear modulus presented in reference (2) are for round-grained sands

$$G = \frac{2\,630(2.17-\epsilon)^2}{1+\epsilon}\sqrt{\bar{\sigma}_o} \tag{10}$$

and for angular grained materials:

$$G = \frac{1230(2.97-\epsilon)^2}{1+\epsilon}\sqrt{\bar{\sigma}_o} \tag{11}$$

The equations for soil motion can be readily adapted to computer solution by expressing them in terms of finite differences. Solutions follow from a process of successive approximations or a relaxation technique. An example of computed soil displacement is shown in Figures 2 and 3 for soil displacements in the vertical and horizontal direction, respectively. This solution is for a vertical load of 100 pounds distributed over a disk with a radius of 4 inches. Displacements are given in terms of micro-inches at points 8 inches apart within the soil. It will be shown later that the MILES transducer responds primarily to the horizontal soil motion. In that respect it is interesting to note that horizontal soil motion near the surface tends to be toward the load point, whereas at greater depths, the soil moves away from the load point. This suggests that the polarity of a transducer output will depend on the soil depth and there may be certain soil depths and load conditions in which nulls in transducer output occur.

## Transducer Response Mechanism

In reference (3), the following general conclusions were made concerning the response mechanism of the MILES line transducer:

(1) The primary response mechanism is related to the magnetostrictive properties of the core material.

(2) The stress causing response of the line transducer is either pure tension or pure compression within the core material.

(3) The tension and compression loads are generated by soil motion in the direction of the line transducer.

The line loading per unit length was shown to be proportional to the difference between soil displacement and line stretch and to the soil shear modulus. The equation expressing this relationship is

$$\frac{dF_L}{dx} = G C_s (u_s - u_L) \tag{12}$$

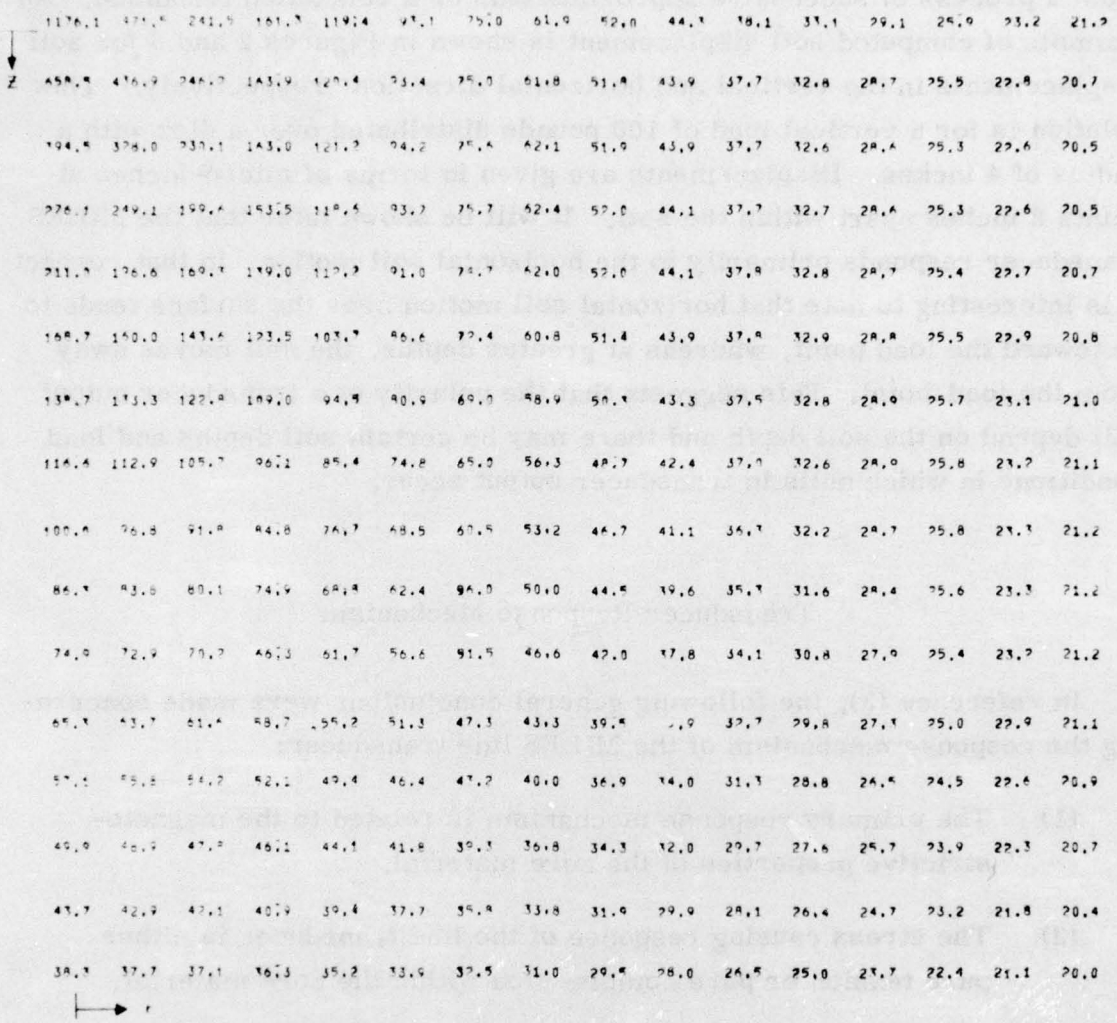


Figure 2. Vertical soil displacements in micro-inches

| | | | | | | | | | | | | | | |
|---|---|---|---|---|---|---|---|---|---|---|---|---|---|---|
| 0. | -114.7 | -66.0 | -46.4 | -36.2 | -29.1 | -24.1 | -20.4 | -17.6 | -15.1 | -13.0 | -11.2 | -9.6 | -8.2 | -6.8 | -5.8 |
| 0. | 61.7 | 22.1 | 1.9 | -5.7 | -8.4 | -9.3 | -9.3 | -8.8 | -8.1 | -7.4 | -6.7 | -5.9 | -5.2 | -4.5 | -3.8 |
| 0. | 40.6 | 38.7 | 24.4 | 13.5 | 6.8 | 2.7 | 0.2 | -1.2 | -2.0 | -2.4 | -2.5 | -2.5 | -2.5 | -2.4 | -2.2 |
| 0. | 24.7 | 32.7 | 28.6 | 21.7 | 15.5 | 10.7 | 7.2 | 4.8 | 3.1 | 1.9 | 1.0 | 0.3 | -0.1 | -0.5 | -0.7 |
| 0. | 16.1 | 25.0 | 26.3 | 23.4 | 19.2 | 15.1 | 11.7 | 9.0 | 6.9 | 5.2 | 3.8 | 2.7 | 1.9 | 1.1 | 0.5 |
| 0. | 11.4 | 19.1 | 22.3 | 22.8 | 19.8 | 17.0 | 14.1 | 11.6 | 9.4 | 7.6 | 6.0 | 4.8 | 3.5 | 2.5 | 1.6 |
| 0. | 8.4 | 14.9 | 18.5 | 19.5 | 18.8 | 17.1 | 15.1 | 13.0 | 11.0 | 9.2 | 7.5 | 6.0 | 4.7 | 3.6 | 2.5 |
| 0. | 6.4 | 11.8 | 15.3 | 17.0 | 17.2 | 16.4 | 15.1 | 13.8 | 12.8 | 10.1 | 8.5 | 7.0 | 5.6 | 4.4 | 3.3 |
| 0. | 5.1 | 9.5 | 12.7 | 14.7 | 15.4 | 15.2 | 14.5 | 13.3 | 11.9 | 10.5 | 9.0 | 7.6 | 6.2 | 5.0 | 3.8 |
| 0. | 4.2 | 7.9 | 10.7 | 12.6 | 13.7 | 13.9 | 13.5 | 12.7 | 11.7 | 10.5 | 9.2 | 7.9 | 6.6 | 5.4 | 4.2 |
| 0. | 3.5 | 6.6 | 9.1 | 10.9 | 12.0 | 12.5 | 12.4 | 11.9 | 11.1 | 10.2 | 9.1 | 7.9 | 6.8 | 5.6 | 4.5 |
| 0. | 2.9 | 5.6 | 7.7 | 9.4 | 10.5 | 11.1 | 11.2 | 11.0 | 10.4 | 9.7 | 8.8 | 7.8 | 6.7 | 5.7 | 4.7 |
| 0. | 2.4 | 4.7 | 6.6 | 8.1 | 9.1 | 9.8 | 10.0 | 9.9 | 9.5 | 9.0 | 8.3 | 7.4 | 6.6 | 5.7 | 4.7 |
| 0. | 2.0 | 3.9 | 5.5 | 6.8 | 7.8 | 8.4 | 8.7 | 8.8 | 8.5 | 8.2 | 7.6 | 7.0 | 6.3 | 5.5 | 4.7 |
| 0. | 1.7 | 3.2 | 4.5 | 5.6 | 6.5 | 7.0 | 7.4 | 7.5 | 7.4 | 7.2 | 6.8 | 6.3 | 5.8 | 5.2 | 4.6 |
| 0. | 1.3 | 2.4 | 3.4 | 4.3 | 5.0 | 5.5 | 5.8 | 6.0 | 6.0 | 6.0 | 5.8 | 5.5 | 5.2 | 4.8 | 4.4 |

Figure 3. Computed horizontal soil displacements in micro-inches

The soil displacement along the line is determined from a solution for soil motion as presented by example in the previous section. At each point along the line, the component of soil displacement in the direction of line $u_s$ is computed. The governing equation for the stretching of the line is

$$\frac{d^2u_L}{dx} + \frac{C_s G}{A_L E}(u_s - u_L) = 0 \tag{13}$$

Under certain conditions, the differences between the soil displacement and line stretch can become very small so that inaccuracies in the use of equation (13) will arise. These inaccuracies can be avoided to a large extent by defining the parameter

$$\Delta u = (u_s - u_L) \tag{14}$$

When this parameter is introduced into equations (12) and (13) there results

$$\frac{d^2(\Delta u)}{dx^2} - \frac{C_s G}{A_L E}\Delta u = \frac{d^2u_s}{dx^2} \tag{15}$$

$$\frac{dF_L}{dx} = C_s G \Delta u \tag{16}$$

The computational procedure followed with the above equations is to first introduce computed soil displacements as a numerical approximation of the second derivative on the righthand side of equation (15). A solution for $\Delta u$ results from use of a relaxation process to numerically solve the equation. Having obtained values for $\Delta u$, the line loading per unit length is calculated from equation (16). The total tension or compression load in the line is then determined by integrating equation (16) from a specified point on the line to infinity or at some distant point where the line loading can be assumed to be zero. The expression that accomplishes this integration is

$$F_L(x) = \int_x^{\infty} C_s G \Delta u \, dx \tag{17}$$

Having determined the tension or compression load in the line at any given point, it is then possible to derive an expression for the electrical output of the line transducer by making use of the magnetostrictive properties of the core material. The change in magnetic induction will be proportional to the stress produced within the core. The total flux change generated by imposition of a load at a given point is therefore

$$\Delta \phi = \frac{A_c}{A_L} \Lambda F(x) \tag{18}$$

where $\Lambda$ change in magnetic induction per unit stress.

If the load at a given point is taken as the amplitude of a sinusoidally imparted load, then the maximum value of rate of change of flux is

$$\dot{\phi} = \Lambda \omega \frac{A_c}{A_L} F(x) \tag{19}$$

The electrical output of the line then becomes

$$e = \int_o^L n \Lambda \omega \frac{A_c}{A_L} F(x) \, dx \tag{20}$$

In general, the load imparted to the line will be proportional to the load applied at the soil surface. This suggests an expression for line output of the form

$$e^* \equiv \frac{e}{\omega W} = \int_o^L n \Lambda \frac{A_c}{A_L} \frac{F(x)}{W} \, dx \tag{21}$$

Note that in the above expression the parameter n is the number of sense windings per unit length. In the MILES transducer, the direction of these

windings reverses every 43 inches. This winding reversal can be accounted for during integration by assigning a polarity to n.

## General Considerations

It will be subsequently shown that the theory set forth in this section provides a reasonable analytical representation of MILES response to low frequency loads imparted at the soil surface. In making use of the theory it should be remembered that certain assumptions have been made so that neither severe demands placed on the theoretical results nor erroneous conclusions are drawn from the analysis.

In deriving the equations for soil motion, two key assumptions were made. First, it was assumed that the soil behaved as a purely elastic media. In general, this is not the case. Particularly for moist clay behavior is more that of a plastic rather than an elastic substance. The other extreme of soil conditions is represented by sand. One may expect that the assumption of elasticity within sand is reasonably valid.

A second underlying assumption in the analysis with respect to soil motion is that the soil properties are uniform in the horizontal direction. In general, for many terrains, some variation in soil properties even over a distance of a few feet may be anticipated. Even where by intent uniform soil properties or conditions have been generated, as in a control testing environment, some horizontal variation of soil properties will exist immediately under the load point because of pressures generated by the load itself in addition to the weight of the soil.

With respect to computation of transducer response, the primary assumption is in the area of how soil displacements are translated into loading per unit length of cable. Again, the experimental results will indicate reasonably good correlation with the theoretical approach presented here. However, the coupling model presented in reference (3) is based on an extremely simplified soil geometry. In general, some variations in the

coupling phenomena will occur because of both line geometry and the distribution of soil displacements in the vicinity of the line.

# SECTION IV
# DESIGN OF EXPERIMENTS

The experimental program was designed to gather data for obtaining basic understanding of the response of MILES transducers to given targets and intruders under various environmental conditions. The specific intent was to generate data that would provide quantitative descriptions of signal coupling to the soil, soil motion, coupling of soil motion to the line transducer, and electrical response of the line transducer. In order to achieve this objective, it was necessary to design the experimental procedures and equipment to achieve controlled loading under controlled environmental conditions. With all key environmental and load conditions rigorously defined, meaningful correlations with analytical models could be carried out.

## Soil Conditioning

Experiments were carried out in three types of soil. Nominally these soils were designated as a loam-gravel mixture, clay, and sand. Each of the soils was carefully examined by an independent engineering test firm and the results of their study are presented in Appendix A. The resulting classifications of soil samples in terms of the unified system of soil classification for engineering purposes (ASTM designation D-2487) are as follows:

1) SM, silty sand, fine to medium grained, brown
   7.8 percent moisture

2) SC, clay-like sand, brown
   16.5 percent moisture

3) SP, sand, medium to fine grained, brown
   4.9 percent moisture

Care was taken to maintain a given soil moisture content during experiments. In general, moisture contents measured before and after a 30 day interval were essentially identical. Maintenance of moisture content was ensured by keeping the soil sample covered with a plastic film when experiments were not in progress.

Generation of desired frost conditions was carried out in a special freeze/thaw facility shown schematically in Figure 4. Soil samples tested covered an area of approximately 480 square feet to a depth of 4 feet. At the 4-foot level are brine-filled coils for either heating or cooling of the soil sample. The frost conditions generated were:

1) Thawed - a condition where the soil is thawed from the surface to some level below that of the buried line transducers.

2) Frozen - a condition where the soil is frozen from the surface to a level below that of the buried line transducers.

3) Partially frozen - where the soil is frozen from the surface to a level above that of the line transducer.

4) Frozen layered - where the soil is frozen above the line transducer but thawed at the soil surface.

The sequence of operations that created these frost conditions is illustrated by Figure 5. The normal procedure was to first conduct tests with a soil sample fully thawed. Next, the sample was frozen by running chilled brine through the cooling coils and by ventilating the test area with Minnesota winter air. The partially frozen condition was generated next by placing a layer of insulating hay at the soil surface and running warm brine through the coils to thaw the soil from below. Finally, the frozen layered condition was created by heating the air above the soil sample immediately after completion of the test under the partially frozen condition.

It should be noted that the partially frozen and frozen layered conditions were transient conditions. In general, there was a span of

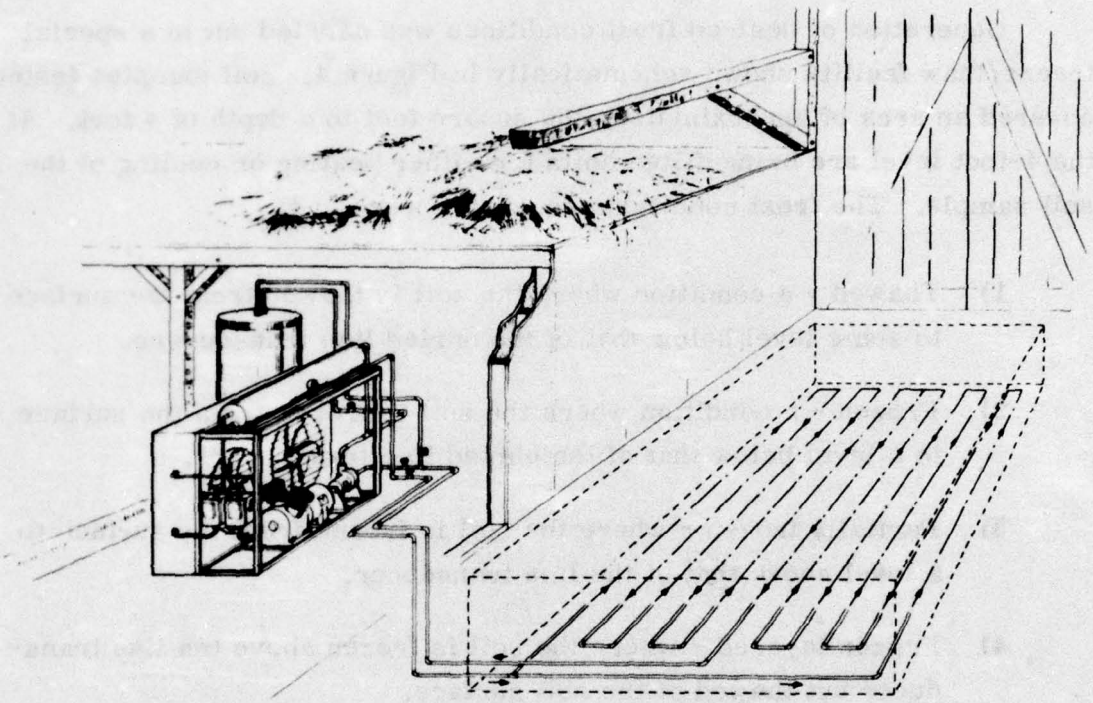

Figure 4. Freeze/thaw facility

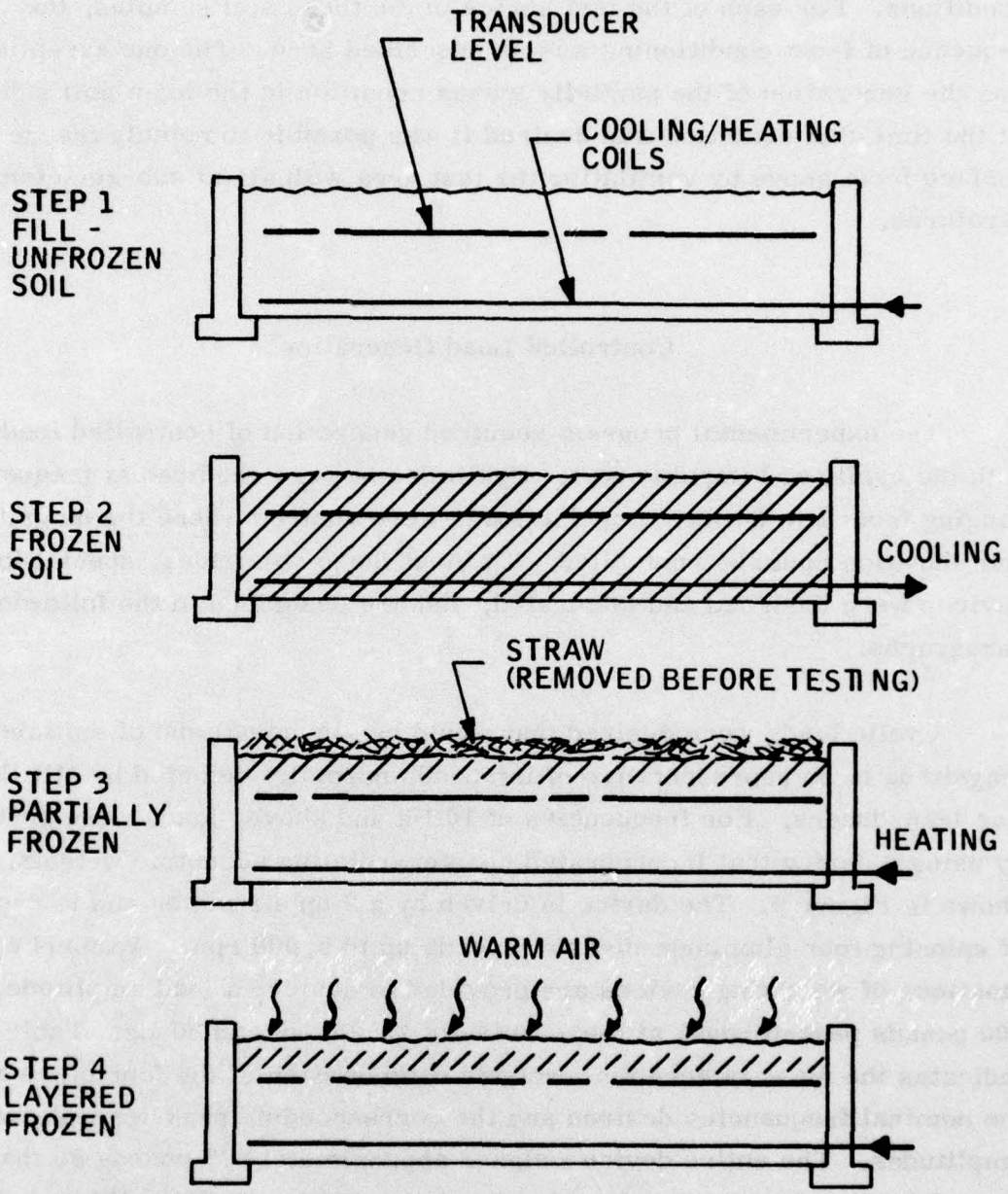


Figure 5. Sequence for generating frost conditions

approximately 12 hours during which tests could be run under these conditions. For each of the test series in the three soil samples, the sequence of frost conditioning was as described here. The one exception was the generation of the partially frozen condition in the loam soil sample. At the time that condition was desired it was possible to rapidly freeze the surface from above by ventilating the test area with air at sub-zero temperatures.

## Controlled Load Generation

The experimental program required generation of controlled loads of both the cyclic and impulse type. Cyclic loads were required at frequencies ranging from 1 to 80 Hz. Impulse loads were desired where the magnitude and duration could be controlled. To meet these objectives, special loading devices were designed and fabricated, and are described in the following paragraphs.

Cyclic loads were desired that would be sinusoidal and of sufficient magnitude to be representative of intruders normally detected by MILES line transducers. For frequencies of 10 Hz and above, loads were generated by using a device that incorporated counter-rotating eccentric weights, as shown in Figure 6. The device is driven by a 2 hp air motor and is capable of spinning four aluminum discs at speeds up to 5,000 rpm. Various combinations of weighting devices are provided to achieve a load amplitude of 100 pounds peak-to-peak at frequencies of 10, 20, 40 and 80 Hz. Table 1 indicates the mass of eccentric weights used on each of the four discs at the nominal frequencies desired and the corresponding peak-to-peak load amplitudes. The entire device weighed approximately 75 pounds so that the net loading to the ground varied from approximately 25 to 125 pounds during a single load cycle.

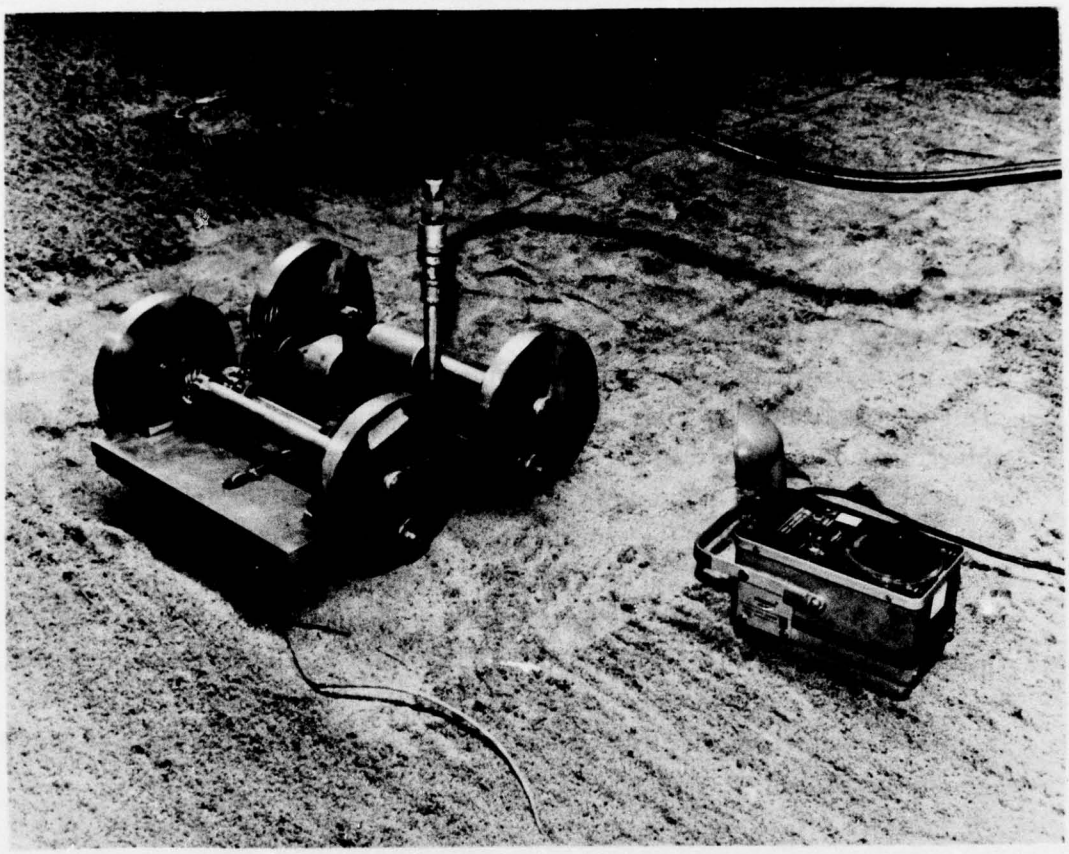

Figure 6. Cyclic load generator for frequencies or 10 Hz and above

TABLE 1. MASS OF ECCENTRIC WEIGHTS FOR CYCLIC LOAD GENERATOR

| Nominal Frequency | Mass/ Disc, gr. | Load Amplitude (p-p) lb. |
|---|---|---|
| 10 | 188.29 | 102 |
| 20 | 48.09 | 104 |
| 40 | 14.09 | 122 |
| 80 | 2.81 | 97 |

The production of cyclic loads at frequencies under 10 Hz required a second type of loading apparatus. Use of counter-rotating eccentrics at very low frequencies would require gigantic eccentric weights in order to produce amplitudes as great as 100 pounds peak-to-peak. A more reasonable approach is shown in Figure 7. For this device a 100-pound weight rests on the soil surface and is attached to a cam-driven lever through a relatively stiff spring. As the air motor drives the cam, displacement of the spring causes a net variation in load to the soil of approximately 30 pounds peak-to-peak. The drive mechanism rests on two large wood beams that are tied into the foundation walls of the test facility. It was demonstrated that loads would not be imparted to the soil through the wood beams by monitoring geophone and line transducer response as a test subject walked across the beams.

Special consideration was given to developing an impulse generator to produce well-defined input signals. A photograph of the device fabricated for this purpose is shown in Figure 8 and a schematic in Figure 9. The device is based on loads produced by falling weight impacting on a preloaded spring (an air-spring in this case). As the weight impacts the spring, a load imparted to the ground rises rapidly to a value equal to the spring preload. The kinetic energy of the weight is absorbed by compression of the spring over the duration of the pulse. At maximum spring compression, a ratchet mechanism locks the weight so that virtually no spring-back occurs. The pulse terminates concurrent with the locking action. A geophone mounted on the unit indicates the resultant motion of the pulse

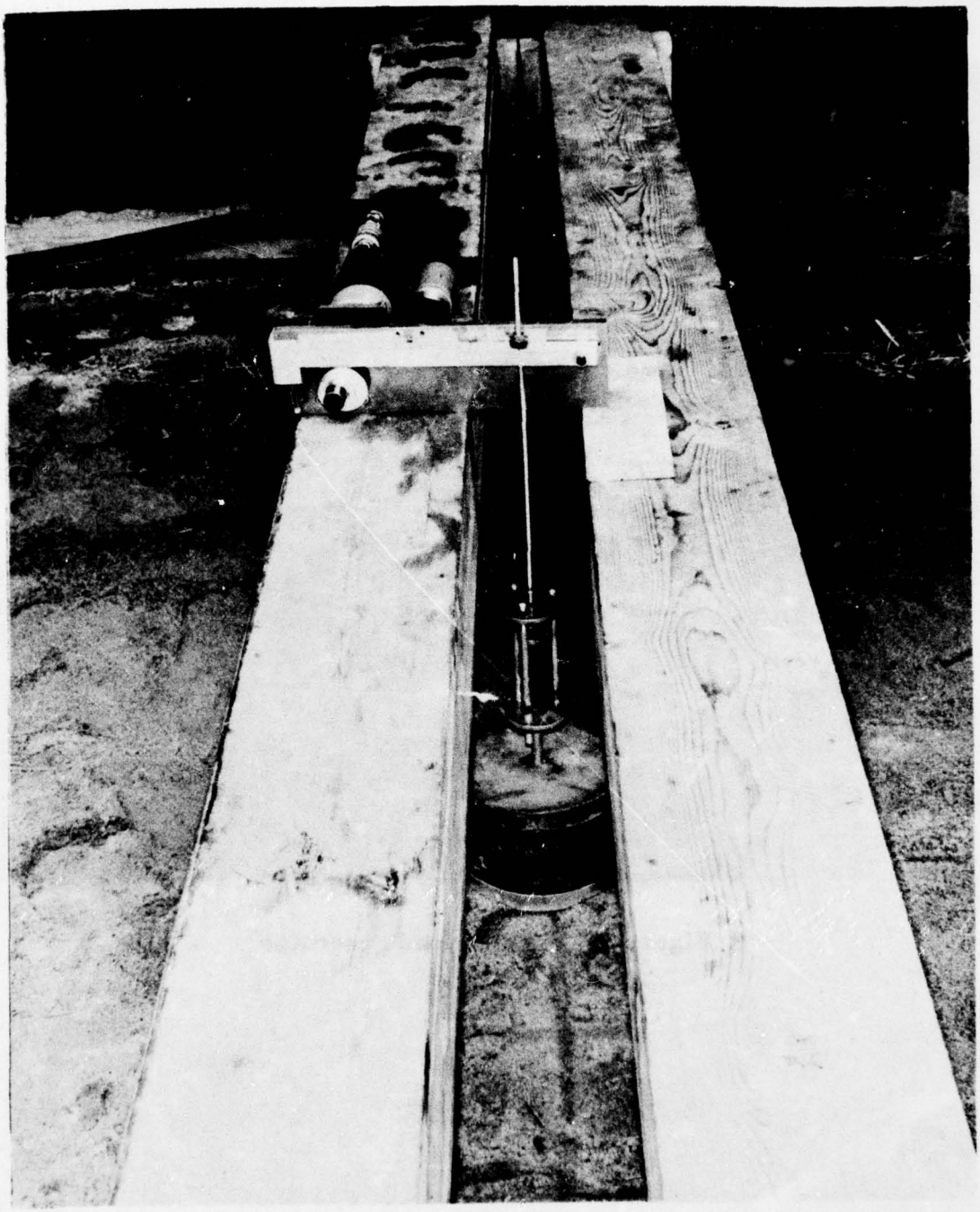

Figure 7. Cyclic load generator for frequencies below 10 Hz

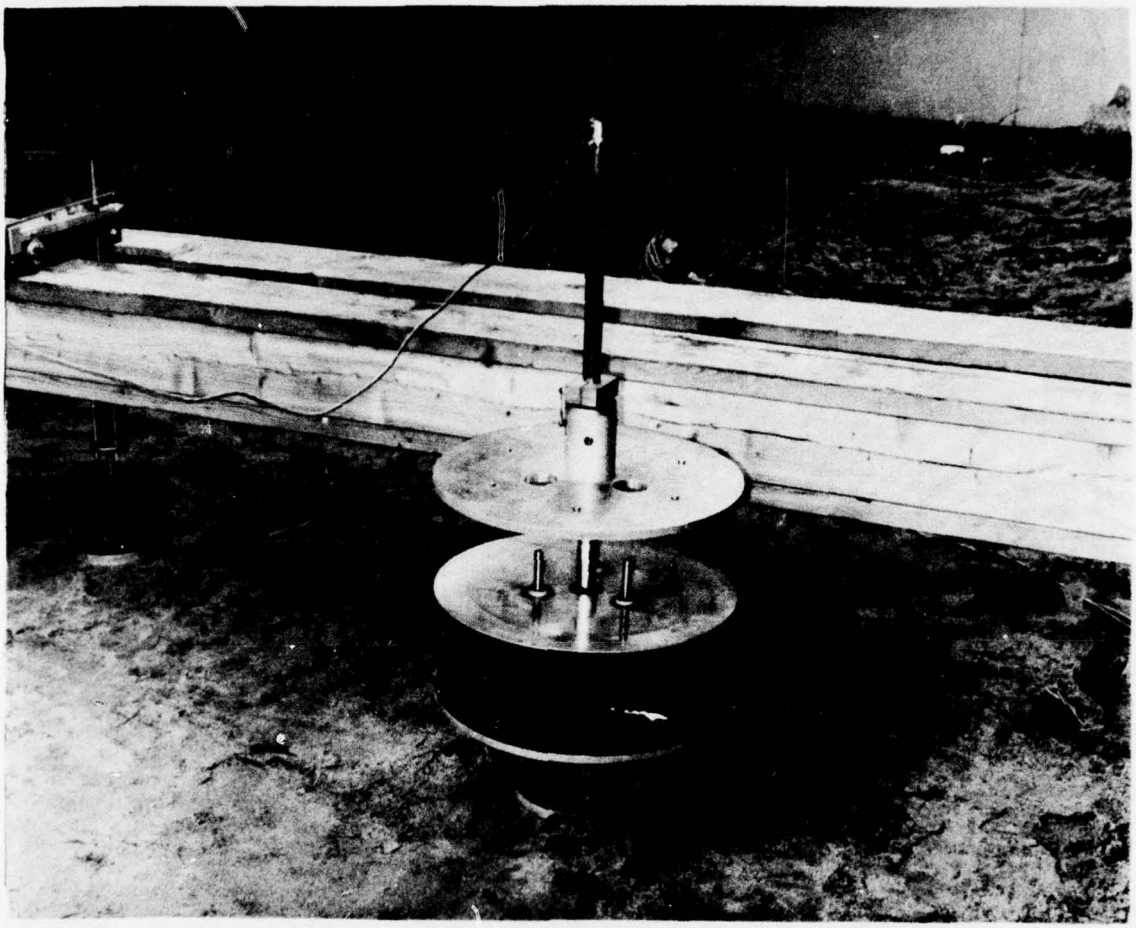

Figure 8. Impulse load generator

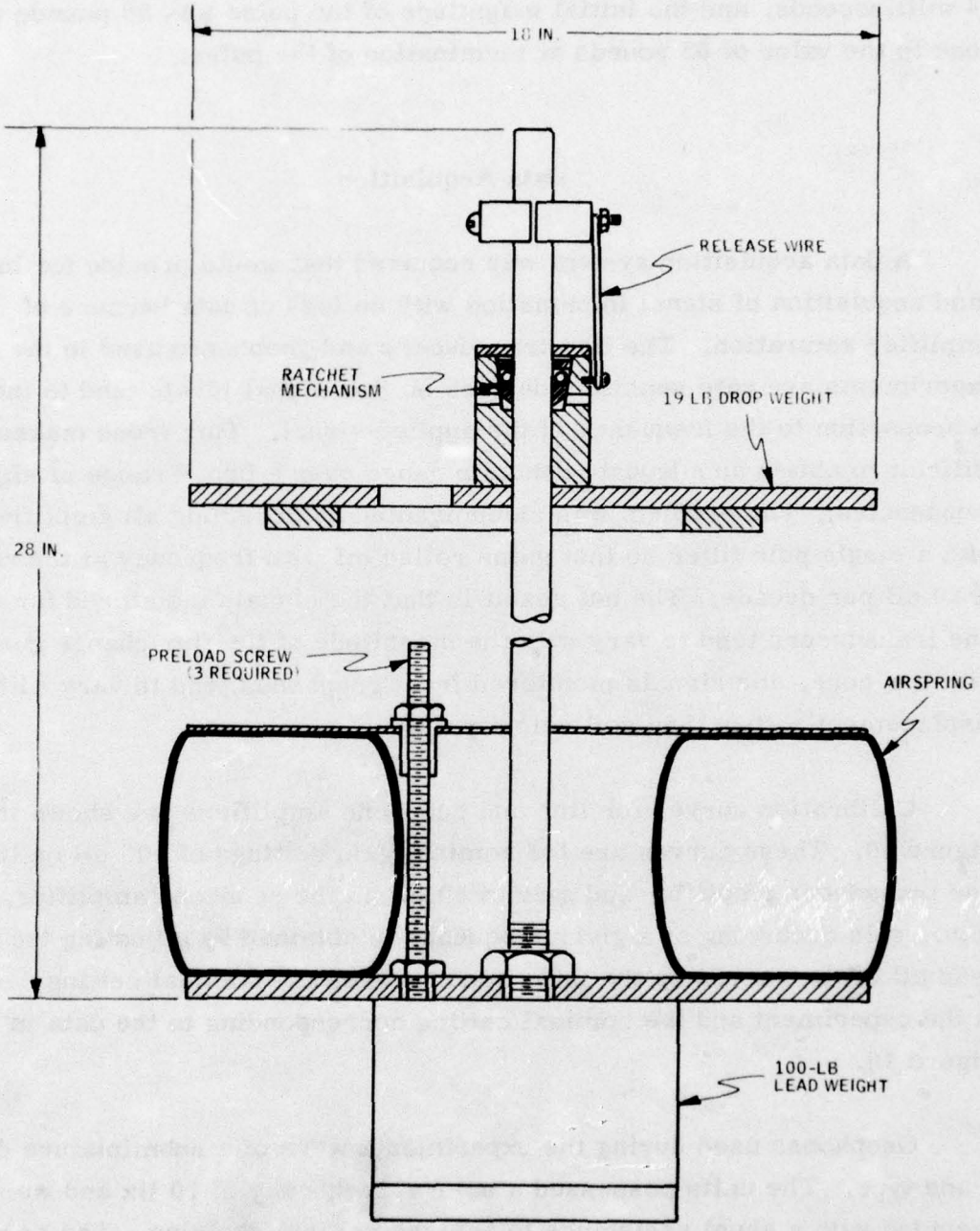


Figure 9. Schematic of impulse load generator

generator. The magnitude and duration of the pulse can be derived from measured parameters using equations developed in Appendix C. For experiments carried out under this study, the nominal pulse duration was 24 milliseconds, and the initial magnitude of the pulse was 50 pounds and rose to the value of 85 pounds at termination of the pulse.

## Data Acquisition

A data acquisition system was required that would provide for broad-band acquisition of signal information with no loss of data because of amplifier saturation. The line transducers and geophones used in the experiments are rate sensitive devices so that signal levels tend to increase in proportion to the frequency of the applied signal. This trend makes it difficult to obtain an adequate dynamic range over a broad range of signal frequencies. The problem was circumvented by providing all amplifiers with a single pole filter so that gains rolled off with frequency at the rate of 20 dB per decade. The net result is that the signals monitored for the line transducers tend to vary with the magnitude of the flux change generated with the core, and signals monitored from geophones tend to vary with soil displacement rather than soil velocity.

Calibration curves for line and geophone amplifiers are shown in Figure 10. These curves are for nominal gain settings of 100 dB on the line transducer amplifier and gain of 80 dB on the geophone amplifier. The actual gain occurring at a given frequency is obtained by adjusting the gains read off of the curves by the difference between the nominal setting occurring in the experiment and the nominal setting corresponding to the data in Figure 10.

Geophones used during the experiments were of a subminiature digital grade type. The units possessed a natural frequency of 10 Hz and were provided with a shunt resistance to achieve critical damping. The resulting calibration of the geophones is shown in Figure 11.

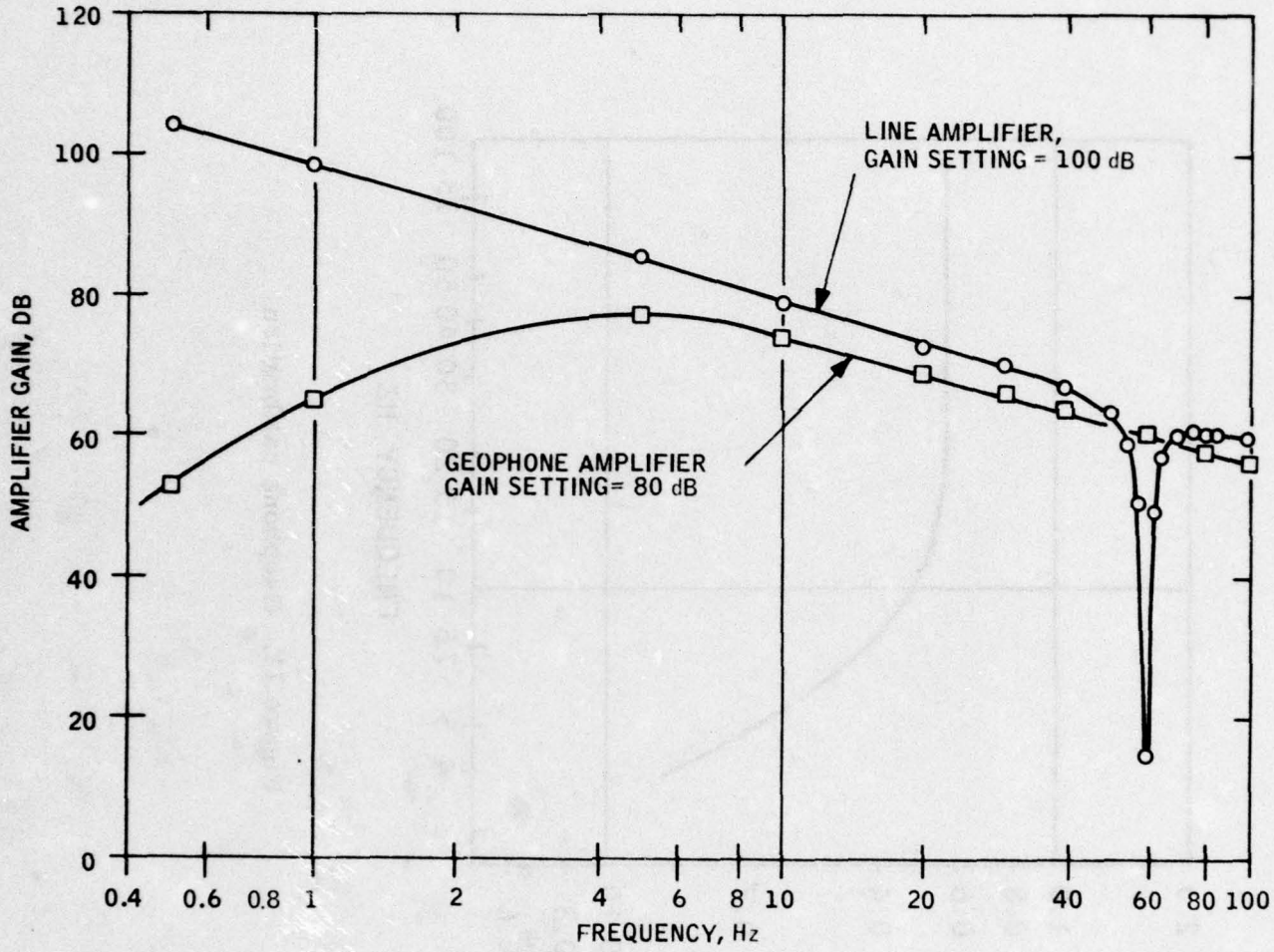


Figure 10. Amplifier gain characteristics

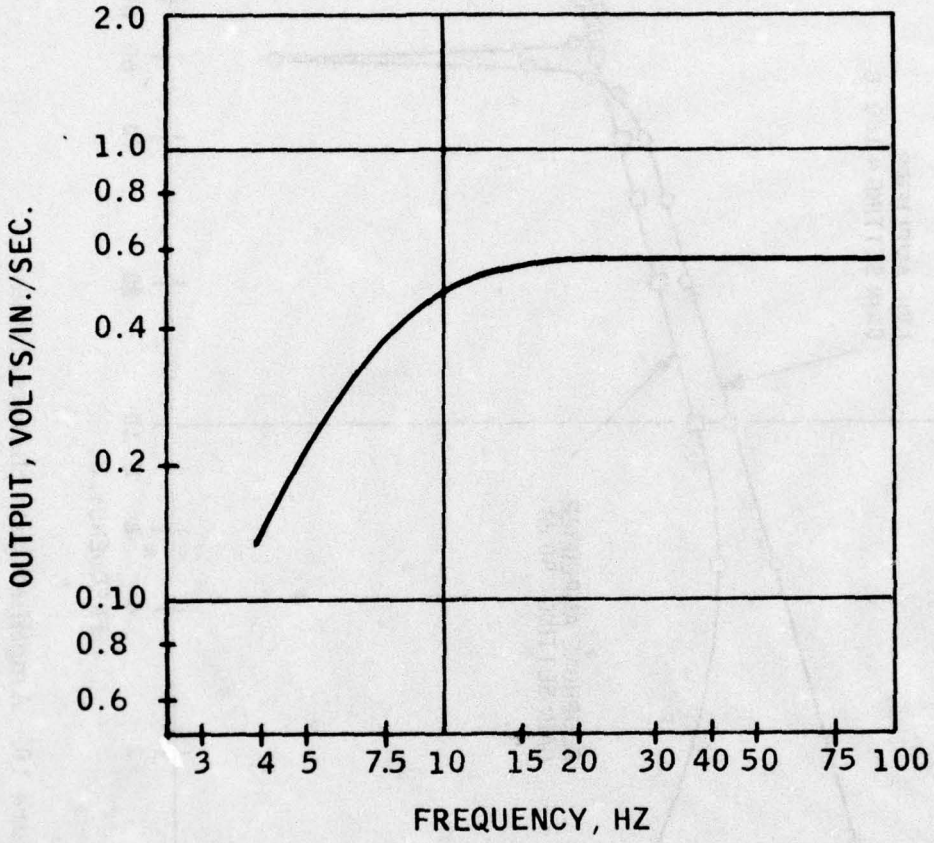


Figure 11. Geophone calibration

## Experimental Layout

A total of five line transducers and six geophones were installed in the freeze/thaw facility. The layout of lines and geophones is illustrated in Figure 12. Each line was approximately 10 meters long and included eight 42 inch sections of sense winding. The flat transducers had a sense winding density of 80 turns/inch and the round transducers 38 turns/inch. As noted in Figure 12, one of the flat transducers was equipped with special devices to achieve near perfect coupling with the soil. The details of the coupling devices are shown in Figure 13. The intent of the coupling devices was to provide an experimental method of evaluating coupling coefficient based on comparisons of outputs for a flat transducer with the coupling devices and one without the coupling devices. Both round and flat line transducers were buried at depths of 9 and 18 inches. Geophone triads were buried at a depth of 9 inches.

Cyclic and impulse data were taken along paths X1 and M shown in Figure 12. Path X1 corresponded to a line that intersected transposition points in the line transducers whereas path M intersected a mid-point between transpositions within the transducers. All experiments were run for a specified values of $R_s$ but reduced data presented in subsequent sections is expressed in actual range from the load point to the line transducer in question. Transducers were nominally oriented in a north-south direction. Prior to installation, all transducers were momentarily subjected to a three-oersted field that complemented the earth's magnetic field. This provision was carried out in order to assure maximum uniformity of the magnetic state within the transducers.

## Experimental Conditions

For each of the previously discussed soil samples and frost conditions, loads were generated for various frequencies, ranges and paths within the test facility. Table 2 is a listing of the test parameters for experiments

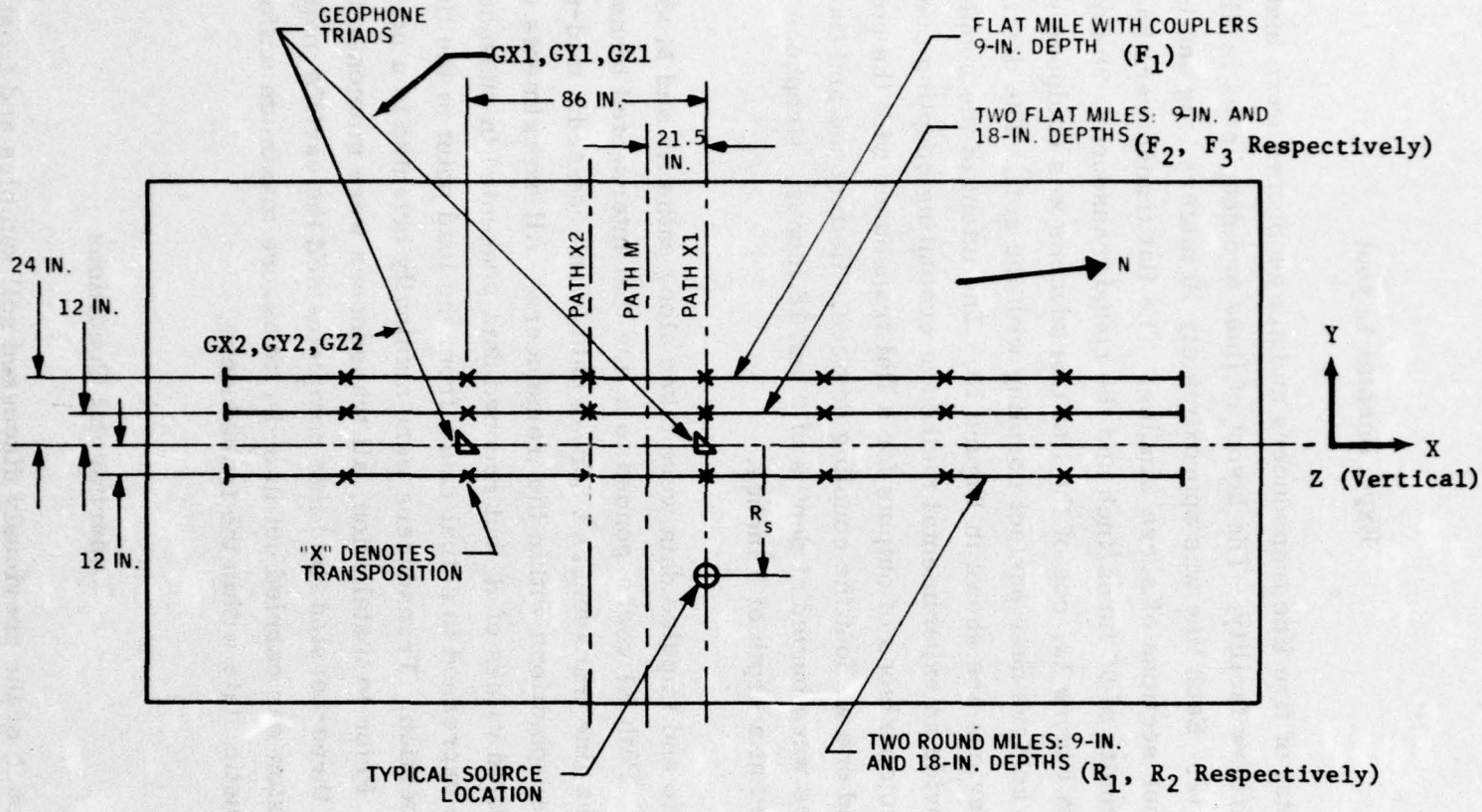


Figure 12. Instrumentation layout in freeze-thaw facility

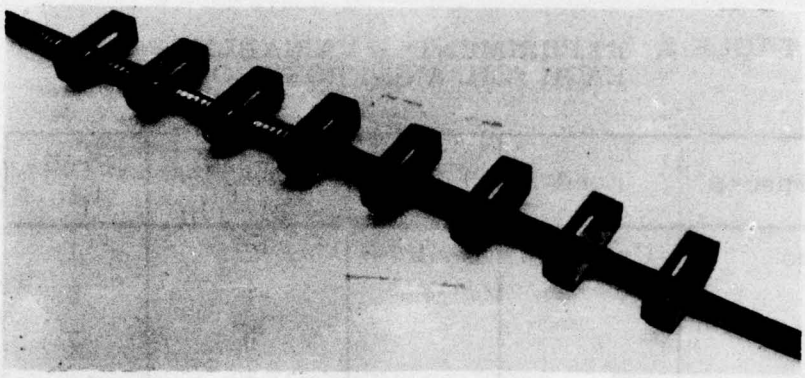

Figure 13. Coupling elements

in which line transducer and geophone data were acquired. In addition to these experiments, attempts were made to detect a resonant condition associated with the vibration of the cyclic load generator at the surface of the soil. These resonant checks were made by continuously varying the load generator frequency with minimum counter-weighting applied. The resonant condition provides an indication of the relative stiffness of the soil near its surface.

TABLE 2. EXPERIMENTAL VARIABLES FOR EACH SOIL AND FROST CONDITION

| Sensors | Load | Paths | Ranges $R_s$, Ft. | Freq Hz |
|---|---|---|---|---|
| Lines | Cyclic | X1 | -2 | 1 |
| | | M | -1 | 5 |
| | | | 0 | 7 |
| | | | 1 | 10 |
| | | | 2 | 20 |
| | | | 3 | 40 |
| | | | 4 | 80 |
| | Impulse | X1 | 0 | - |
| | | M | 3 | - |
| Geophones | Cyclic | X1 | 0 | 10 |
| | | M | | 20 |
| | | X2 | | 40 |
| | | | | 80 |
| | Impulse | X1 | 0 | - |
| | | M | 3 | - |

# SECTION V
# EXPERIMENTAL RESULTS

This section summarizes the experimental data acquired for MILES line transducers and geophones. The geophone data serve to characterize the nature of the soil motion generated under various load conditions. The line transducer data serve to characterize the response of the transducer as a function of load frequency and magnitude, range, and soil condition. Geophone data in response to cyclic loads are presented in terms of the amplitude of soil displacement in micro-inches divided by the amplitude of the load imposed at the soil surface. Line data is presented in terms of the parameter, e*, defined by equation (21).

The presentation of line transducer data in terms of this parameter accounts for increases in signal with frequency because signal is proportional to the rate of change of magnetic flux within the core material. Also, the signal would tend to increase with the load applied at the soil surface because the magnitude of the flux change within the core is proportional to the load applied at the surface.

## Soil Motion

An attempt was made to characterize the motion of the soil in response to cyclic loads through geophone measurements. Figures 14, 15 and 16 illustrate measured soil displacement for loam, clay, and sand samples, respectively, under thawed and frozen conditions. Superimposed on these data are computed soil displacements for a uniform soil shear modulus and for a shear modulus that varies with soil depth in accordance with equation (11).

In the thawed soil, it is evident that the variation in soil displacement with range is somewhat greater than predicted by either analytical result.

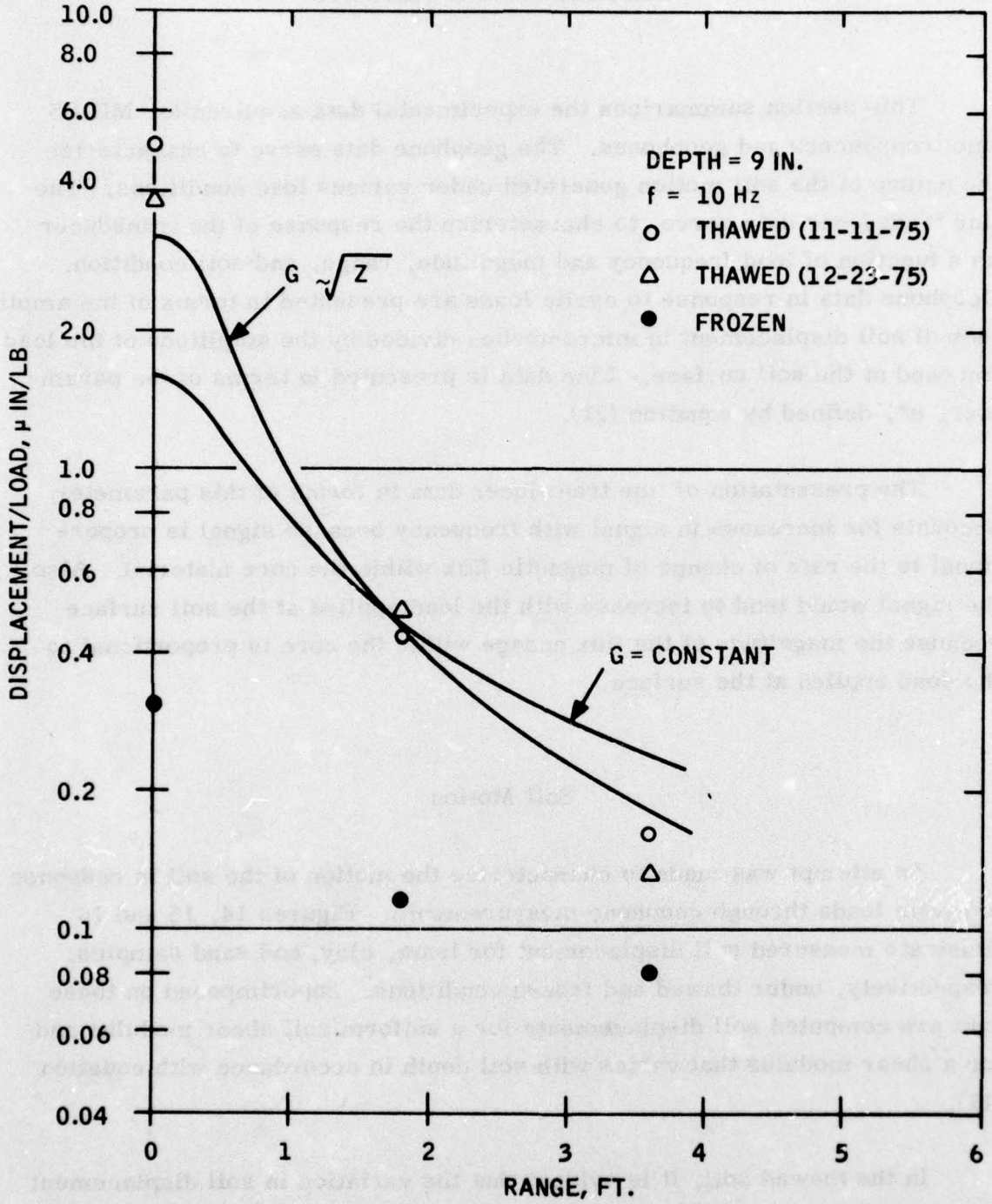


Figure 14. Measured vertical soil displacement in loam

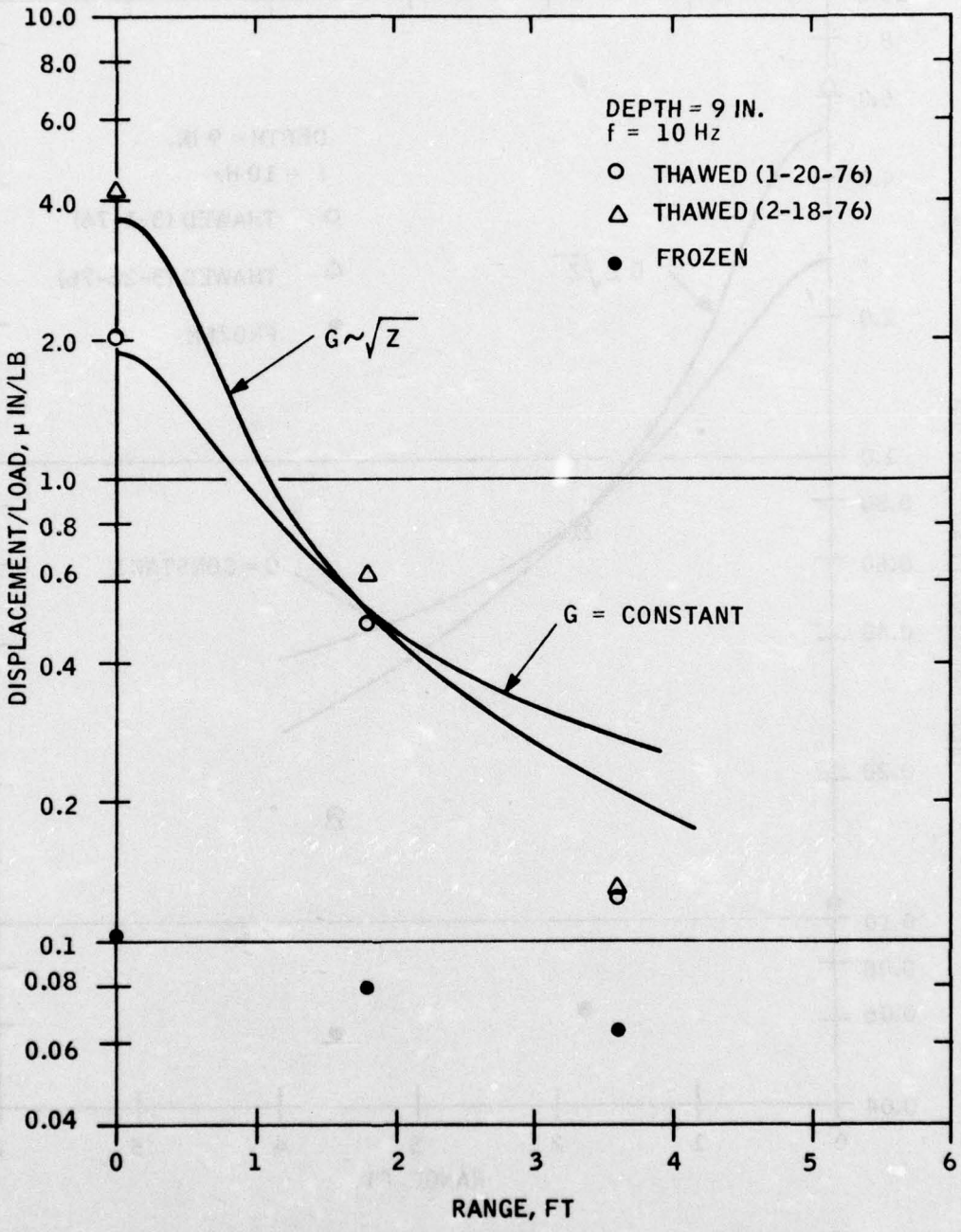


Figure 15. Measured vertical soil displacement in clay

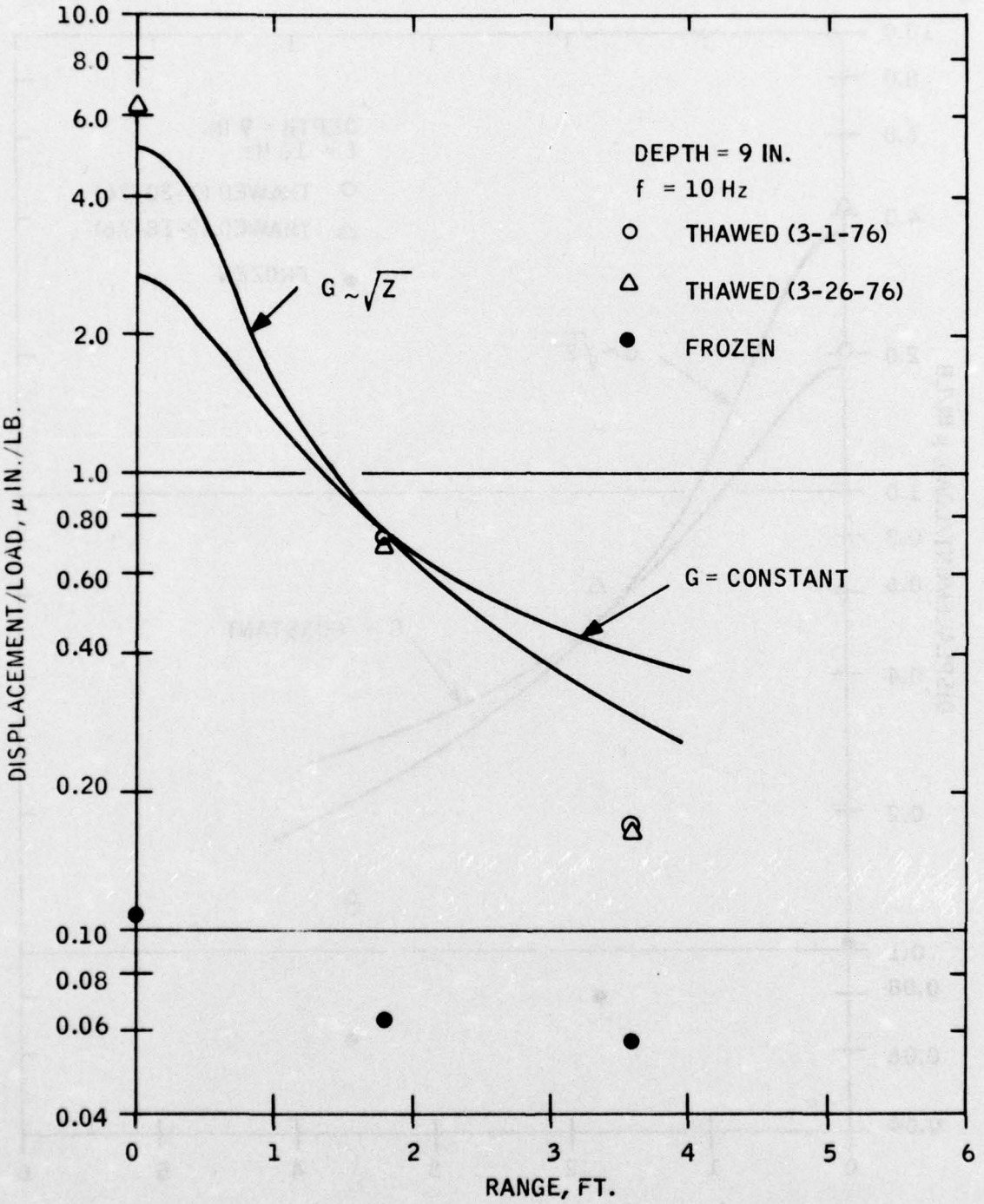


Figure 16. Measured vertical soil displacement in sand

However, better correlation is obtained when it is assumed that the soil shear modulus does increase with depth. Data acquired for the frozen soil condition is somewhat in question because of the relatively small variation of displacement with range that is observed. It is entirely possible that the measured displacement was not only that produced within the soil sample by the applied load, but, in part, due to the displacement relative to the surrounding terrain of the entire frozen soil sample contained within the freeze/thaw facility. This relative motion could have existed because the soil in the surrounding terrain remained mostly thawed during the winter of 1975-1976. The frozen soil sample was thus equivalent to a relatively rigid block floating on relatively compliant soil.

The waveforms generated by cyclic loads are shown in Figures 17 and 18 for all three soil samples and for ranges of 0 and 3.6 feet. For cases where the load is applied directly above the geophone, the waveforms are exceptionally clean, and relatively uninfluenced by background noise. In the thawed soil at a range of 3.6 ft., it is noted that the clay sample remains relatively quiet whereas the loam sand samples exhibit somewhat noisier waveforms. It is probable that waveforms for the loam and sand samples were influenced by seismic waves propagating at random throughout the freeze/thaw facility. The waveform for clay remains relatively clean because of the attenuation of seismic waves due to internal damping. Waveforms in frozen soil are relatively clean. It is possible that with the stiffer frozen soils, energy reflected off of foundation walls was insignificant.

The dynamic characteristics of the various soil samples were further evaluated by attempting to measure the condition of resonance associated with the vertical vibration of the cyclic load generator at the soil surface. Figure 19 illustrates displacements measured by use of a geophone mounted on the cyclic load generator.

In general, resonant conditions were detected at frequencies of 80 Hz and below for the case of thawed soils. For frozen conditions, all resonances were well above 80 Hz. For the case of loam soil, resonances were

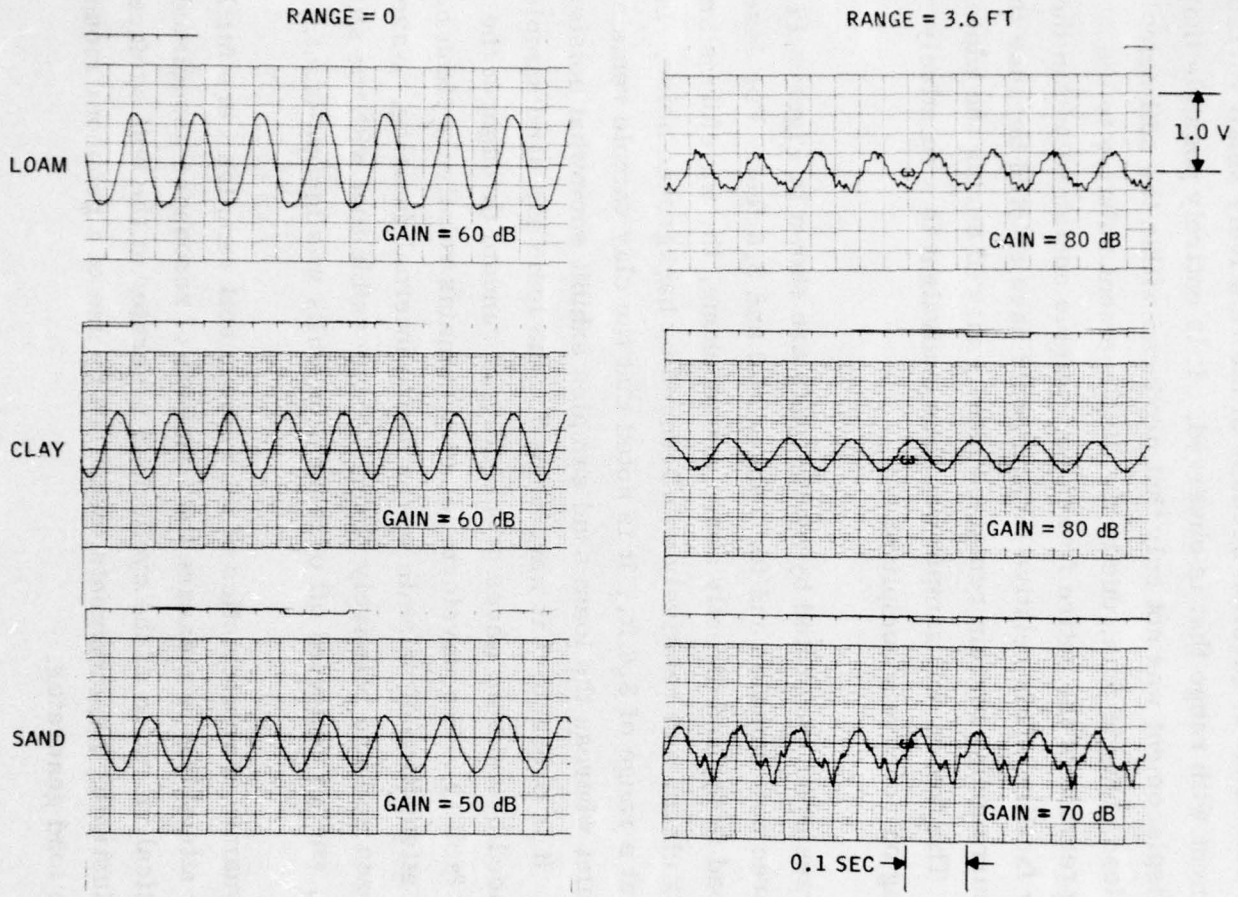


Figure 17. Vertical geophone traces for thawed soils, frequency = 10 Hz

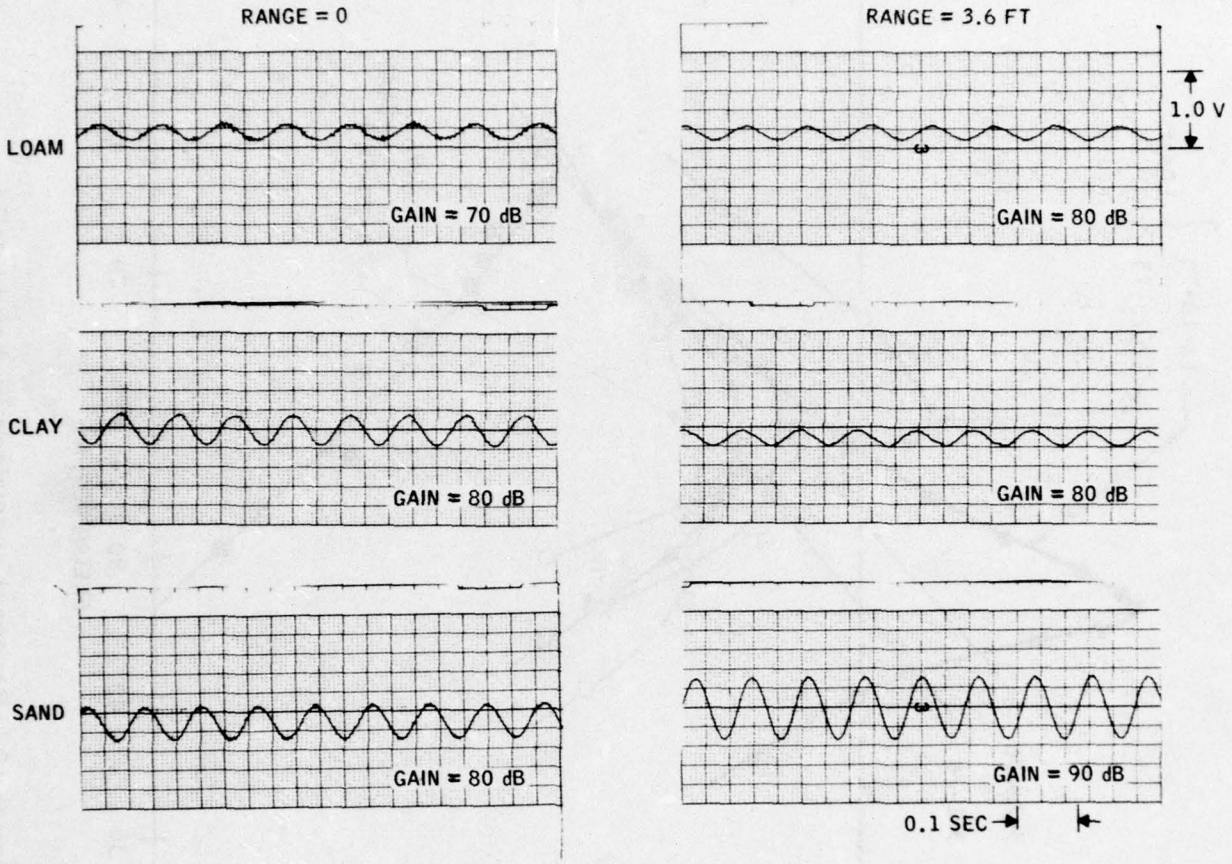


Figure 18. Vertical geophone traces for frozen soils, frequency 10 Hz

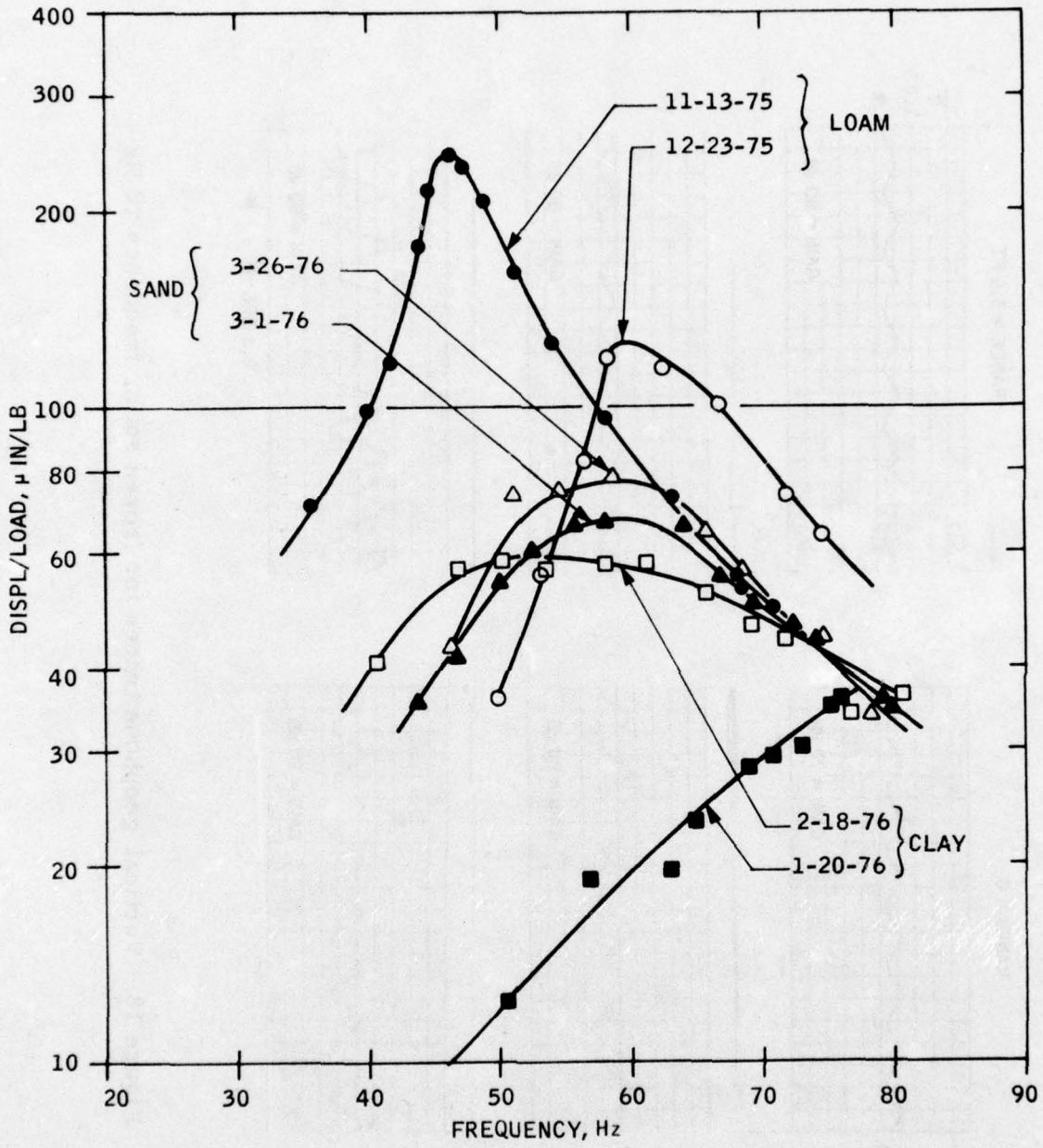


Figure 19. Resonant conditions in thawed soils

measured on two dates separated by approximately six weeks. A significant variation in the resonant frequency is noted; apparently it is caused by progressive compaction of the soil with time. For clay soil, the resonant point corresponding to tests run on the earlier date was apparently well above 80 Hz, whereas one month later the resonant condition was at approximately 52 Hz. It is possible that the process of freezing and thawing resulted in frost heaving and increased porosity within the clay sample; hence, the relative soil stiffness decreased with time. For the sand sample, resonant data taken on two dates separated by 25 days exhibits no significant difference.

The overall conclusion drawn from these data is that significant variations in dynamic properties of soil will occur with time. This conclusion applies only to signal information at relatively high frequencies (>20 Hz).

## Line Transducer Data

### Sensitivity at Mid-points and Transpositions

The discussion presented in reference 3 indicates that the primary mode of line transducer response is due to magnetostriction and that sensitivity at mid-points between transpositions should be substantially greater than that at transpositions. In order to substantiate that conclusion, line transducer response was measured at several positions along the line for a cyclic load of 10 Hz. The data is presented in Figure 20 in terms of relative output. It is clear from this data that at the transpositions the output of the transducer is substantially less than that exhibited at the mid-point. In general, throughout the experimental study, data taken along path M exhibited much higher sensitivity than data taken along path X1. For this reason, the analysis of data for the line transducer deals primarily with data taken along path M.

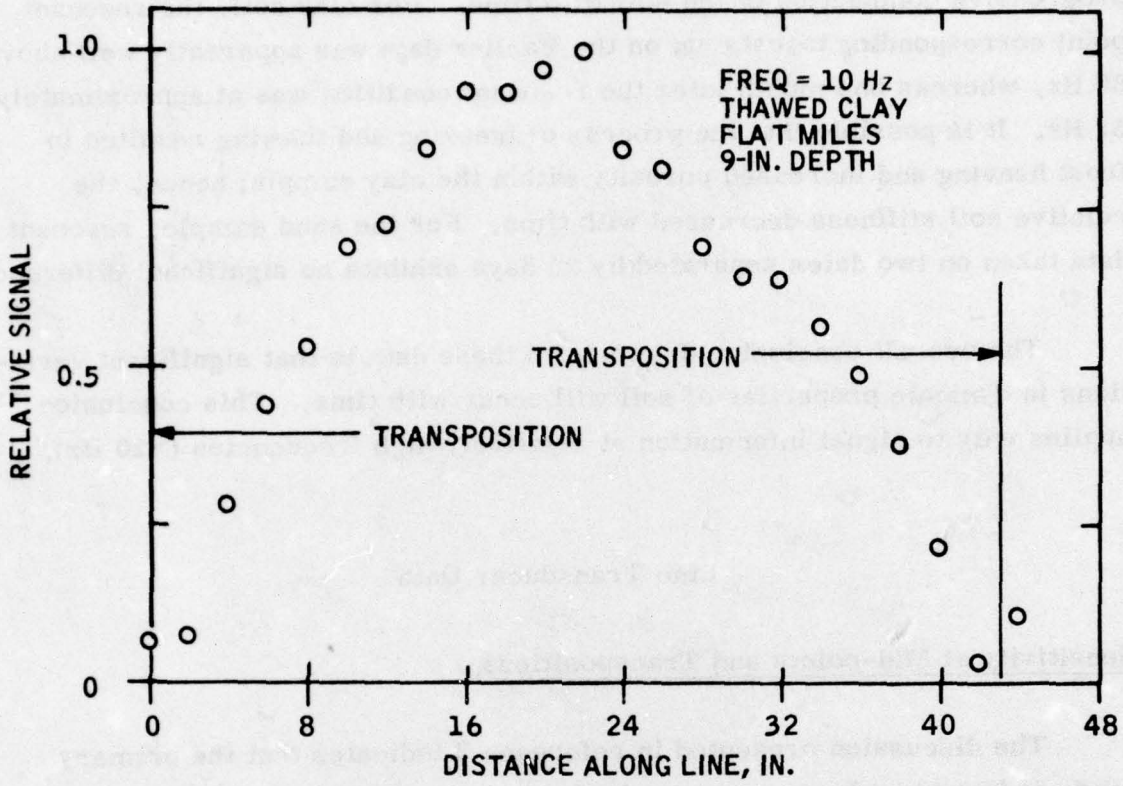


Figure 20. Longitudinal variation in MILES response

## Frequency Effects

In the theoretical background presented in a previous section, it was suggested that the motion of the soil at relatively low frequencies could be characterized in terms of the steady state equations of elasticity. This means that the soil displacement should be proportional to the magnitude of the load applied at the surface of the soil. As long as the frequency of the input signal results in seismic wavelengths that are substantially greater than the distance between the load source and the transducer, the magnitude of the resulting soil displacement for a given load should not change.

If one begins with this postulate and then follows through the derivation of the equations for transducer response presented in the theoretical background, it follows that the magnitude of the output signal of the line should be proportional to the input load and to the frequency of the applied signal. In order to test this postulate, data was acquired in a thawed clay for frequencies ranging from 1 to 80 Hz. The results are presented in Figure 21 and 22 for flat and round transducers, respectively. The data clearly show that for frequencies under 20 Hz, the transducer response can be characterized at a given range by a single value of the parameter e*. At frequencies of 40 and 80 Hz there is an evident departure of the data from that of lower frequencies. This departure is to be expected in that at 40 Hz wavelengths of approximately 10 feet might be encountered and at 80 Hz the wavelength would be approximately 5 feet. Hence, a condition is reached where the distance between the signal source and the transducer is of the same order of magnitude as seismic wavelengths.

Based on these data it is concluded that a single value of e* defines the sensitivity of both flat and round transducers at a given range at any given frequency under 20 Hz. For cases of frozen soil this conclusion will continue to be valid in that seismic wavelengths would be substantially longer because of the much higher anticipated propagation velocity. Based on this conclusion, subsequent discussions of transducer response to cyclic loads place emphasis on data taken at only one frequency (10 Hz).

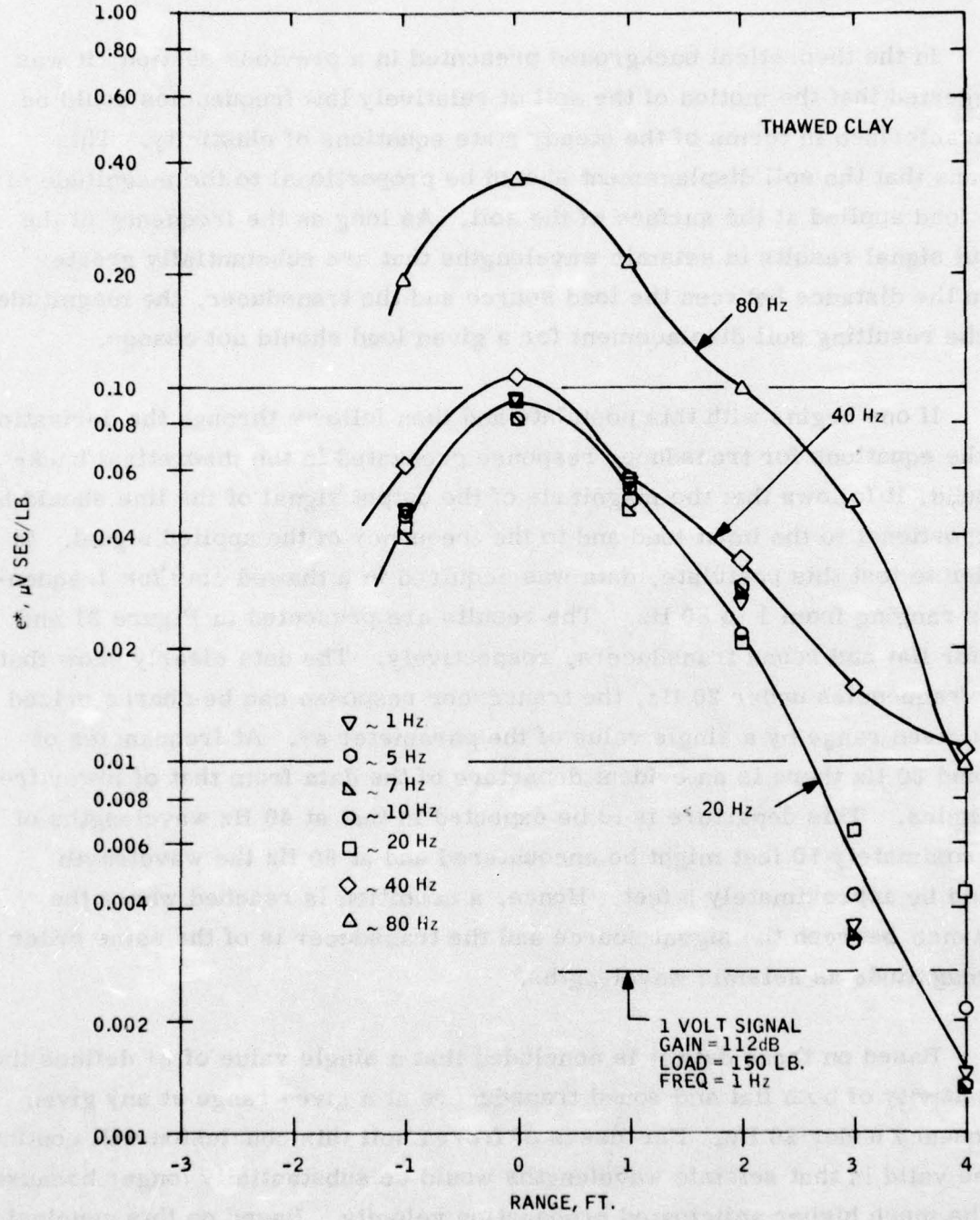


**Figure 21. Effect of load frequency on flat transducer response**

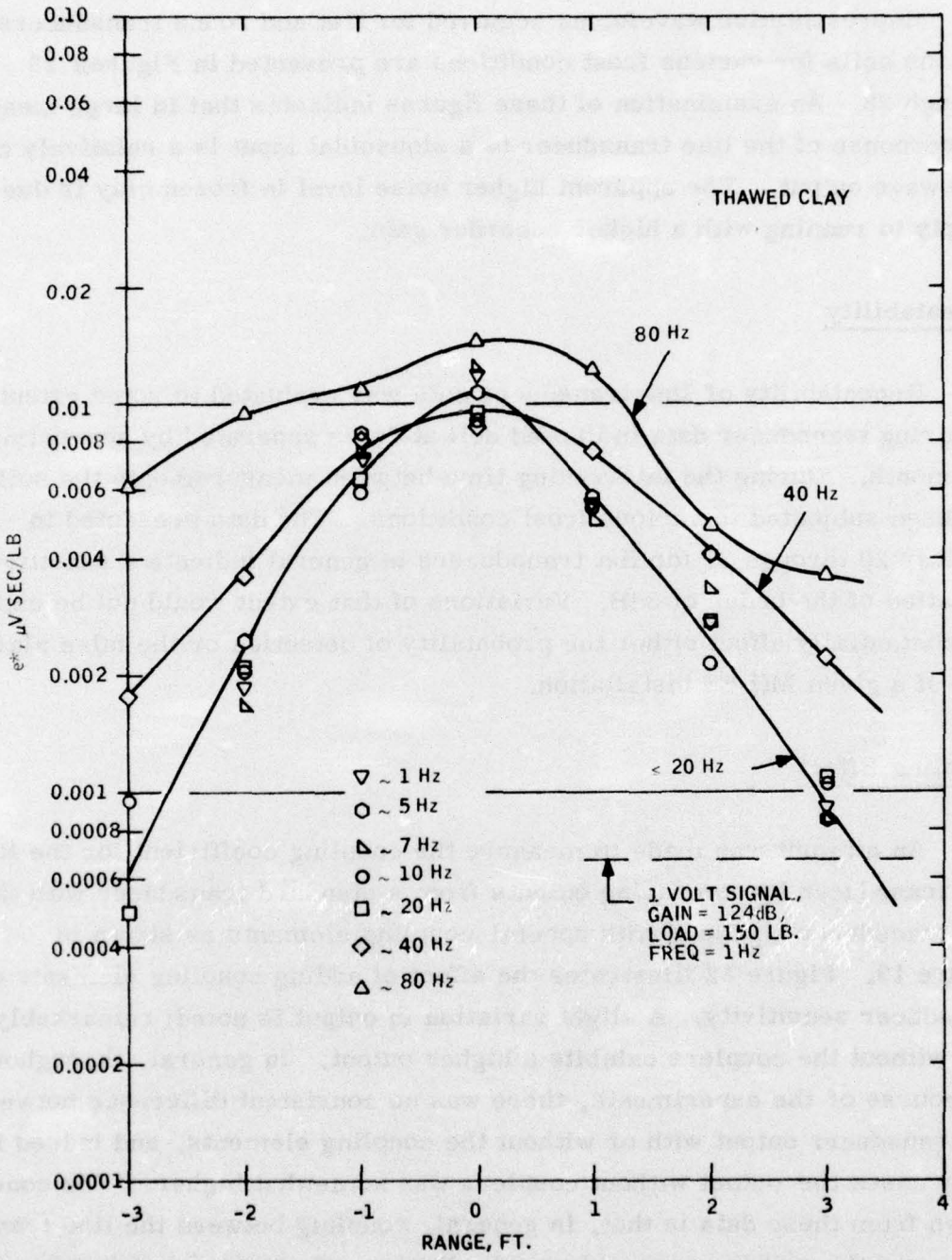


**Figure 22. Effect of load frequency on round transducer response**

## Cyclic Waveform

Representative waveforms acquired for flat and round transducers in various soils for various frost conditions are presented in Figures 23 through 28. An examination of these figures indicates that in large measure the response of the line transducer to a sinusoidal input is a relatively clean sine wave output. The apparent higher noise level in frozen clay is due simply to running with a higher recorder gain.

## Repeatability

Repeatability of line transducer data was evaluated to some extent by acquiring transducer data in thawed soil at dates separated by approximately one month. During the intervening time between measurements the soils had been subjected to various frost conditions. The data presented in Figures 29 through 31 for flat transducers in general indicate a sensitivity variation of the order of 3dB. Variations of that extent would not be expected to substantially affect either the probability of detection or the false alarm rate of a given MILES installation.

## Coupling Effect

An attempt was made to measure the coupling coefficient for the flat line transducer by comparing outputs from a standard transducer with those of a transducer equipped with special coupling elements as shown in Figure 13. Figure 32 illustrates the effect of adding coupling elements on transducer sensitivity. A slight variation in output is noted; remarkably the line without the couplers exhibits a higher output. In general, throughout the course of the experiments, there was no consistent difference between the transducer output with or without the coupling elements, and indeed in many cases the output without couplers was somewhat higher. The conclusion drawn from these data is that, in general, coupling between the line transducer and the soil is reasonably good. Design efforts aimed at improved coupling probably would not yield fruitful results.

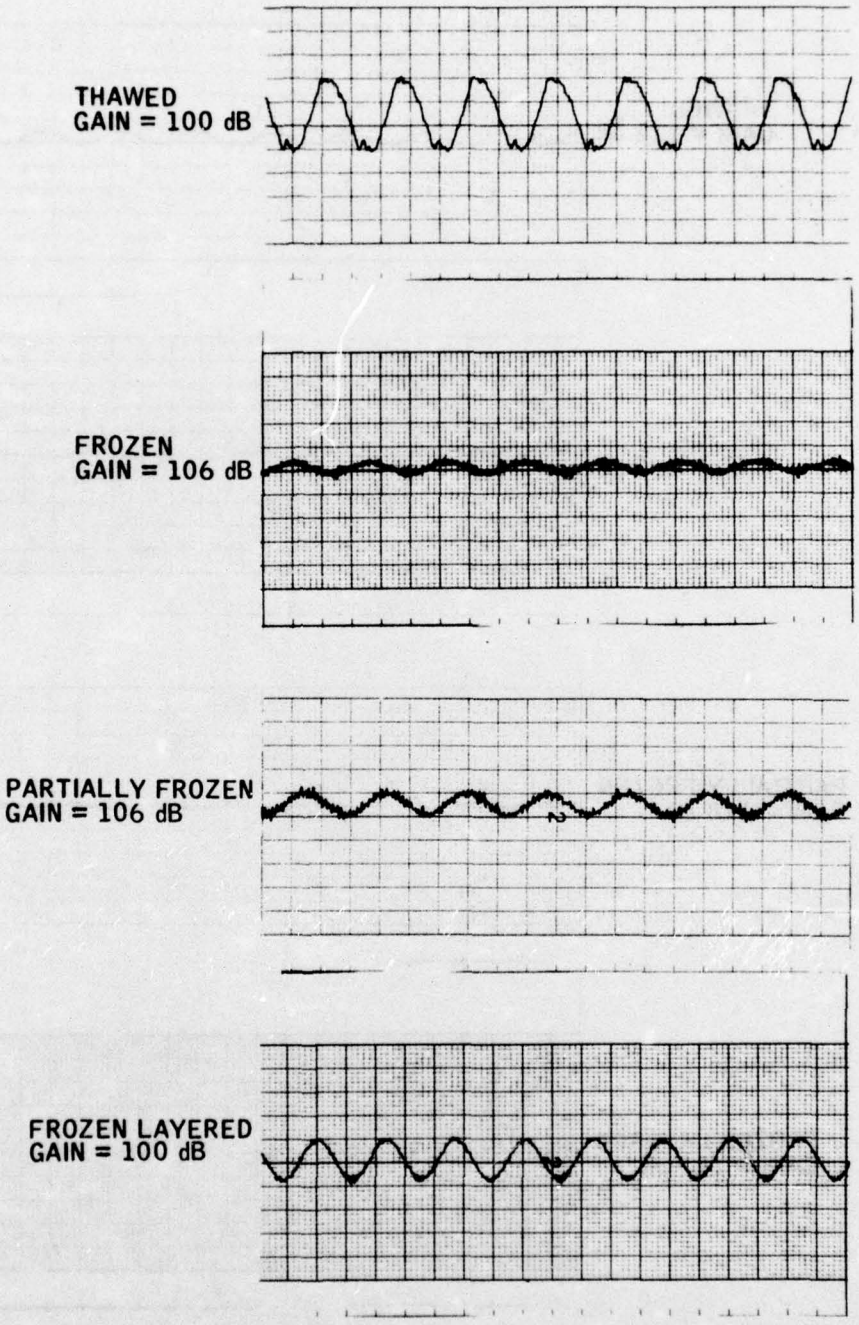


Figure 23. Waveforms produced by 10 Hz cyclic load; flat MILES in loam

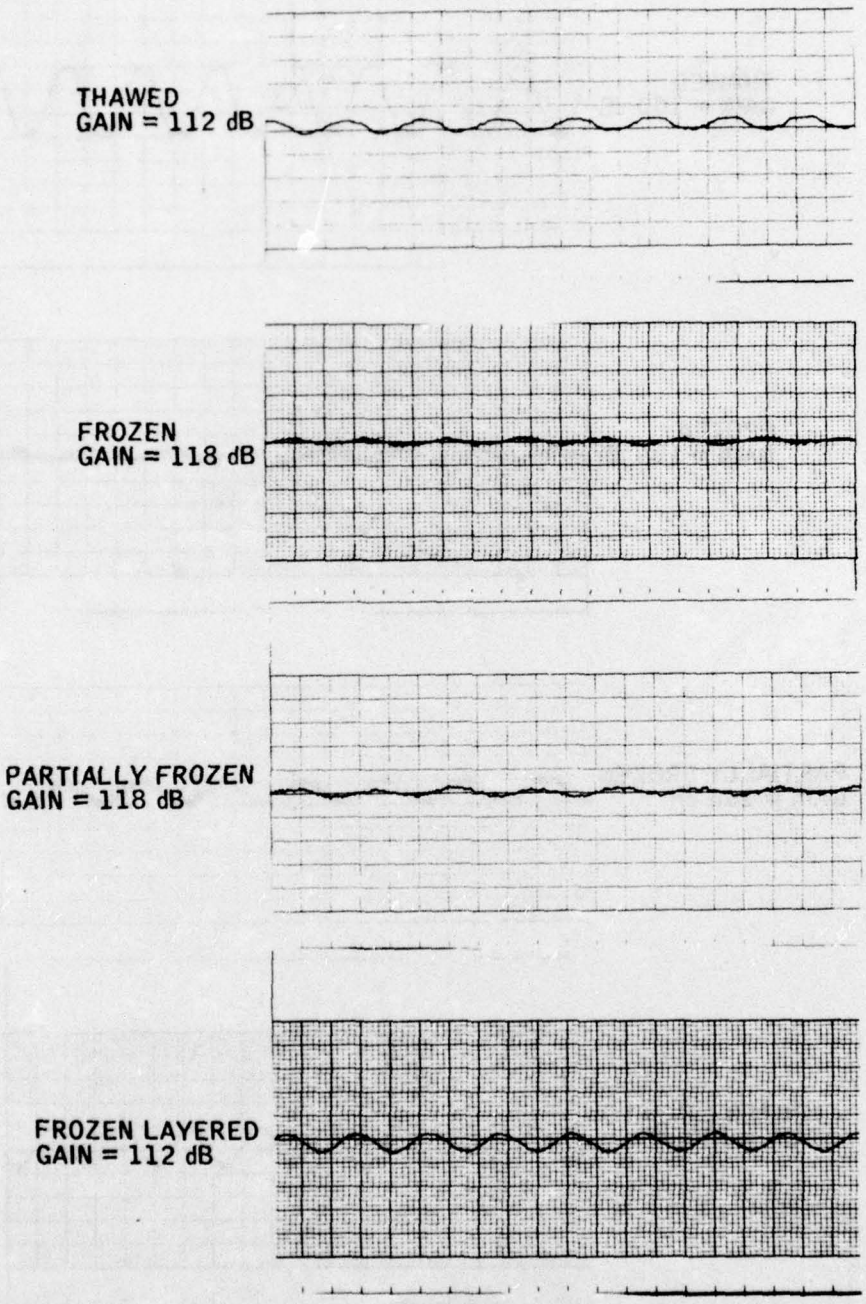


Figure 24. Waveforms produced by 10 Hz cyclic load, round MILES in loam

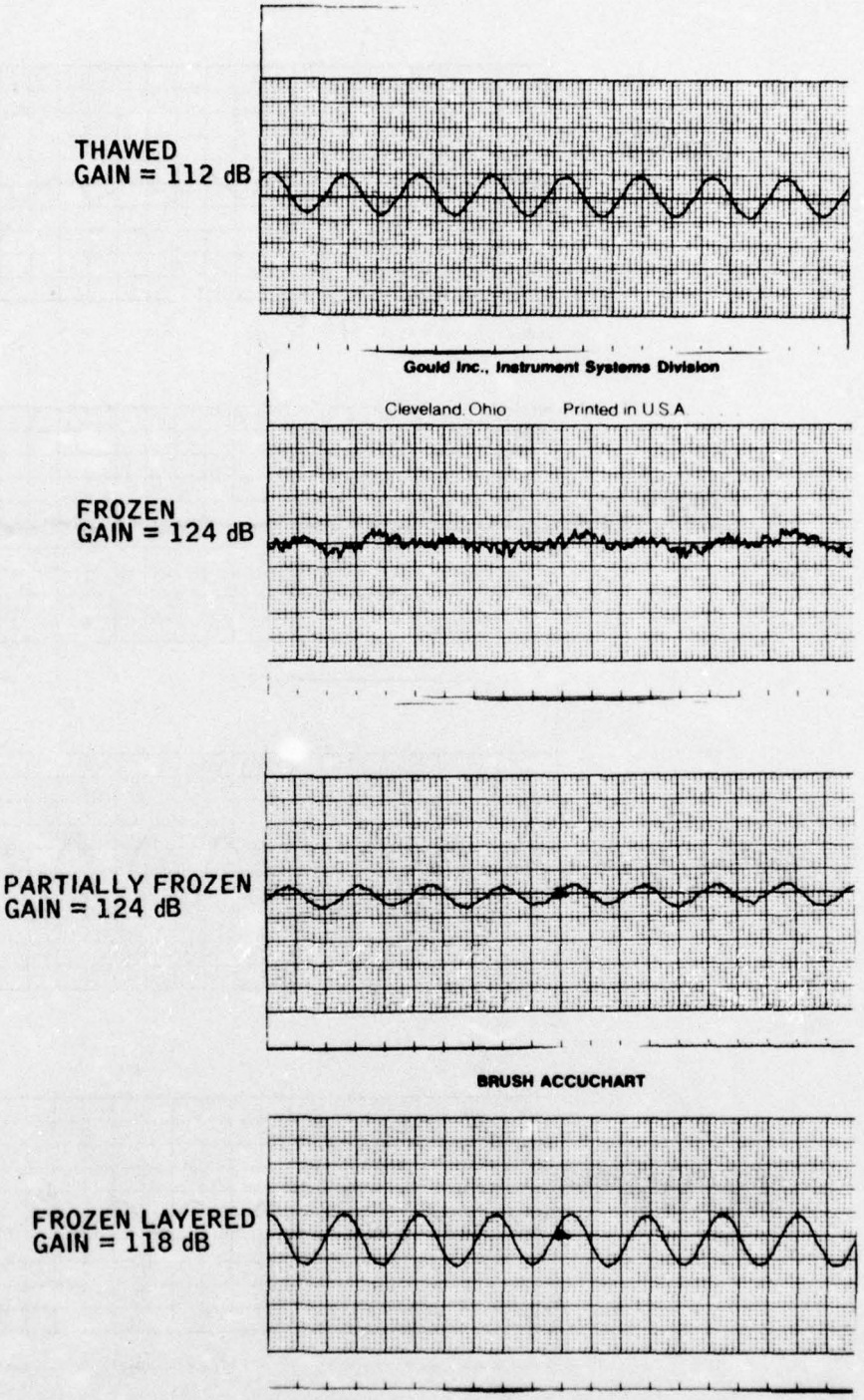


Figure 25. Waveforms produced by 10 Hz cyclic load; round MILES in clay

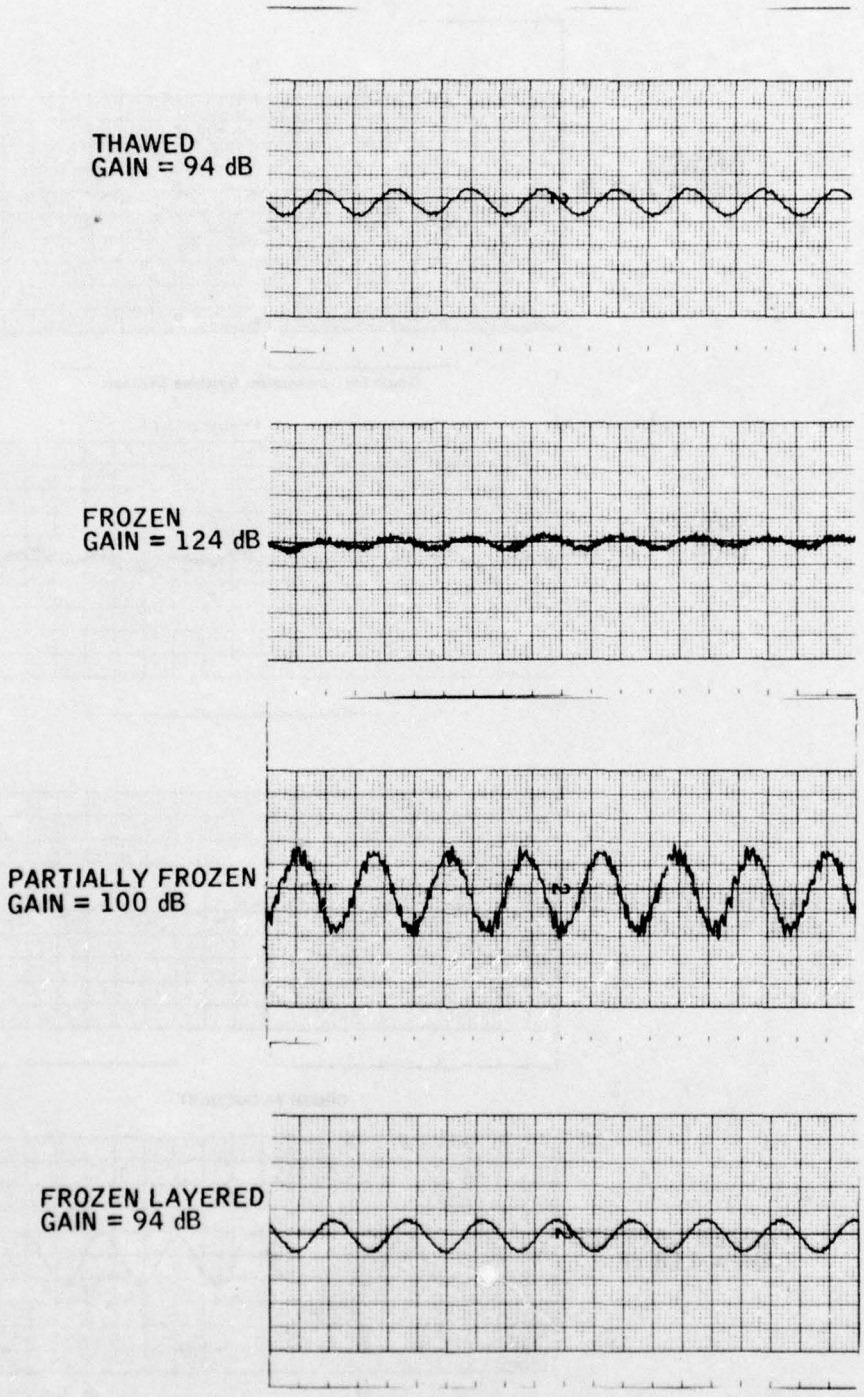


Figure 26. Waveforms produced by 10 Hz cyclic load; flat MILES in sand

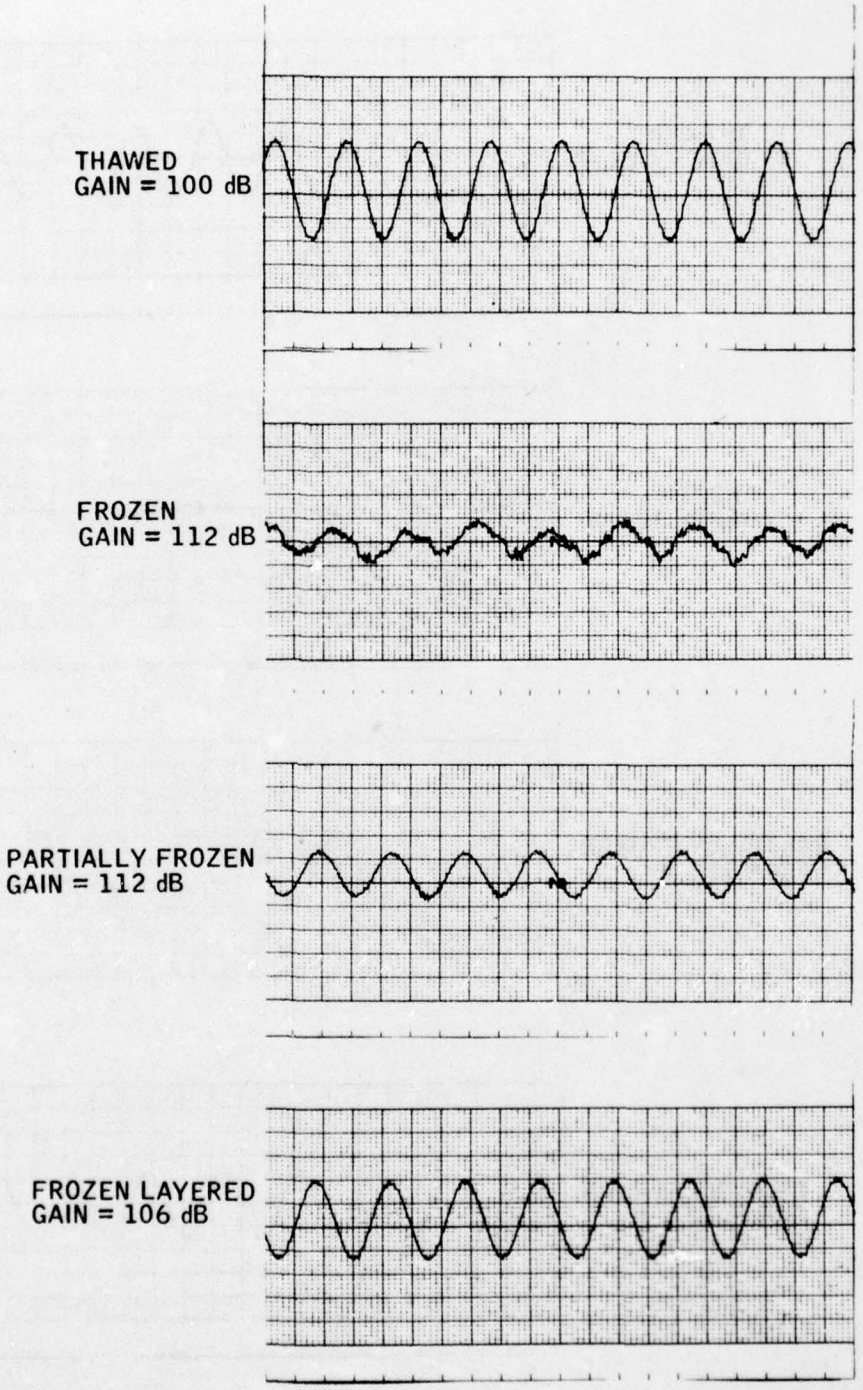


Figure 27. Waveforms produced by 10 Hz cyclic load; flat MILES in clay

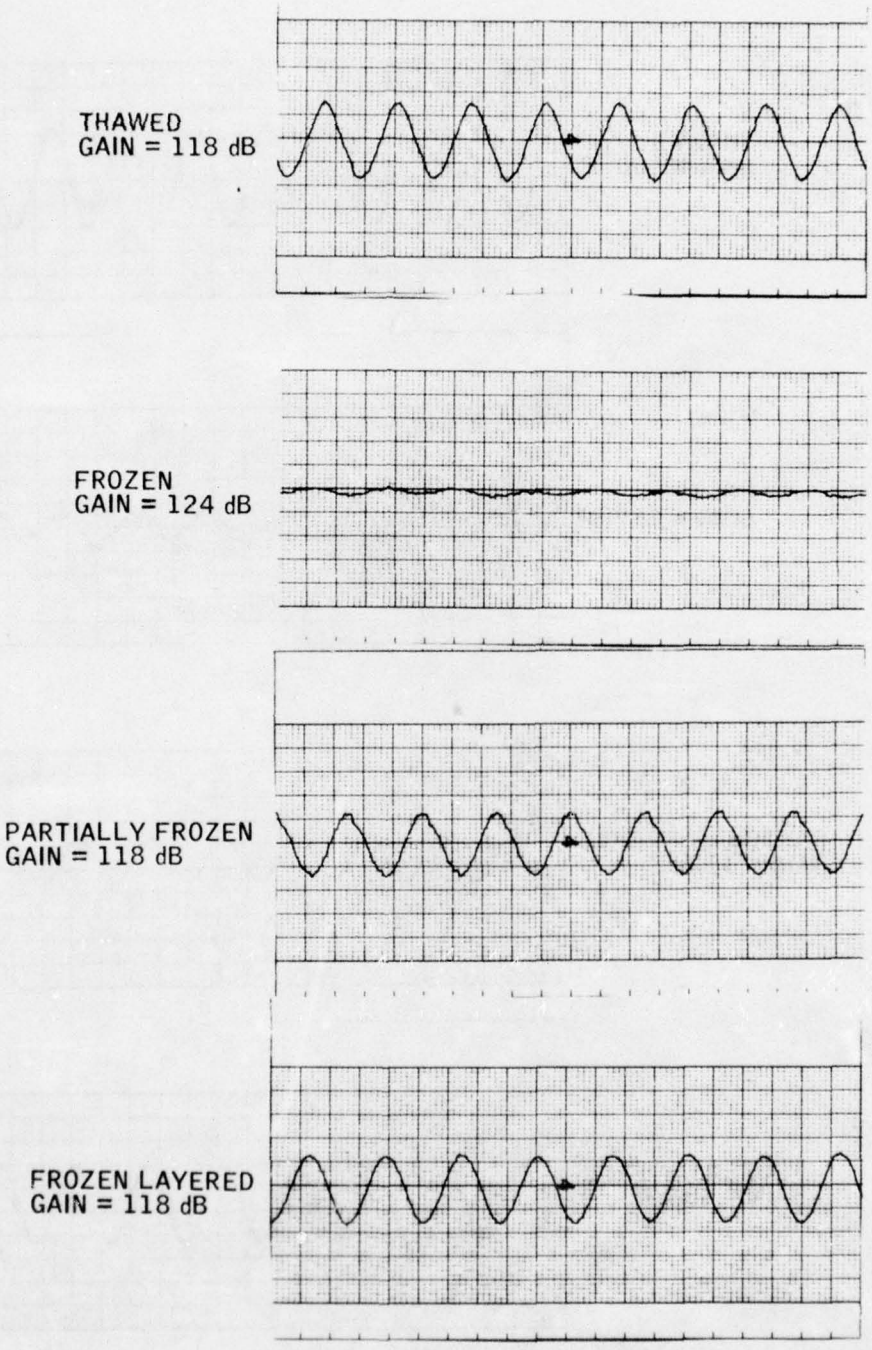


Figure 28. Waveforms produced by 10 Hz cyclic load; round MILES in sand

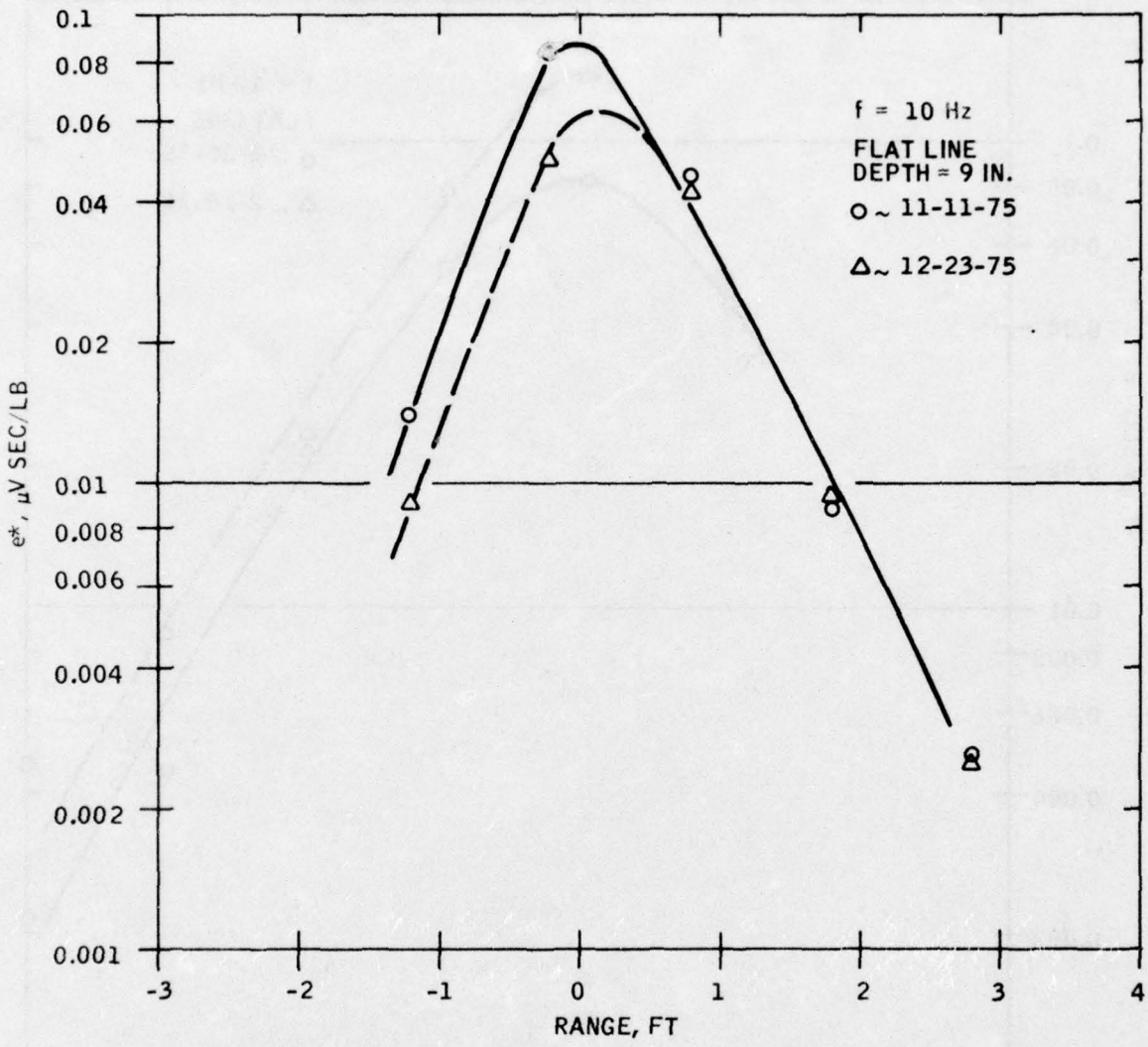


Figure 29. Repeatability of line data in thawed loam

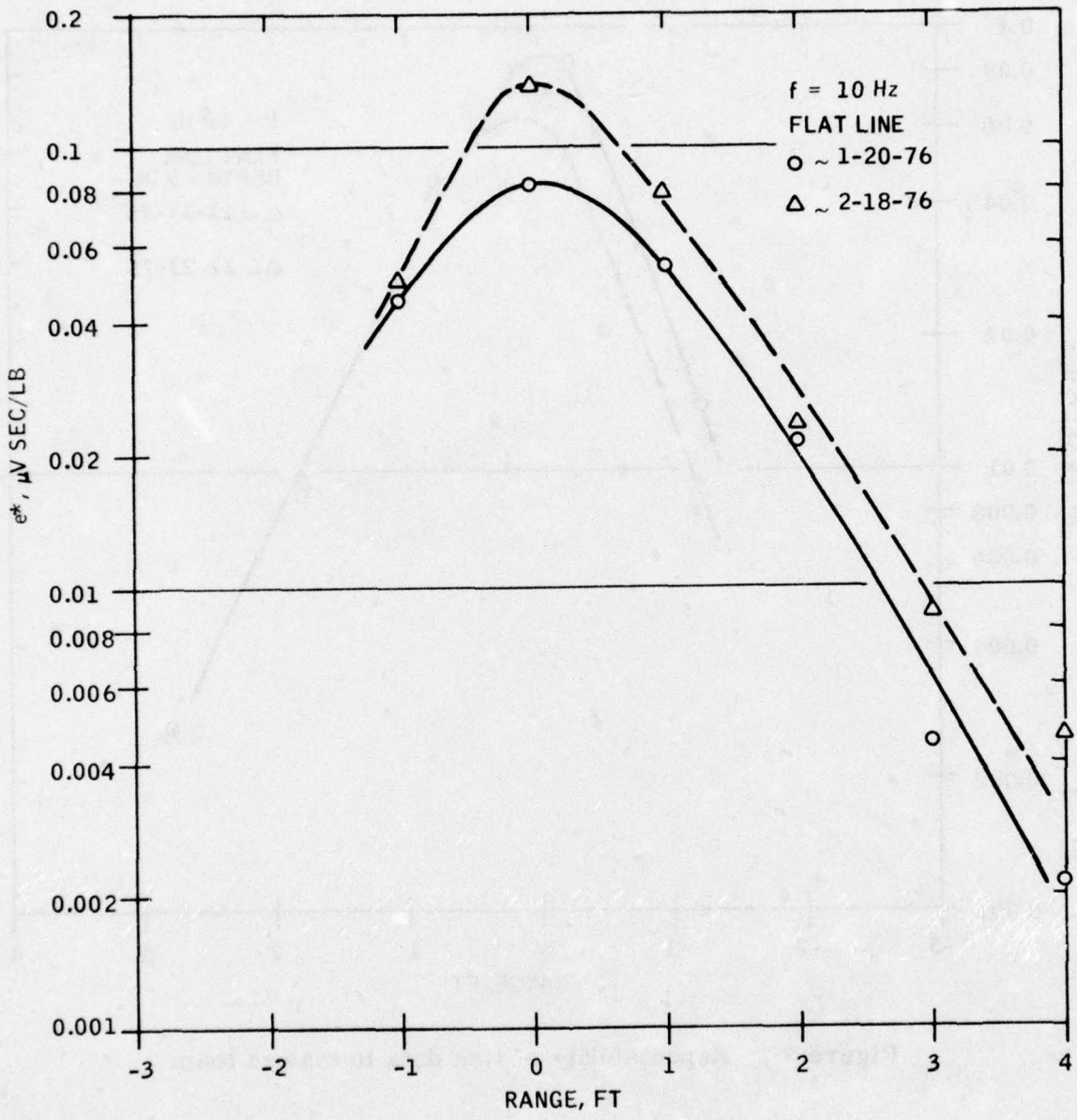


Figure 30. Repeatability of line data in thawed clay

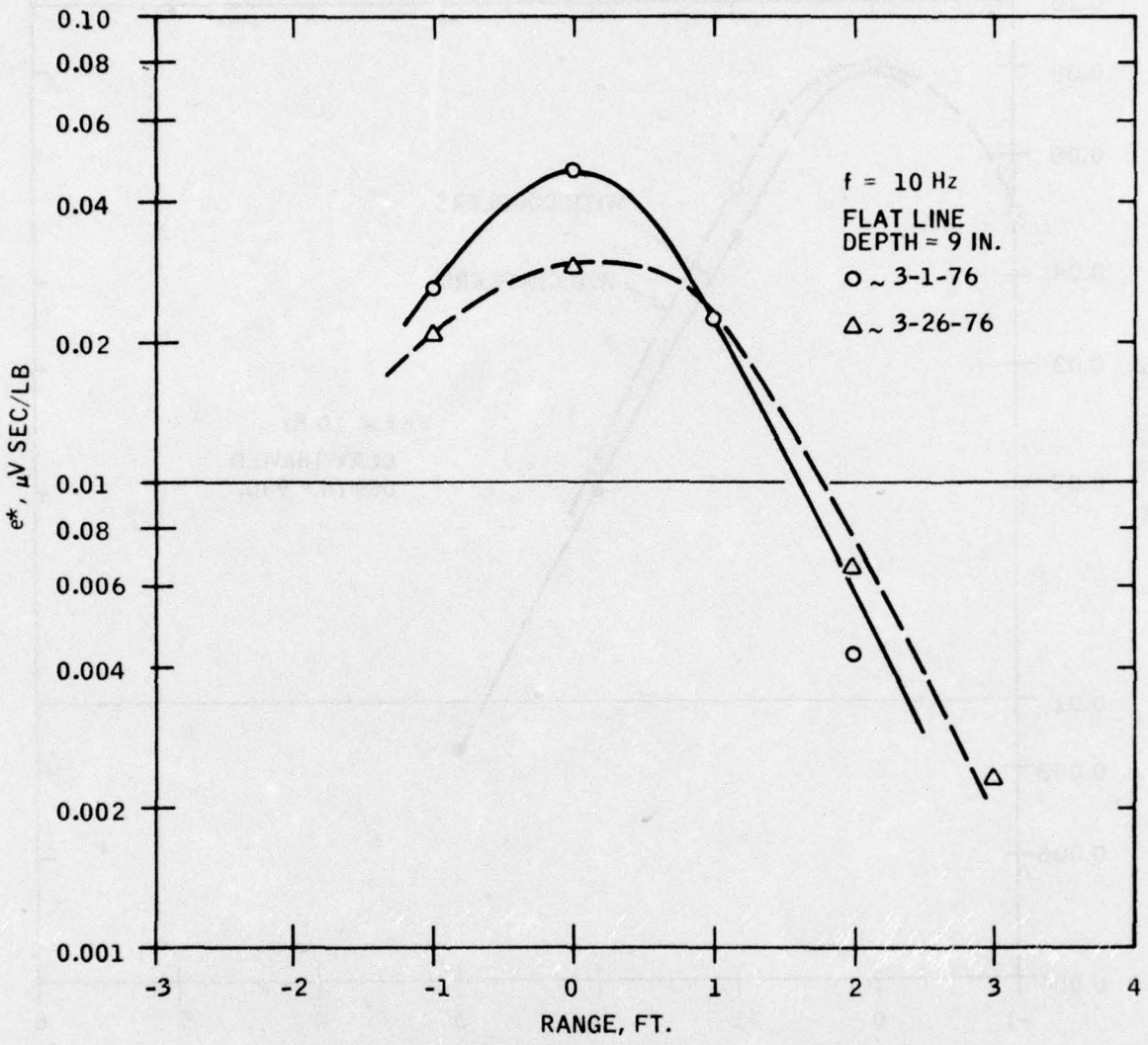


Figure 31. Repeatability of line data in thawed sand

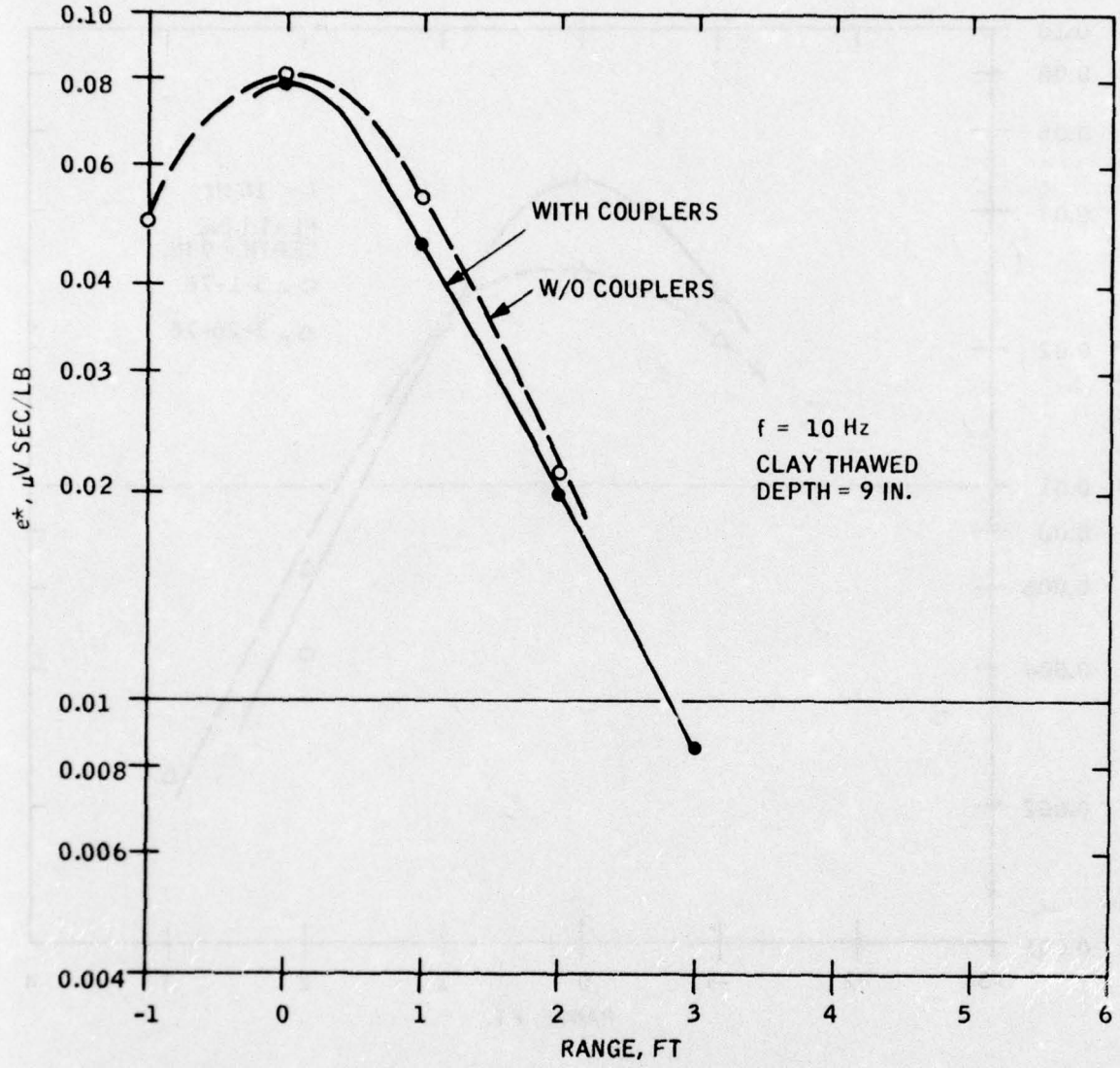


Figure 32. Effect of coupling elements

## Effect of Depth

Data was acquired on round and flat transducers buried at both 9- and 18-inch depths. These experiments are presented in Figures 33, 34 and 35 for loam, clay, and sand soil samples, respectively. The test results are for thawed soil. The trend that appears common to all soil samples and both round and flat transducers is a flattening out of the curve of sensitivity versus range for the deeper burial. For line transducers buried in sand, and for the round transducers buried in loam, sensitivity at all values of range increased at the greater depth. It can be concluded from these data that with burial at 18 inches rather than 9 inches a high probability of detection can be maintained at ranges of 3 to 4 feet from the line, with reduced probability of false alarms because of relatively lower sensitivity directly above the line. This same trend was observed for the various frost conditions generated within the soil during the experimental program.

## Effect of Frost

Data was acquired for the conditions of thawed, totally frozen, partially frozen, and frozen layered conditions as defined in Section IV. Actual frost depths generated are listed in Table 3.

TABLE 3. FROST DEPTHS IN PARTIALLY FROZEN AND FROZEN-LAYERED SOILS

| Soil | Partially Frozen | Frozen Layered |
|---|---|---|
| Loam | Surface to 3 in. | 1 in. to 6 in. |
| Clay | Surface to 8 in. | 1.5 in. to 7 in. |
| Sand | Surface to 6 in. | 1 in. to 5 in. |

In order to realistically evaluate the effect of frost, a threshold range was defined as the range at which a 1 volt signal is produced by a 150 pound peak-to-peak amplitude signal at 1 Hz. For the flat transducer it was assumed that the signal would be generated through a gain of 112 dB, and for the round transducer the gain setting would be 124 dB. This difference in gain setting offsets the inherent higher sensitivity of the 80-turn flat transducer.

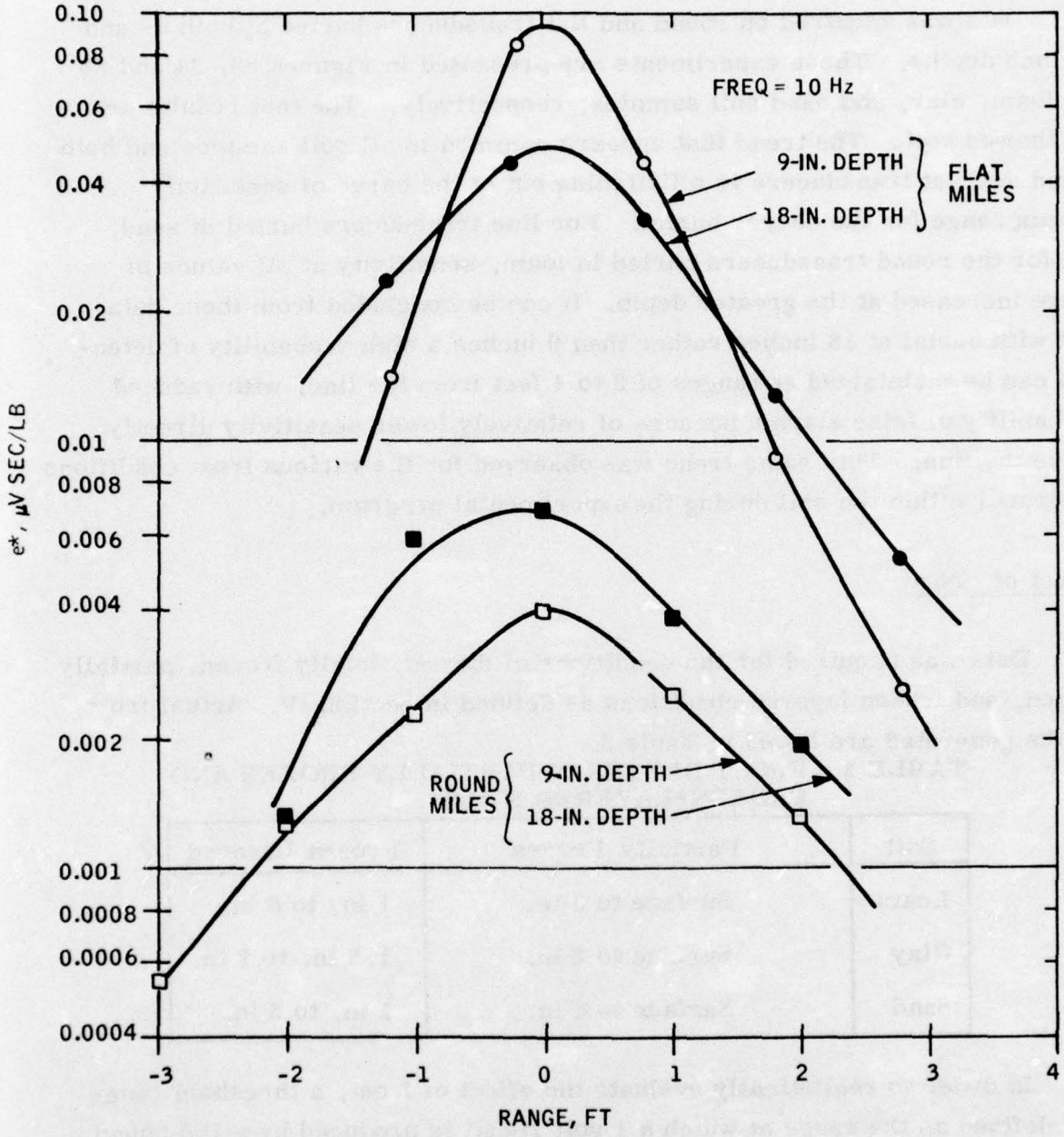


Figure 33. Effect of depth on transducer response in loam

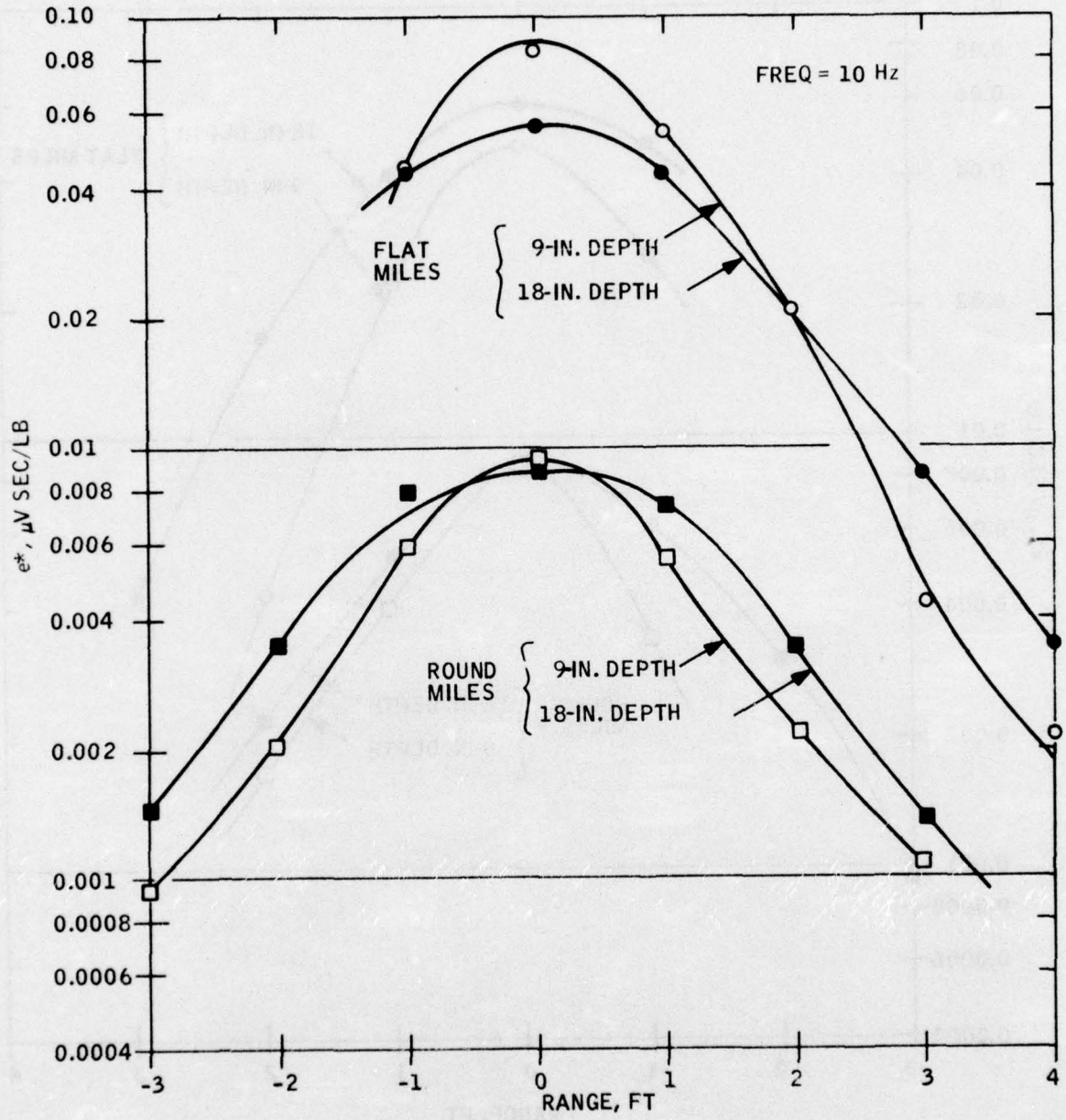


Figure 34. Effect of depth on transducer response in clay

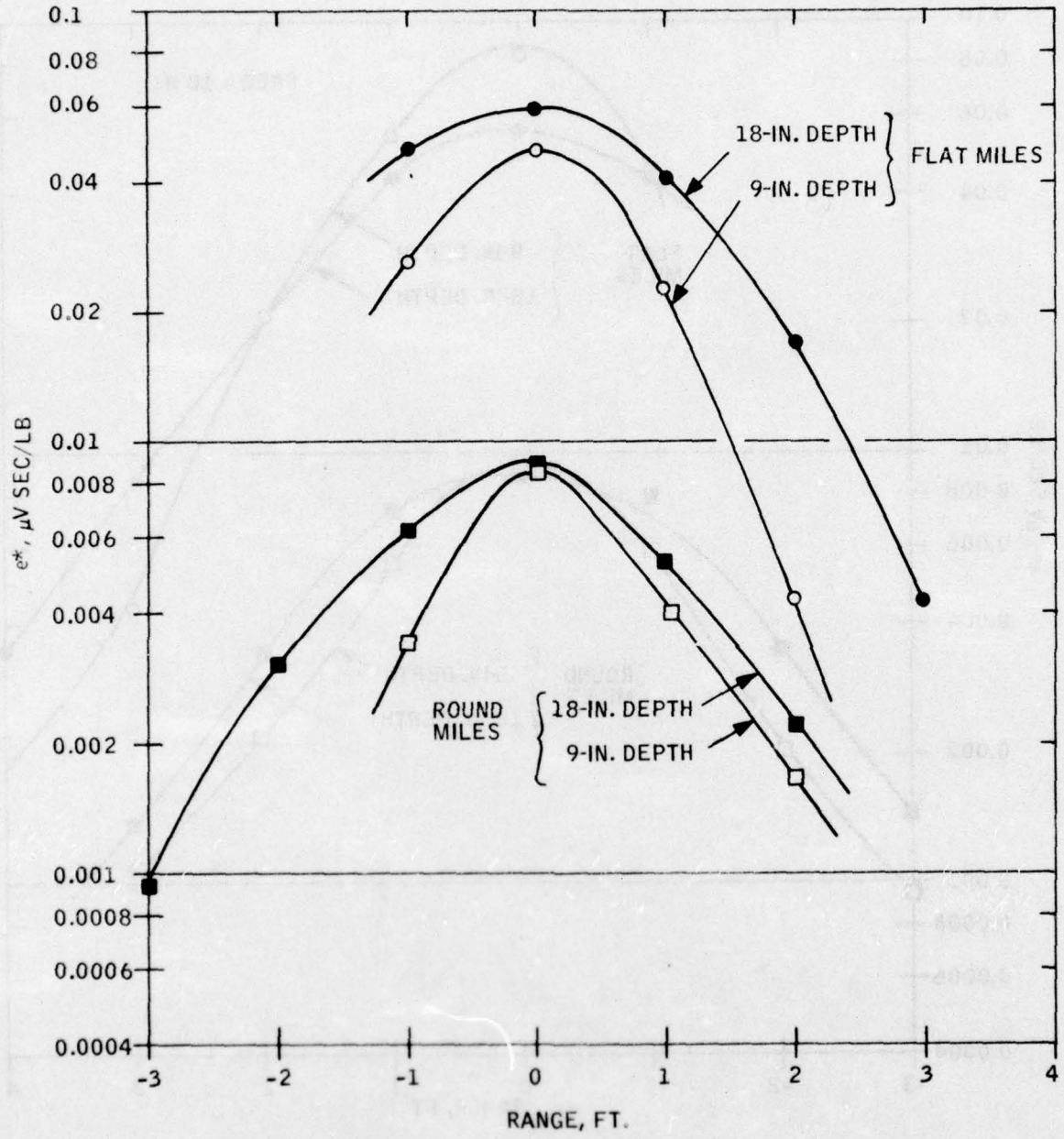


Figure 35. Effect of depth on transducer response in sand

Data acquired for various frost conditions is presented in Figures 36 through 41. Each figure is for a given soil sample and a given transducer. The e* value corresponding to a 1 volt threshold signal is indicated on each curve. The threshold range parameter for each frost condition corresponds to the intersecting point of the experimental curve with the threshold level.

A summary of threshold ranges is presented in Table 4. In interpreting these results, it is essential that each of the sets of experimental data be examined carefully so that meaningful correlation of the data with anticipated operational environments can be made. Beginning with Figures 36 and 37 for the flat and round transducers, respectively, it is seen that significant attenuation occurred for the conditions of totally frozen and partially frozen ground. It is probable that some increase in electronics gain would be desirable to offset the frost effect under this situation. Of interest is the relatively high sensitivity obtained with the frozen layered condition. Actually, the thickness of the frozen layer was approximately 6 inches where that of the partially frozen layer was 3 inches. One would therefore expect greater attenuation with the frozen layered condition. That this greater attenuation did not occur, means that under the frozen layer condition, a continuous shelf of frozen ground did not exist. Discontinuities in the frozen ground may have occurred either because of migration of water within the soil, or simply that the layer had developed cracks because of surface loadings.

It will be subsequently shown for other soil samples that many layered conditions did not produce significant reduction in threshold range. For the loam sample the partially frozen condition was generated by rapid freezing of the soil surface by sub-zero air that was ventilated into the test area. Under this condition of rapid freezing, a continuous shelf of ice probably was generated.

Data for round and flat transducers in clay is presented in Figures 38 and 39. For the condition of a totally frozen ground, attenuation is significant enough to drop the output level below the threshold of detection for all ranges.

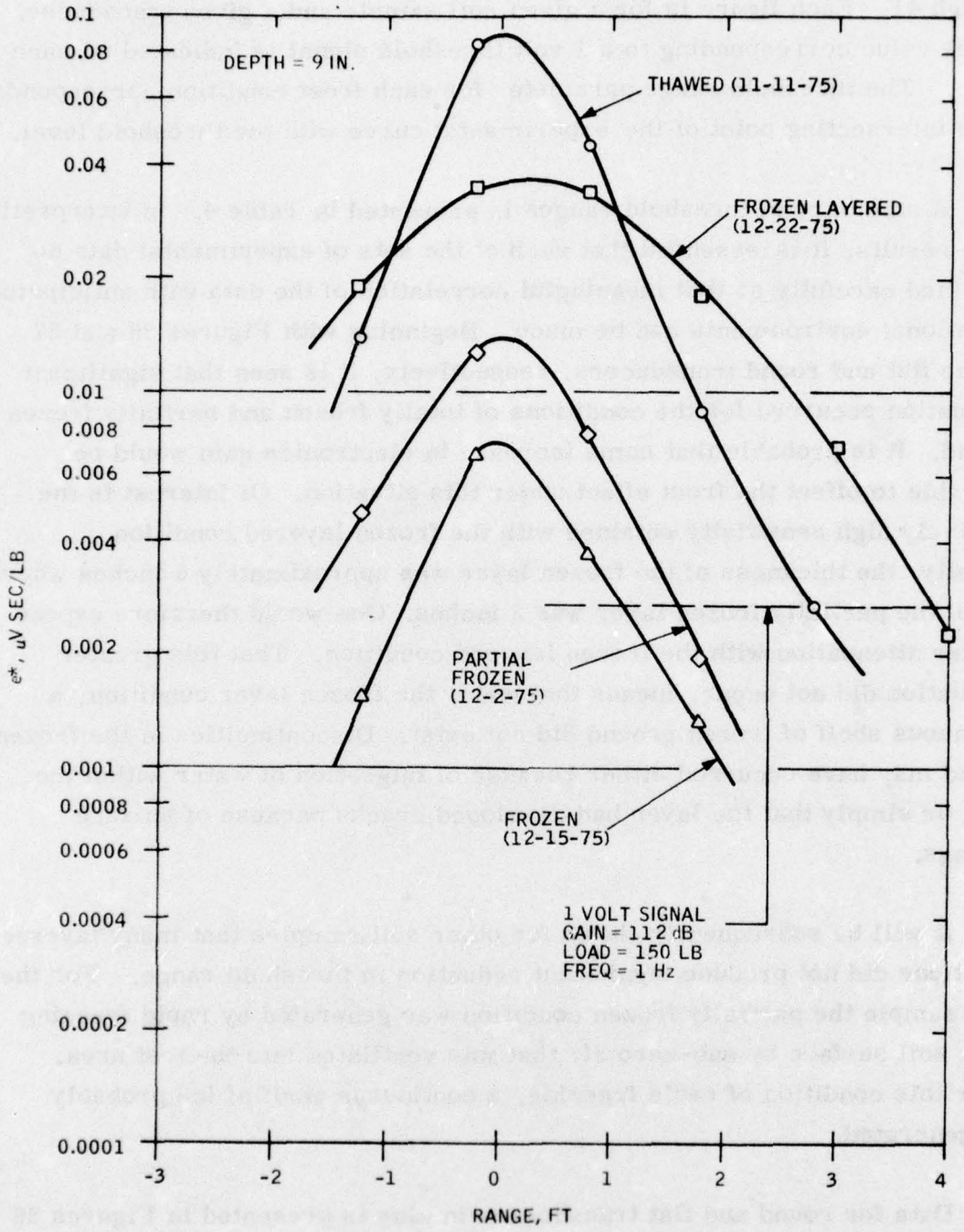


Figure 36. Effect of frost on flat MILES response in loam

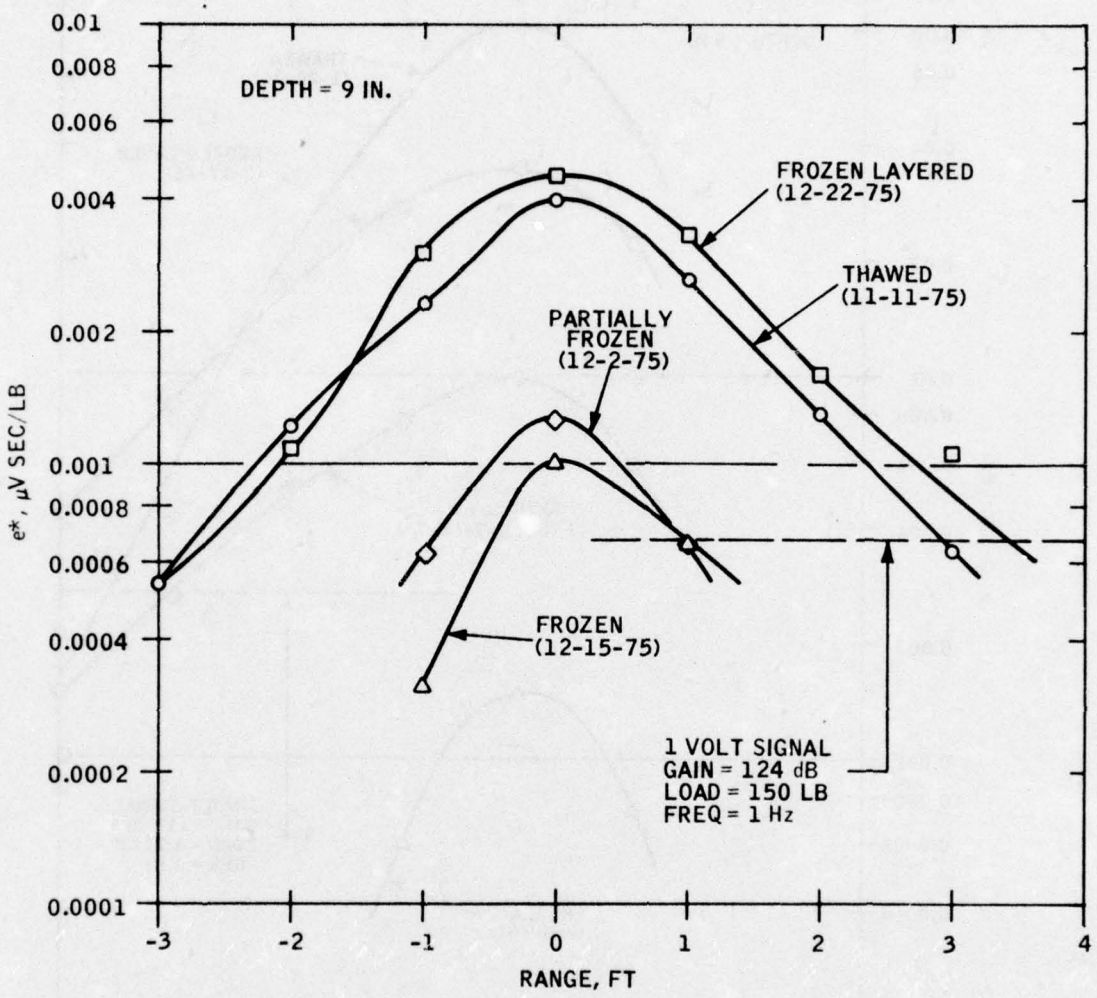


Figure 37. Effect of frost on round MILES response in loam

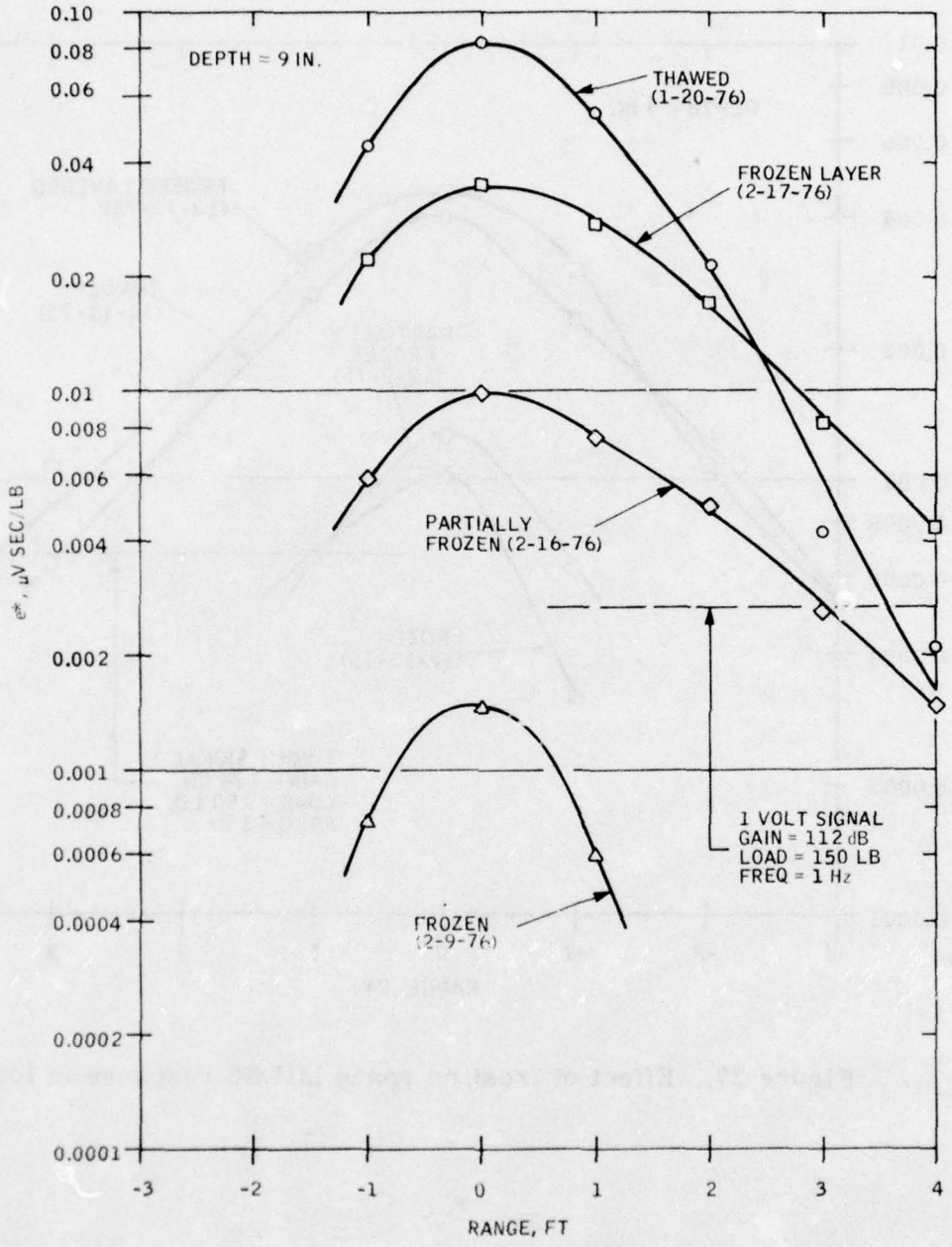


Figure 38. Effect of frost on flat MILES response in clay

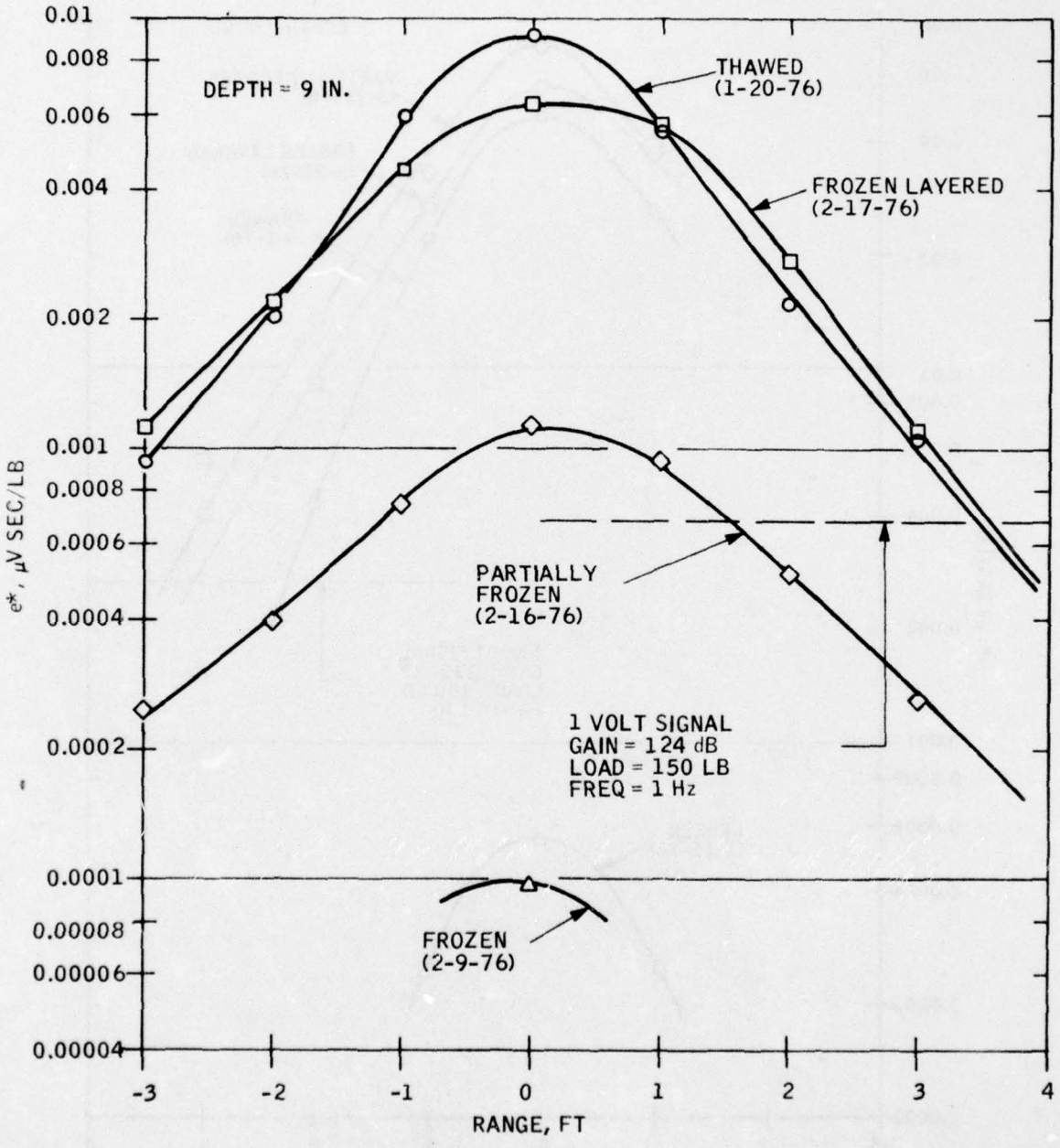


Figure 39. Effect of frost on round MILES response in clay

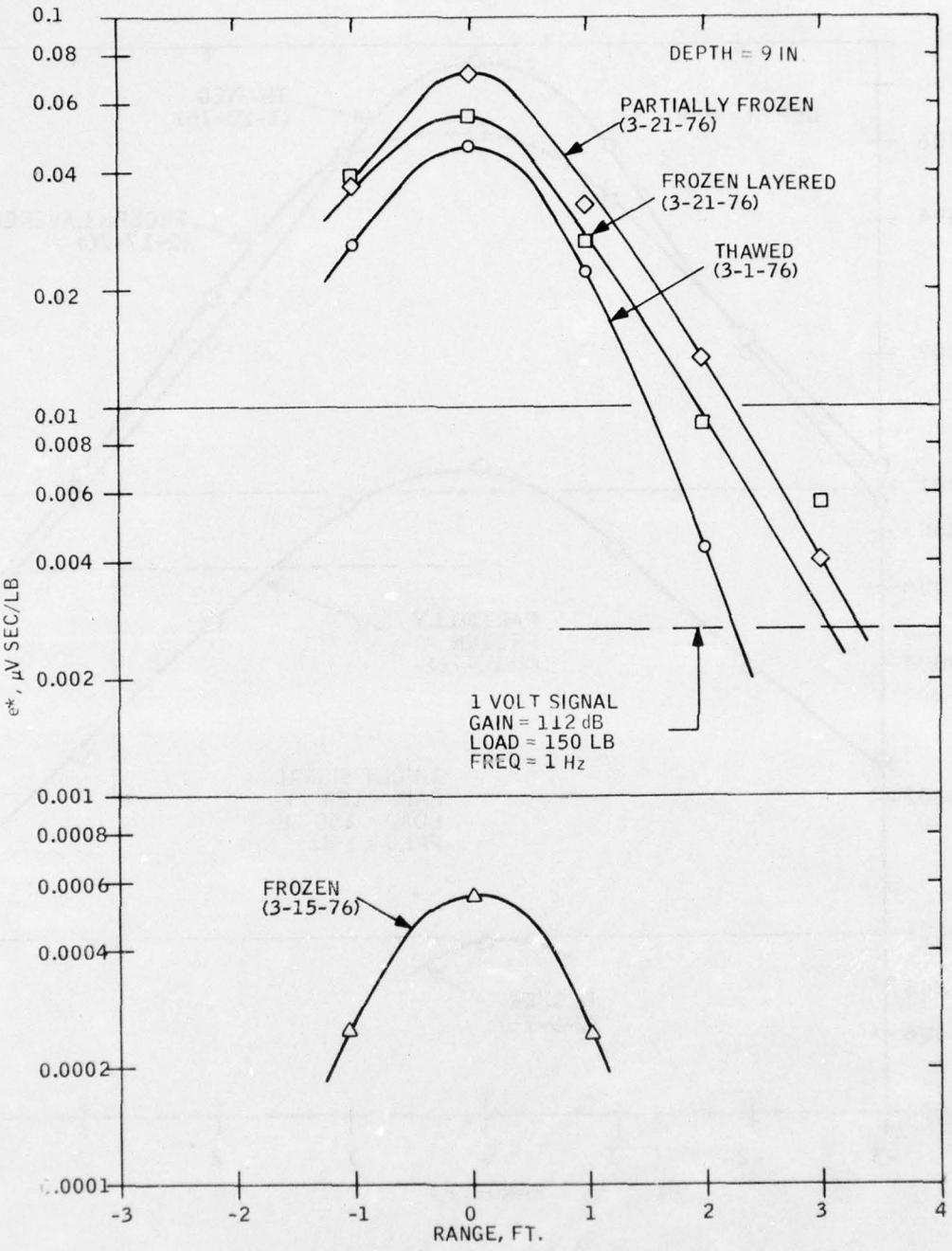


Figure 40. Effect of frost on flat MILES response in sand

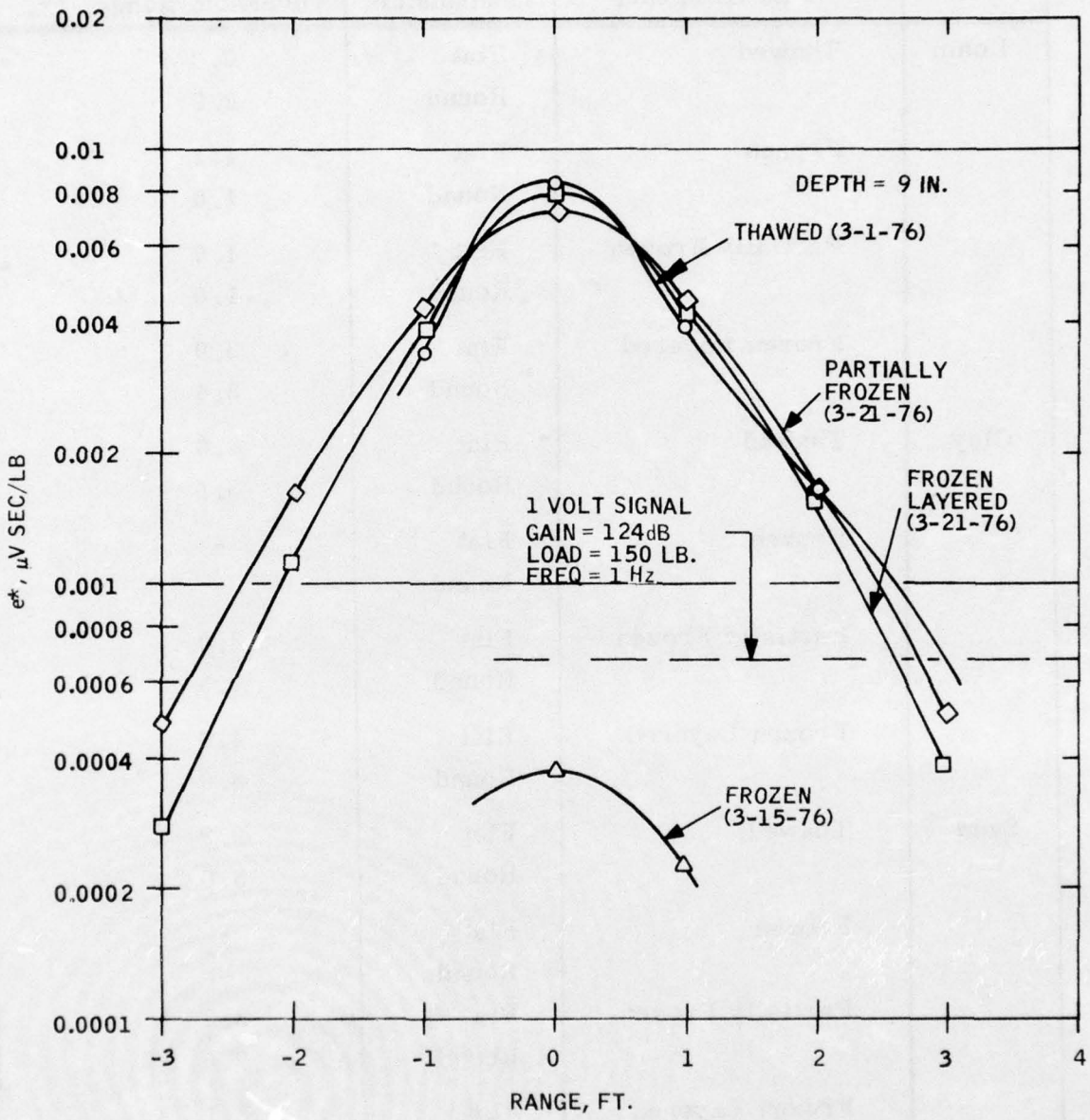


Figure 41. Effect of frost on round MILES response in sand

TABLE 4. THRESHOLD RANGE FOR VARIOUS SOIL CONDITIONS, 9-IN. DEPTH

| Soil | Frost Condition | Transducer | Threshold Range, Ft. |
|---|---|---|---|
| Loam | Thawed | Flat | 2.8 |
| | | Round | 2.9 |
| | Frozen | Flat | 1.1 |
| | | Round | 1.0 |
| | Partially Frozen | Flat | 1.6 |
| | | Round | 1.0 |
| | Frozen Layered | Flat | 3.9 |
| | | Round | 3.4 |
| Clay | Thawed | Flat | 3.6 |
| | | Round | 3.5 |
| | Frozen | Flat | - |
| | | Round | - |
| | Partially Frozen | Flat | 3.0 |
| | | Round | 1.5 |
| | Frozen Layered | Flat | 4.6 |
| | | Round | 3.6 |
| Sand | Thawed | Flat | 2.3 |
| | | Round | 3.0 |
| | Frozen | Flat | - |
| | | Round | - |
| | Partially Frozen | Flat | 3.3 |
| | | Round | 2.8 |
| | Frozen Layered | Flat | 3.1 |
| | | Round | 2.6 |

With the flat transducer, layering caused some attenuation, but at the same time the fall-off in sensitivity with range was not as great as with the thawed sample. As a result, only a small reduction in threshold range was obtained. For the round transducer, the partially frozen condition resulted in a significant reduction in threshold range.

Data for a round and flat transducers in sand is presented in Figures 40 and 41 for the various frost conditions. For both round and flat transducers in frozen ground, the attenuation is large enough to reduce the output to below threshold level at all ranges. However, for all layered conditions no significant attenuation of output occurs. Indeed, for the flat transducer, a more sensitive and flatter response curve is obtained under the layered condition. It is probable that for these layered conditions a continuous shelf of ice did not exist.

Response to Impulse Loading

The response of the line transducer to a broader range of frequencies than represented by the cyclic loads was obtained by subjecting the soil to impulse loads using the impulse load generator described in Section IV. Line transducer data taken along path M and path X1 is shown in Figures 42 and 43, respectively. The lowest trace on each of the figures is the output of the geophone mounted on the impulse load generator. Note that a slight impulse is imparted to the ground when the drop hammer is released. This is because at the release point the drop weight goes into free fall so that the net load imparted to the ground is reduced.

At the impact point, a relatively large displacement is generated. The resulting sinusoidal displacement is due to the elastic properties of the soil. In general, the springiness of the soil could result in an impact load generator lifting off the ground on rebound; however, if the weight of the generating device exceeds the magnitude of the input load by factor of 2, no bounce should occur.

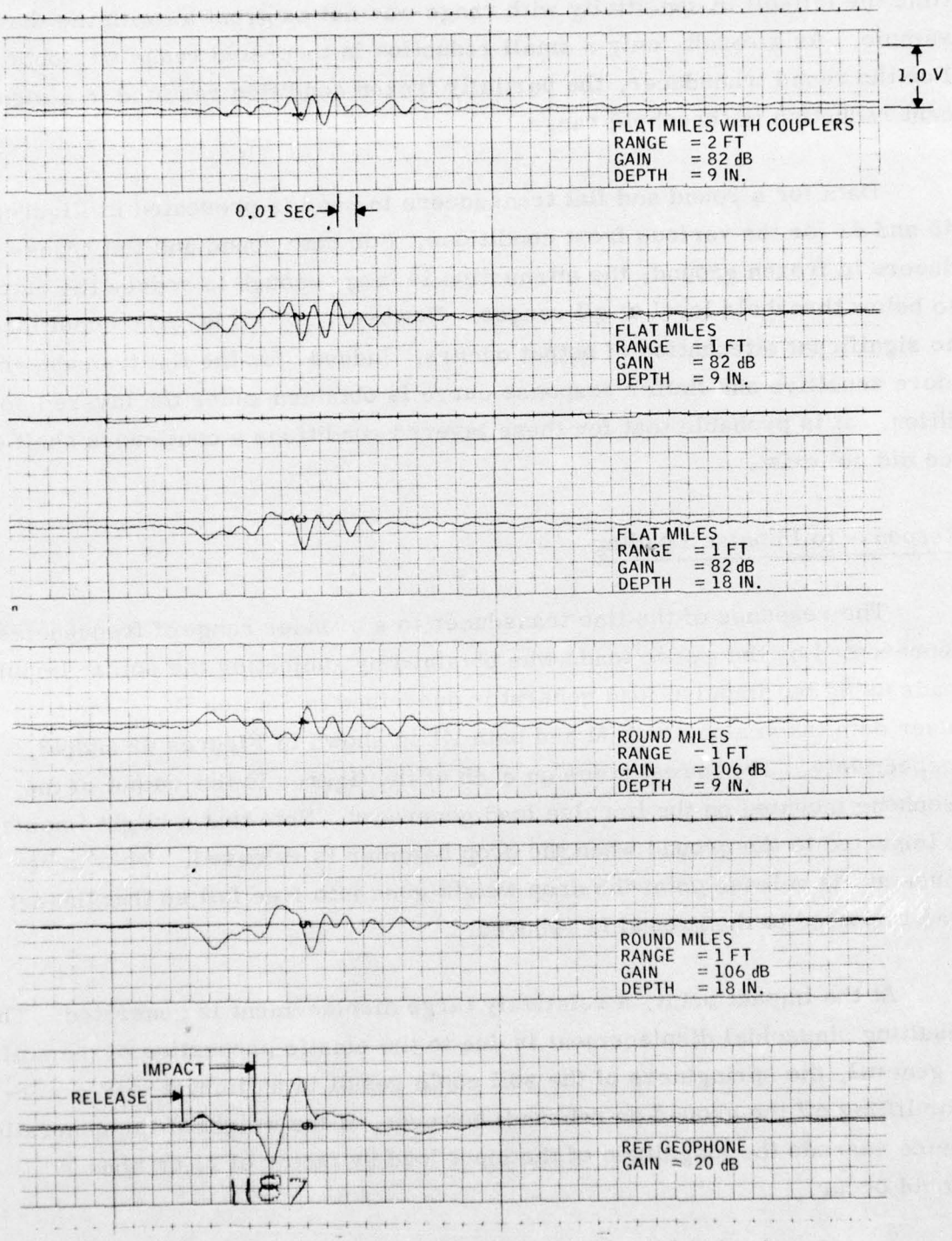


Figure 42. Response of lines to impulse load; path M, sand

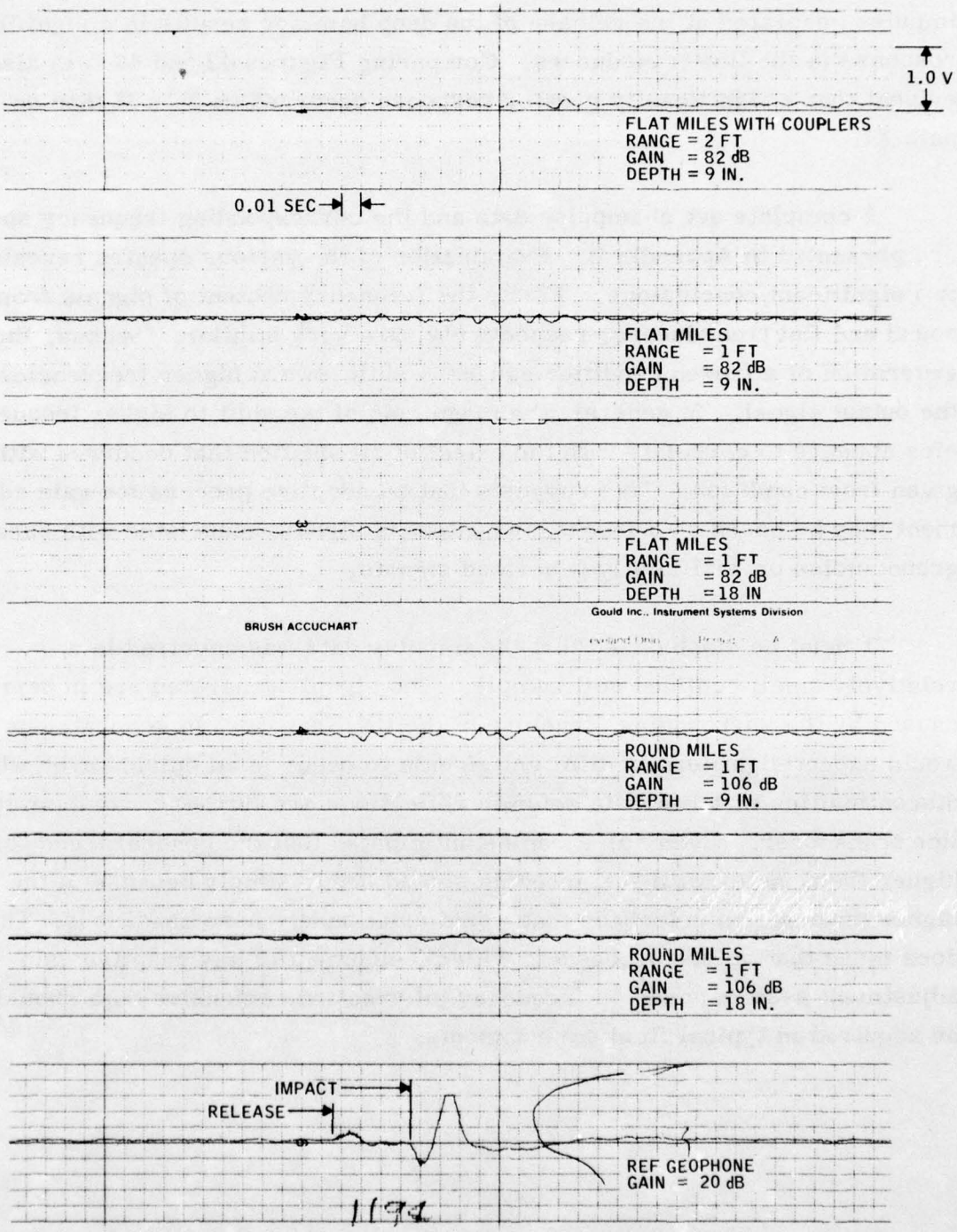


Figure 43. Response of lines to impulse load; path X1, sand

For both the flat and the round lines, it is seen that the response is primarily that of a ringing frequency of the order of 100 Hz. Even the slight impulse generated at the release of the drop hammer results in a significant response in the line transducers. Comparing Figures 42 and 43 it is also evident that a significantly greater response occurred on path M than on path X1.

A complete set of impulse data and the corresponding frequency spectra are presented in Appendix B. Examination of the various spectra reveals two significant conclusions. First, the frequency content of signals from round and flat transducers, respectively, are very similar. Second, the generation of a frozen condition causes a shift toward higher frequencies in the output signal. In general, the magnitude of the shift to higher frequencies appears to correlate with the extent of attenuation that occurred with a given frost condition. This suggests that an adaptive process for gain adjustment may be based on a frequency content in signals associated with background noise or artificially generated signals.

It must be emphasized that the impulse data was acquired in a relatively small confined soil sample. The signals generated are in part caused by the surrounding structure of the test facility. In general, one would expect significantly different signals to occur in an outside area where discontinuities that result in seismic reflections are further away from the line transducer. Even so, it can be anticipated that the general trend toward higher frequencies with soil freezing should occur simply because of the higher propagation velocities that would exist under those conditions. This does mean that before proceeding with development of any adaptive gain adjustment system based on frequency information, extensive data should be acquired in typical field environments.

# SECTION VI
# THEORETICAL CORRELATION

The theoretical model described in Section III has been exercised to obtain comparisons with experimental data presented on Section V. In general, good correlation is obtained with experimental data. Where experiment and theory significantly differ, certain basic assumptions can be shown to limit the theory.

## Effect of Depth

Figure 44 illustrates a comparison of experimental data and theoretical curves for a flat transducer at depths of 9 and 18 inches. Similar curves for the round transducer would be identical in shape but with a lower sensitivity. For sand, the correlation as shown is remarkably good. Good correlation should be expected in this case in that the elastic properties of sand would probably most closely match those assumed in the theoretical model. A review of experimental data for clay and loam in the previous section will readily show that the agreement with theory would not be as good as shown in Figure 44. Some disagreement is to be expected simply because of the plastic properties inherent in both clay and the loam. Further investigation of depth effects was carried out theoretically by computing output at depths down to 45 inches. As shown in Figure 45, even at 45 inches adequate sensitivity is obtained.

## Effect of Frost

Flat transducer output for the case of thawed, frozen, and partially frozen ground was computed based on the theory in Section III. In computing the response for frozen ground, no direct measurement of soil shear modulus was available. Therefore, it was necessary to select a soil shear modulus

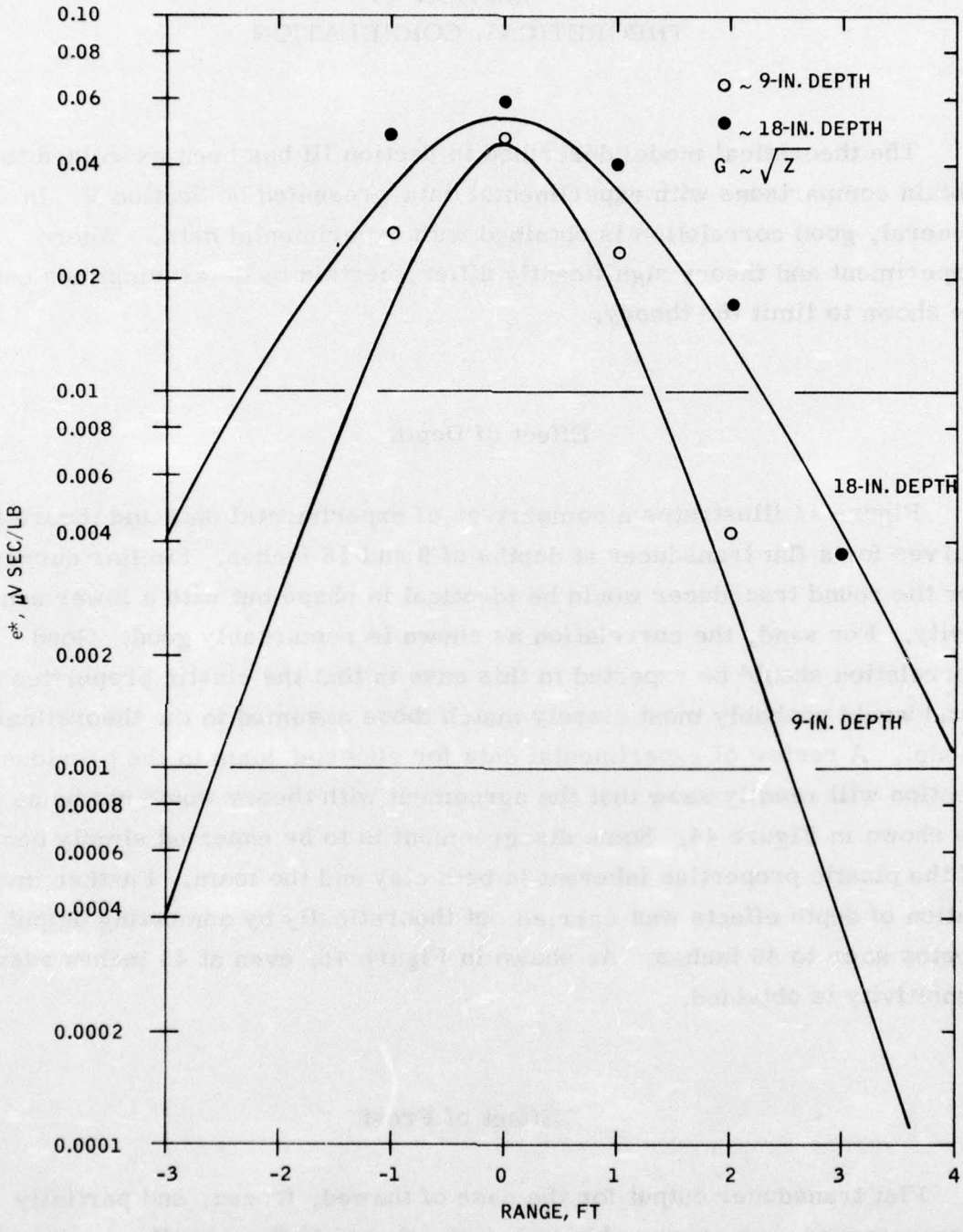


Figure 44. Comparison of theory and experiment for 9- and 18-inch depths in thawed sand

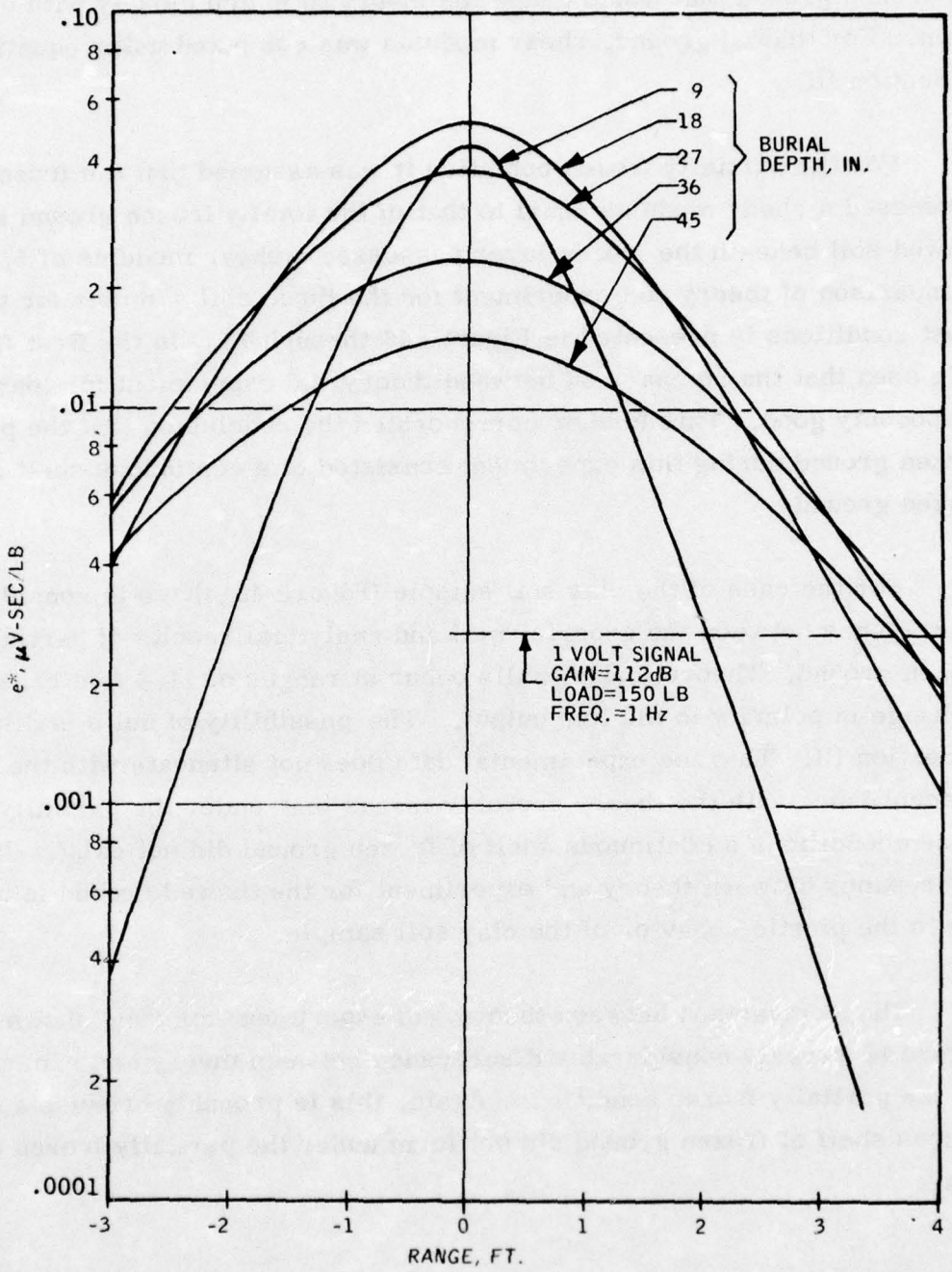


Figure 45. Theoretical extension of burial depth effect

for frozen ground that would cause the theory to match closely with experiment. For thawed ground, shear modulus was computed using equation (11) in Section III.

For the partially frozen condition it was assumed that the frozen layer possessed a shear modulus equal to that of the totally frozen ground and the thawed soil beneath the frozen layer possessed a shear modulus of 5,000 psi. Comparison of theory and experiment for the three soil samples for various frost conditions is presented in Figures 46 through 48. In the first figure, it is seen that the comparison between theory and experiment for loam is reasonably good. This further corroborates the conclusion that the partially frozen ground during this experiment consisted of a continuous shelf of frozen ground.

For the case of the clay soil sample (Figure 46), there is considerable discrepancy between the experimental and analytical results of partially frozen ground. Theoretically, nulls occur at ranges of ±1.6 feet because of a change in polarity in the line output. The possibility of nulls is discussed in Section III. That the experimental data does not attenuate with the range in accordance with the theory probably means that under the partially frozen conditions a continuous shelf of frozen ground did not exist. The discrepancy between theory and experiment for the thawed ground is probably due to the plastic behavior of the clay soil sample.

The comparison between theory and experiment for sand shown in Figure 48 reveals considerable discrepancy between theory and experiment for the partially frozen conditions. Again, this is probably because a continuous shelf of frozen ground did not form under the partially frozen condition.

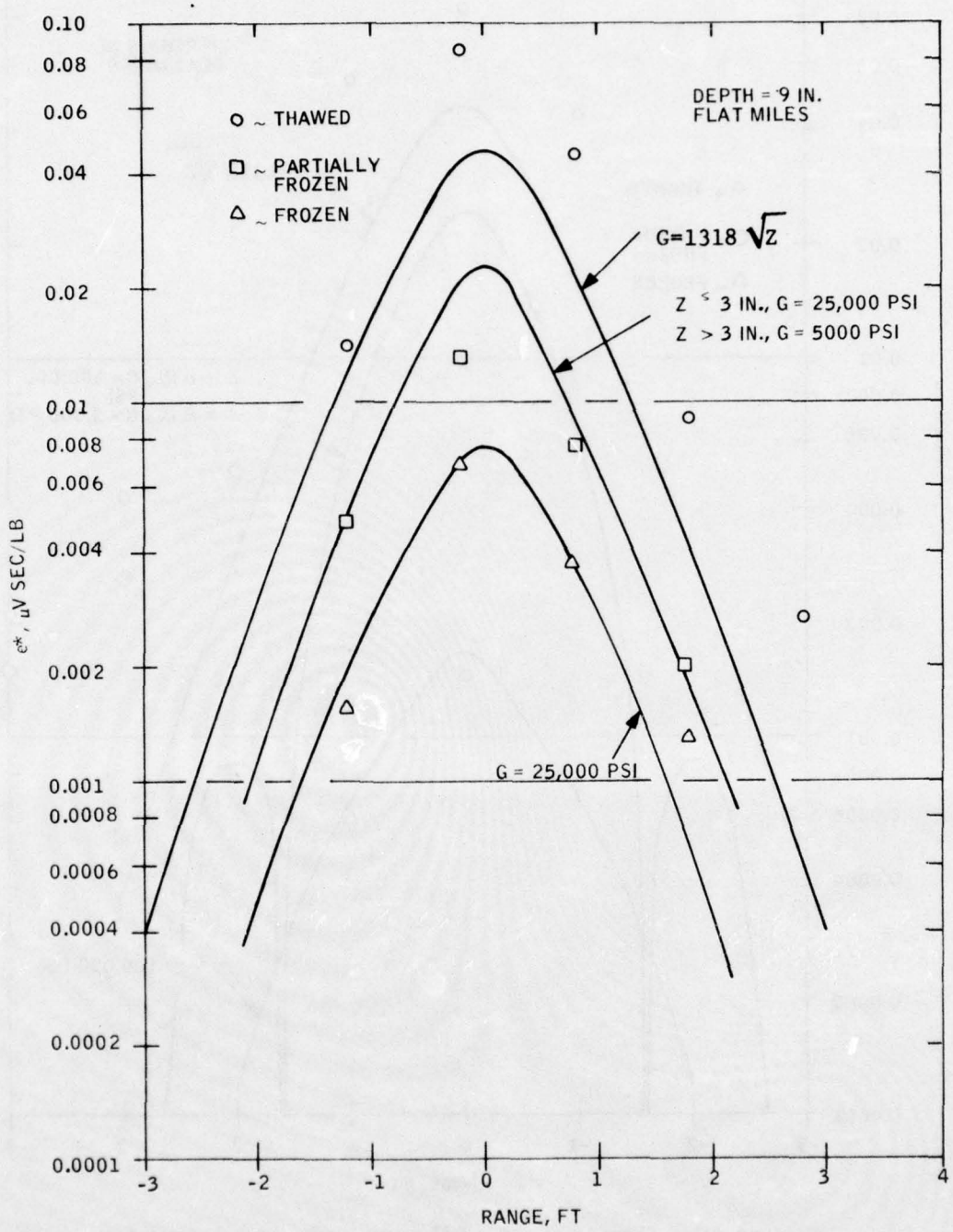


Figure 46. Comparison of theory and experiment for various frost conditions in loam

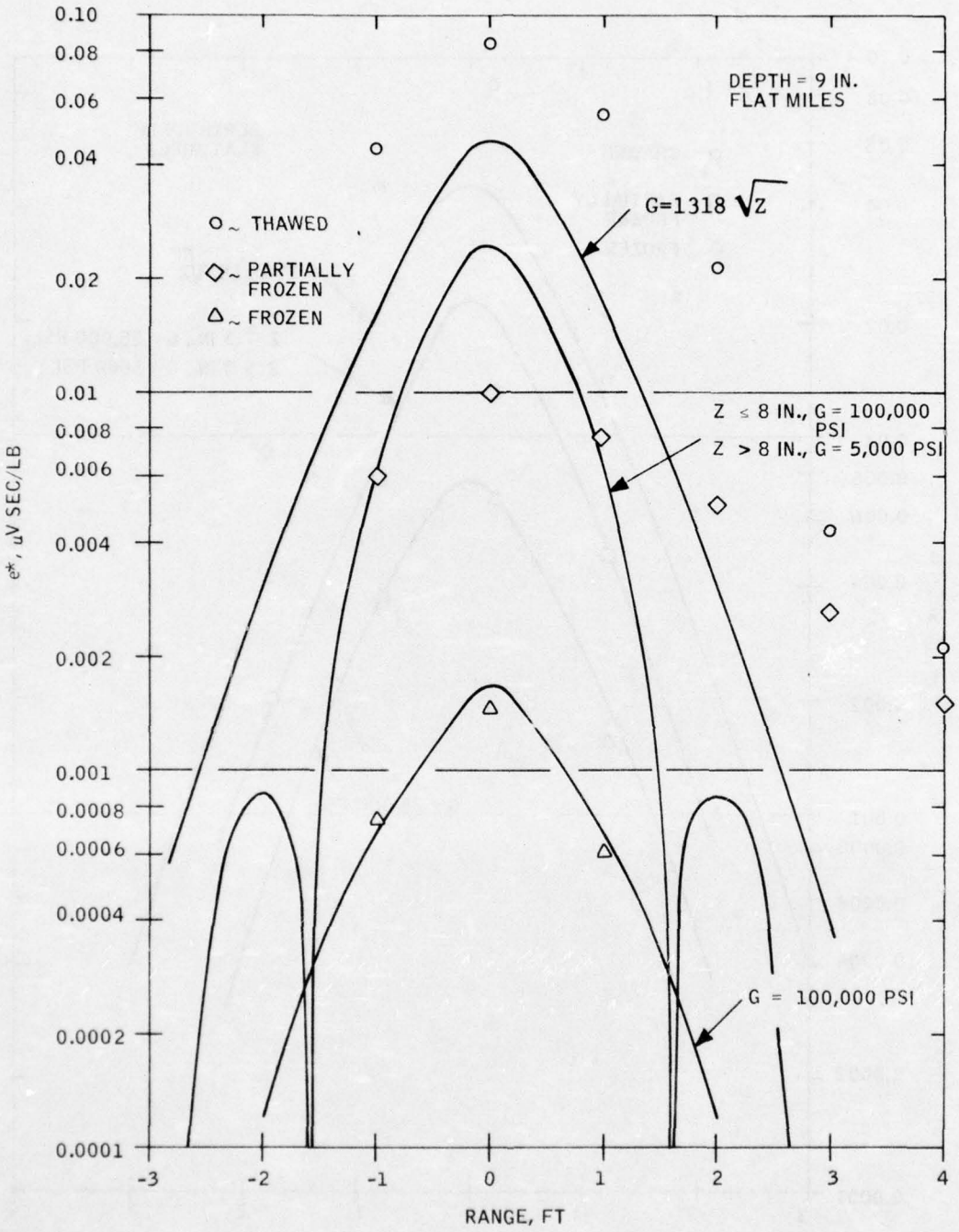


Figure 47. Comparison of theory and experiment for various frost conditions in clay

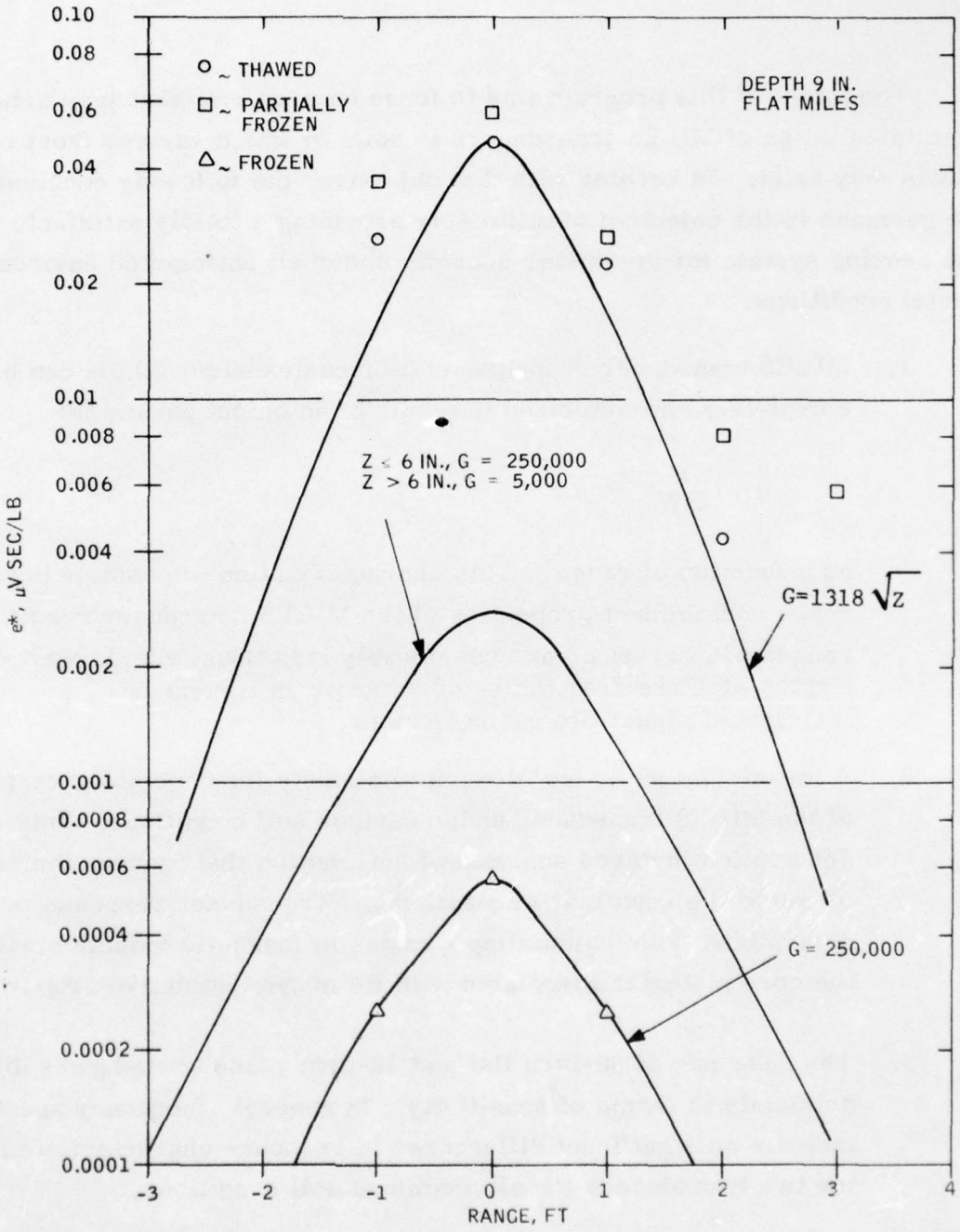


Figure 48. Comparison of theory and experiment for various frost conditions in sand

AD-A031 741 HONEYWELL INC HOPKINS MINN GOVERNMENT AND AERONAUTIC--ETC F/G 17/10
ENERGY PROPAGATION AND COUPLING STUDIES FOR LINE TRANSDUCERS.(U)
AUG 76 J B STARR F30602-75-C-0186

UNCLASSIFIED RADC-TR-76-239 NL

2 OF 2
AD
A031741

END

DATE
FILMED
12-76

## SECTION VII
## CONCLUSIONS

The intent of this program was to focus on problems that may arise from installation of MILES transducers in soils in which various frost conditions may exist. In keeping with that objective, the following conclusions are germane to the objective of ultimately providing a totally satisfactory line sensing system for perimeter security under all anticipated environmental conditions.

1. MILES transducer response at frequencies under 20 Hz can be completely characterized in terms of an output parameter

$$e^* = \frac{e}{\omega W}$$

as a function of range. This characterization is possible because range containment properties of the MILES transducer result in ranges of interest being considerably less than seismic wavelengths at those frequencies of interest in current and anticipated signal processing schemes.

2. A meaningful analytical description exists for describing response of the MILES transducer under various soil conditions. This description involves analysis of soil motion that ignores inertial terms in the equations of elasticity. Transducer response is determined from calculating changes in magnetic induction within the core material associated with its magnetostrictive properties.

3. The response of 80-turn flat and 38-turn round transducers differ primarily in terms of sensitivity. In general, frequency spectra indicate no significant differences in response characteristic for the two transducers for all examined soil conditions.

4. The most severe effect of frost on transducer response occurs in totally frozen ground. Layered conditions may produce a

significant effect when the layer corresponds to a solid shelf of frozen ground. For most layered conditions produced during the experimental program, significant reductions in transducer sensitivity did not occur. In general, there is a high probability of obtaining satisfactory performance in frozen ground if the transducer is buried at a level below that of the frost penetration.

5. Superior performance is obtained with line transducers buried at 18 inches rather than at 9 inches. For a given range of detection, a lower sensitivity directly above the line results. This will lead to reduction of false alarms due to wind and small animals.

6. Where significant attenuation occurs under various frost conditions, there is a tendency of transducer response to impulse loads to shift to higher frequencies. This suggests that the development of an adaptive gain adjustment system based on frequency domain information may be possible.

## SECTION VIII
## RECOMMENDATIONS

Based on the results of this program, several courses of action may be followed in order to arrive at a solution for minimizing the effect of ground frost on performance of MILES transducers. Certain actions may be taken immediately that are relatively simple and will greatly increase the probability of obtaining satisfactory operation. Other possible courses of action will require further analysis and experiment to provide a high degree of confidence in the particular approach.

The following are courses of action that may be undertaken immediately to improve performance in the presence of ground frost.

1. Lines should be buried at 18 inches. In many locales this will ensure that frost penetration does not exceed the burial depth of the line. In addition, burial at 18 inches provides better performance in thawed ground than does a 9-inch burial depth.

2. Where possible, a layer of insulating material may be placed at the ground surface in order to limit frost penetration. This layer may be simply a few inches of straw.

3. Where possible, the soil composition within a few feet of the line should be sand. This will ensure that the moisture content is kept relatively low so that formation of a solid shelf of frozen ground will be highly improbable.

Beyond these immediate actions, further investigation should be undertaken which should lead to a more permanent and general solution for achieving satisfactory performance in the presence of ground frost.

1. Investigation of burial depths beyond 18 inches should be undertaken. Analytical results generated using the theoretical model described in this report suggest that burial depths up to 45 inches will continue to provide excellent line transducer performance. Experimental validation of this conclusion is needed.

2. Feasibility of an adaptive gain adjustment system based on frequency domain information should be examined. This investigation should be based primarily on experiments conducted in a typical field environment for various frost conditions.

3. A similar program for adaptive gain adjustment, based on soil temperature measurements, should be examined. Such a program would concentrate on developing criteria for detection conditions in which frozen ground has penetrated beyond the depth of the line transducer.

4. Extensive outdoor testing should be undertaken to examine the effects of partially frozen and frozen layered conditions in a more typical field environment. This investigation will address the questions regarding the probability of formation of continuous shelves of frozen ground above line transducers.

## REFERENCES


1. Timoshenko, S. and J.N. Goodier, "Theory of Elasticity", McGraw-Hill Book Company, Inc. 1951.

2. Richart, F.E. Jr., J.R. Hall, Jr. and R.D. Woods, "Vibrations of Soils and Foundations," Prentice-Hall, Inc., 1970.

3. Starr, J.B., "Stress Sensitive Line Transducers," Proceedings of the Second Symposium on the Design, Development and Testing of Unattended Ground Sensors, U.S. Army Engineer Waterways Experiment Station, 11-12 May 1976 (to be published).

## LIST OF SYMBOLS

| | |
|---|---|
| $A_C$ | Cross-sectional area of transducer core |
| $A_L$ | Total cross-sectional area of line |
| $C_S$ | Coupling coefficient between soil motion and transducer loading |
| e | Transducer output signal ($\mu$V) |
| e* | Transducer output parameter, $\frac{e}{\omega W}$ ($\mu$V sec/lb.) |
| E | Young's Modulus for line material |
| $F_L$ | Tension/compression load within the line |
| G | Soil shear modulus |
| r | Radial coordinate |
| $r_o$ | Radius of loading disk |
| u | Radial displacement of soil |
| $u_L$ | Displacement of line due to stretch |
| $u_S$ | Displacement of soil along line |
| $\Delta u$ | Difference between $u_S$ and $u_L$ |
| w | Vertical soil displacement |
| W | Vertical load applied at soil surface |
| x | Coordinate measured along line |
| z | Vertical coordinate |
| $\epsilon$ | Soil void ratio |
| $\lambda$ | Lame' constant |
| $\Lambda$ | Magnetic induction change per unit stress |
| $\nu$ | Poisson's ratio |
| $\overline{\sigma_o}$ | Normal stress due to soil overpressure |
| $\phi$ | Magnetic flux in core material |

# APPENDIX A

## SOIL TEST REPORT

An Expansion of Soil Engineering Services, Inc.

BRAUN ENGINEERING TESTING

MINNEAPOLIS/ST. PAUL 6800 S. County Rd. 18, P.O. Box 35106, Mpls., Mn. 55435 / 612-941-5600
NORTHERN MINNESOTA 3219 E. 10th Avenue, Hibbing, Mn. 55746 / 218-263-8868

J. S. BRAUN P. E., President
P. H. ANDERSON, Vice Pres. Operations
C. G. KRUSE P. E., Vice Pres. Engineering
D. R. MONAHAN P. E., Vice Pres. Testing

March 19, 1976

Honeywell Inc.
600 Second Street N.E.
Hopkins, Minnesota 55343

Attention: Mr. James Starr
M.S. H2150

RE: 76-48 LABORATORY TESTS OF SOIL
P. O. #412192-A1

Dear Mr. Starr:

Enclosed are the results of Laboratory Tests you requested on various soil samples furnished by your office.

If we may be of further assistance, kindly contact us at your convenience.

Very truly yours,

BRAUN ENGINEERING TESTING, INC.

Donald R. Monahan, P.E.
Vice President - Testing

DRM/gm

Enclosures

# GRAIN SIZE ACCUMULATION CURVE

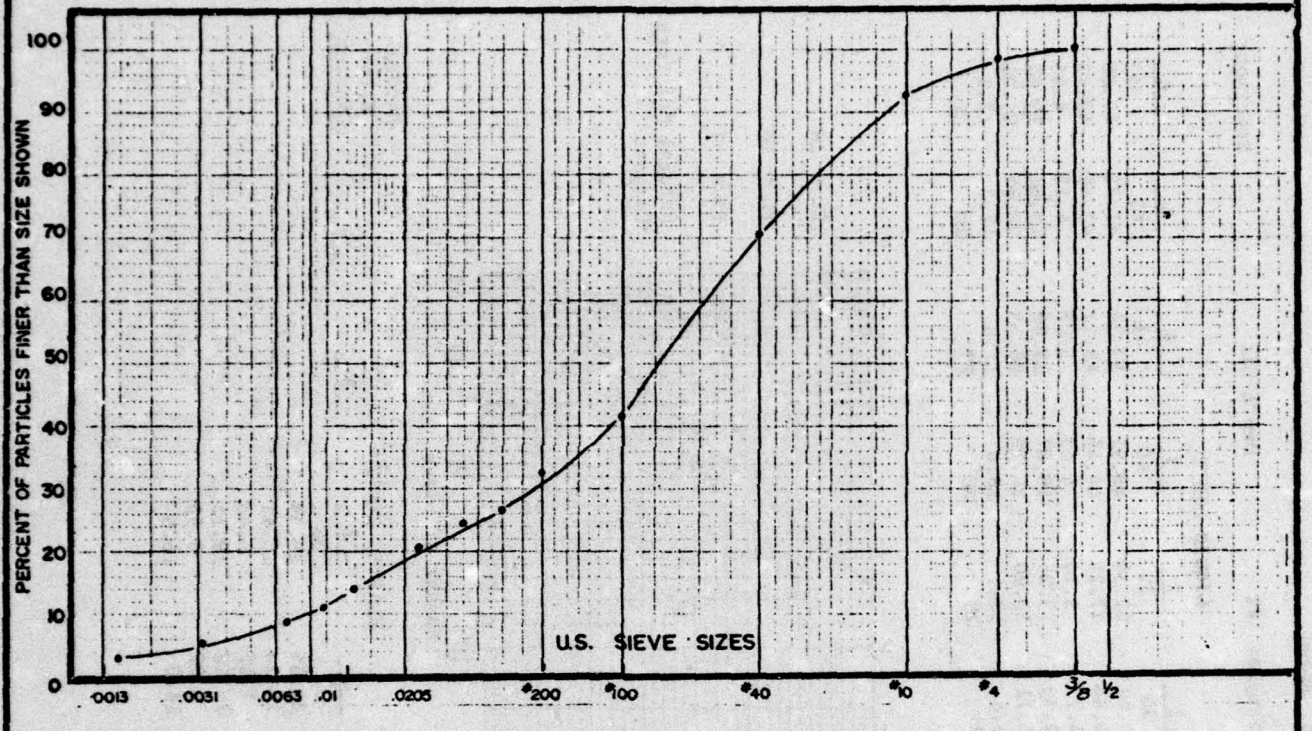


**PROJECT:** 76-48
for Honeywell Inc.
P. O. #412192-A1

**NOTES:** Sample #1
Specific Gravity = 2.65

| | | | |
|---|---|---|---|
| GRAVEL | COARSE | | 2 |
| | MEDIUM | | |
| | FINE | 2 | |
| SAND | COARSE | 6 | 66 |
| | MEDIUM | 22 | |
| | FINE | 38 | |
| SILT AND CLAY | | 32 | |

**CLASSIFICATION:**
SM, Silty Sand, Fine to Medium-Grained, Brown
(ASTM: D2487)

## LIQUID & PLASTIC LIMIT TESTS

Project: 76-48 Honeywell, Inc. Date: 3/17/76

Soil: SM, Silty Sand, Brown

Boring: Sample: #1 Depth/El: Specimen:

### LIQUID LIMIT

| Run | 1 | 2 | 3 | 4 | 5 | 6 |
|---|---|---|---|---|---|---|
| Tare No. | 36 | 39 | 40 | 41 | 42 | 43 |
| Tare + Wet Soil, g. | 49.41 | 52.39 | 48.91 | 53.34 | 47.71 | 47.88 |
| Tare + Dry Soil, g. | 44.64 | 47.25 | 44.46 | 48.27 | 43.56 | 43.73 |
| Water, g. | 4.77 | 5.14 | 4.45 | 5.07 | 4.15 | 4.15 |
| Tare, g. | 19.33 | 19.35 | 19.67 | 19.82 | 19.61 | 19.52 |
| Dry Soil, g. | 25.71 | 27.90 | 24.79 | 28.45 | 23.95 | 24.21 |
| Moist. Cont., % | 18.8 | 18.4 | 18.0 | 17.8 | 17.3 | 17.1 |
| No. of blows | 17 | 23 | 20 | 23 | 26 | 31 |

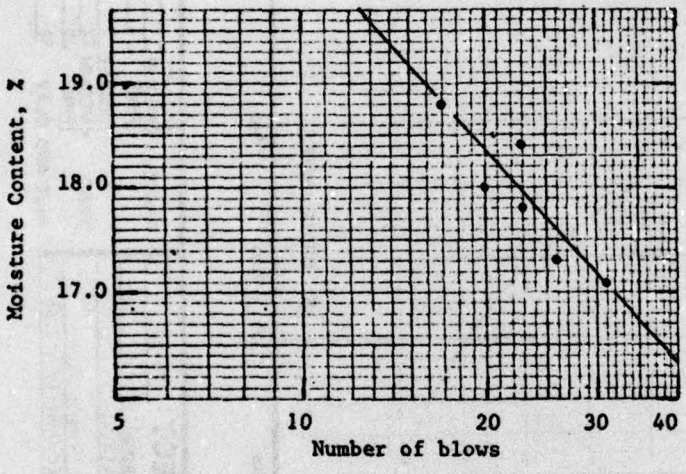


LL = 18

PL = 16

PI = 2

Natural Moisture Content

### PLASTIC LIMIT

| Run | 1 | 2 | 3 | 4 | Natural Water Content |
|---|---|---|---|---|---|
| Tare No. | 37 | 38 | | | |
| Tare + Wet Soil, g. | 27.36 | 29.59 | | | |
| Tare + Dry Soil, g. | 26.24 | 28.11 | | | |
| Water, g. | 1.12 | 1.48 | | | |
| Tare, g. | 19.22 | 19.15 | | | |
| Dry Soil, g. | 7.02 | 8.96 | | | |
| Moist. Cont., % | 16.0 | 16.5 | | | |

Remarks:

# GRAIN SIZE ACCUMULATION CURVE

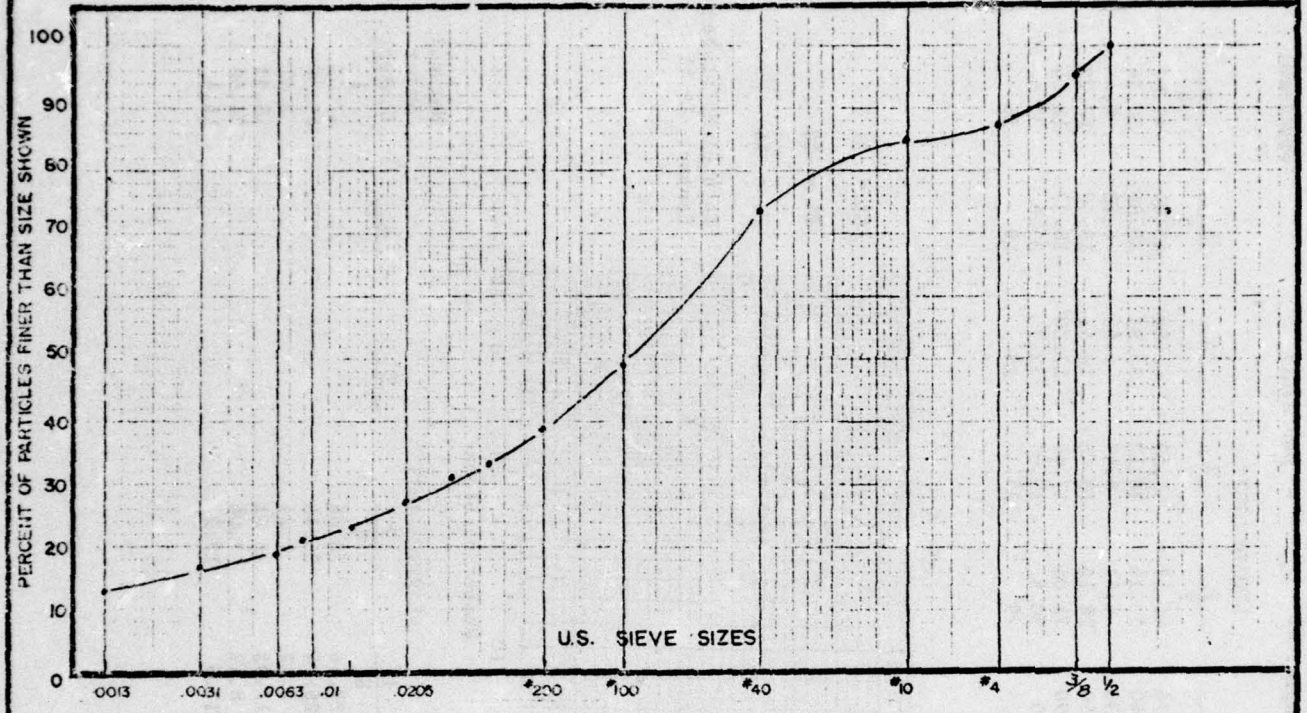


**PROJECT:** 76--8
for Honeywell Inc.
P.O. #412192-A1

**NOTES:** Sample #2
Specific Gravity = 2.69

| | | | |
|---|---|---|---|
| GRAVEL | COARSE | | 12 |
| | MEDIUM | 5 | |
| | FINE | 7 | |
| SAND | COARSE | 3 | 49 |
| | MEDIUM | 12 | |
| | FINE | 34 | |
| SILT AND CLAY | | 39 | |

**CLASSIFICATION:**
SC, Clayey Sand, Brown
(ASTM: D2487)

## LIQUID & PLASTIC LIMIT TESTS

Project: 76-48 Honeywell, Inc. Date: 3/17/76

Soil: SC, Clayey Sand, Brown

Boring: Sample: #2 Depth/El: Specimen:

### LIQUID LIMIT

| Run | 1 | 2 | 3 | 4 | 5 | 6 |
|---|---|---|---|---|---|---|
| Tare No. | 1 | 2 | 3 | 4 | 5 | 6 |
| Tare + Wet Soil, g. | 46.76 | 45.57 | 41.59 | 41.56 | 43.04 | 42.82 |
| Tare + Dry Soil, g. | 40.40 | 39.16 | 36.12 | 35.91 | 36.86 | 36.36 |
| Water, g. | 6.36 | 6.41 | 5.47 | 5.65 | 6.18 | 6.46 |
| Tare, g. | 18.50 | 18.15 | 18.45 | 18.61 | 18.49 | 18.22 |
| Dry Soil, g. | 21.90 | 21.01 | 17.67 | 17.30 | 18.37 | 18.14 |
| Moist. Cont., % | 29.0 | 30.5 | 31.0 | 32.7 | 33.6 | 35.6 |
| No. of blows | 33 | 29 | 25 | 23 | 19 | 16 |

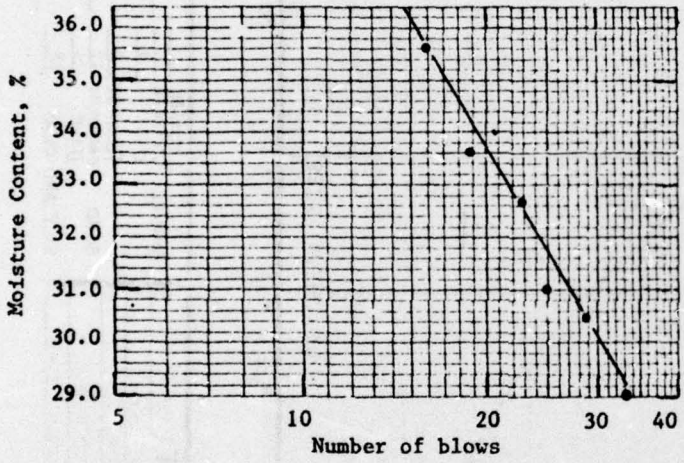


LL = 31

PL = 17

PI = 14

Natural Moisture Content 15.4%

### PLASTIC LIMIT

| Run | 1 | 2 | 3 | 4 | Natural Water Content |
|---|---|---|---|---|---|
| Tare No. | 8 | 9 | | | 1 |
| Tare + Wet Soil, g. | 27.46 | 26.66 | | | 47.02 |
| Tare + Dry Soil, g. | 26.04 | 25.45 | | | 43.21 |
| Water, g. | 1.42 | 1.21 | | | 3.81 |
| Tare, g. | 17.92 | 18.41 | | | 18.53 |
| Dry Soil, g. | 8.12 | 7.04 | | | 24.68 |
| Moist. Cont., % | 17.5 | 17.2 | | | 15.4 |

Remarks:

# GRAIN SIZE ACCUMULATION CURVE

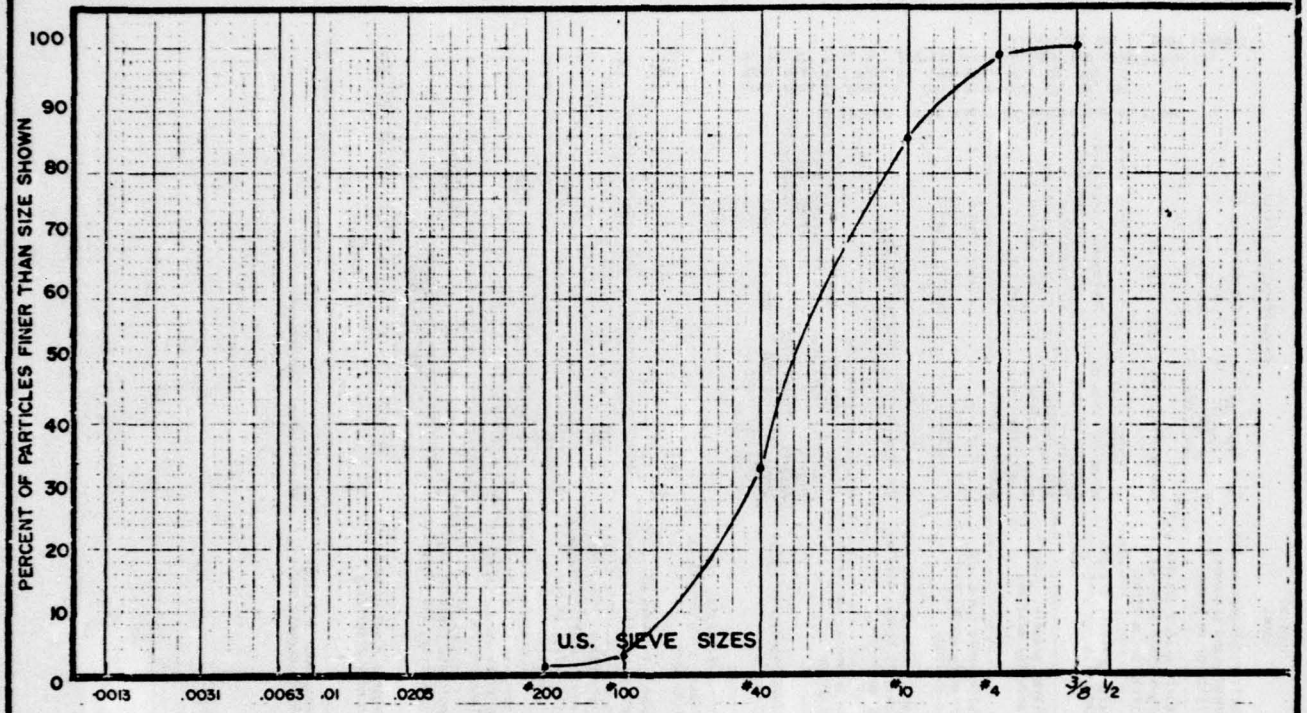


**PROJECT:** 76-48
for Honeywell Inc.
P.O. #412192-A1

**NOTES:** Sample #3
Specific Gravity = 2.69

| | | | |
|---|---|---|---|
| GRAVEL | COARSE | | 2 |
| | MEDIUM | | |
| | FINE | 2 | |
| SAND | COARSE | 12 | 97 |
| | MEDIUM | 53 | |
| | FINE | 32 | |
| SILT AND CLAY | | 1 | |

**CLASSIFICATION:**
SP, Sand, Medium to Fine-Grained, Brown
(ASTM: D2487)

# UNIFIED SYSTEM
## CLASSIFICATION OF SOILS FOR ENGINEERING PURPOSES
## ASTM DESIGNATION D-2487

| Major Divisions | | | Group Symbols | Typical Names | Classification Criteria | |
|---|---|---|---|---|---|---|
| Coarse-Grained Soils More than 50% retained on No. 200 sieve | Gravels 50% or more of coarse fraction retained on No. 4 sieve | Clean Gravels | GW | Well-graded gravels and gravel-sand mixtures, little or no fines | $C_u = D_{60}/D_{10}$ | Greater than 4 |
| | | | | | $C_c = \frac{(D_{30})^2}{D_{10} \times D_{60}}$ | Between 1 and 3 |
| | | | GP | Poorly graded gravels and gravel-sand mixtures, little or no fines | Not meeting both criteria for GW | |
| | | Gravels with Fines | GM | Silty gravels, gravel-sand-silt mixtures | Atterberg limits plot below "A" line or plasticity index less than 4 | Atterberg limits plotting in hatched area are borderline classifications requiring use of dual symbols |
| | | | GC | Clayey gravels, gravel-sand-clay mixtures | Atterberg limits plot above "A" line and plasticity index greater than 7 | |
| | Sands More than 50% of coarse fraction passes No. 4 sieve | Clean Sands | SW | Well-graded sands and gravelly sands, little or no fines | $C_u = D_{60}/D_{10}$ | Greater than 6 |
| | | | | | $C_c = \frac{(D_{30})^2}{D_{10} \times D_{60}}$ | Between 1 and 3 |
| | | | SP | Poorly graded sands and gravelly sands, little or no fines | Not meeting both criteria for SW | |
| | | Sands with Fines | SM | Silty sands, sand-silt mixtures | Atterberg limits plot below "A" line or plasticity index less than 4 | Atterberg limits plotting in hatched area are borderline classifications requiring use of symbols |
| | | | SC | Clayey sands, sand-clay mixtures | Atterberg limits plot above "A" line and plasticity index greater than 7 | |
| Fine-Grained Soils 50% or more passes No. 200 sieve | Silts and Clays Liquid limit 50% or less | | ML | Inorganic silts, rock flour, silty or clayey fine sand | | |
| | | | CL | Inorganic clays of low to medium plasticity, gravelly clays, sandy clays, silty clays, lean clays | | |
| | | | OL | Organic silts and organic silty clays of low plasticity | | |
| | Silts and Clays Liquid limit greater than 50% | | MH | Inorganic silts, micaceous or diatomaceous silts, elastic silts | | |
| | | | CH | Inorganic clays of high plasticity, fat clays | | |
| | | | OH | Organic clays of medium to high plasticity | | |
| Highly organic soils | | | Pt | Peat, muck and other highly organic soils | Visual-manual identification | |

Classification on basis of percentage of fines
Less than 5% Pass No. 200 sieve--GW, GP, SW, SP
More than 12% Pass No. 200 sieve--GM, GC, SM, SC
5% to 12% Pass No. 200 sieve----Borderline classification requiring use of dual symbols

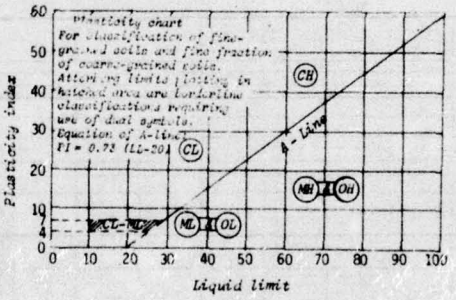

# APPENDIX B

# TIME AND FREQUENCY DOMAIN RESPONSE OF LINE TRANSDUCERS TO IMPULSE LOADS

Data presented in Figures B-1 through B-48 represents line transducer response to impulse loads. These data were acquired with the impulse generator positioned on path M with $R_S = 0$. According Figure 12, this arrangement places the load generator at a range of 1 foot from both round and flat transducers. The data presented here are for round and flat transducers buried at a 9-inch depth.

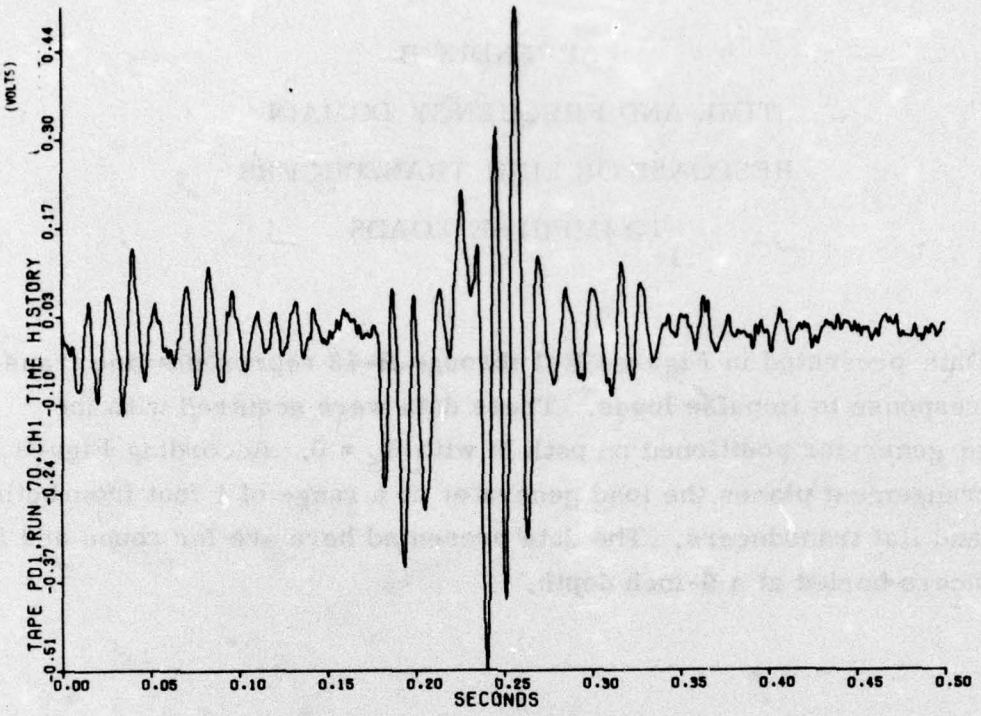


Figure B-1. Time history of flat MILES response - thawed loam

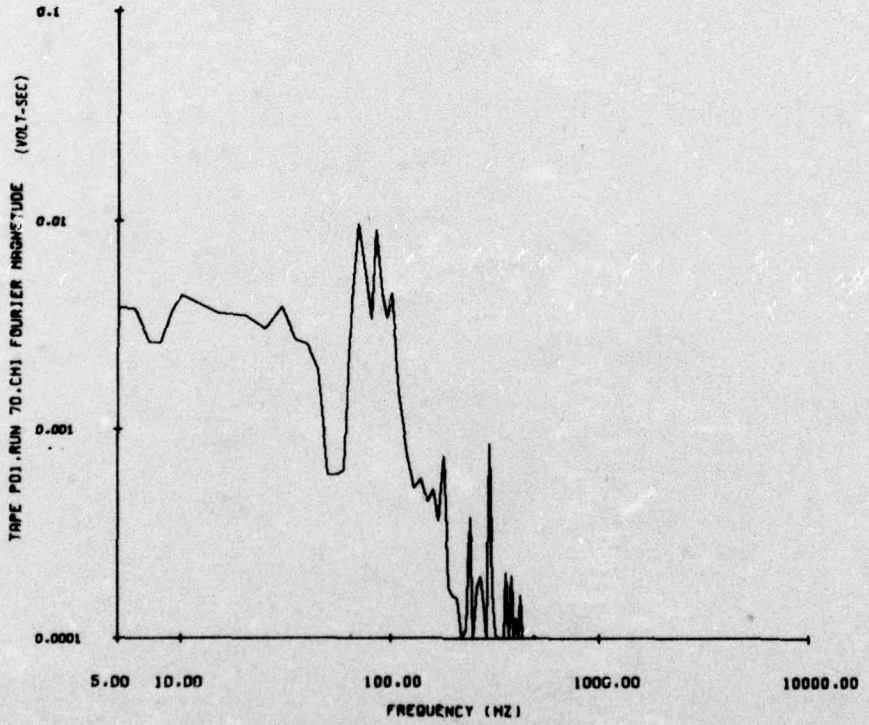


Figure B-2. Frequency spectrum of flat MILES response - thawed loam

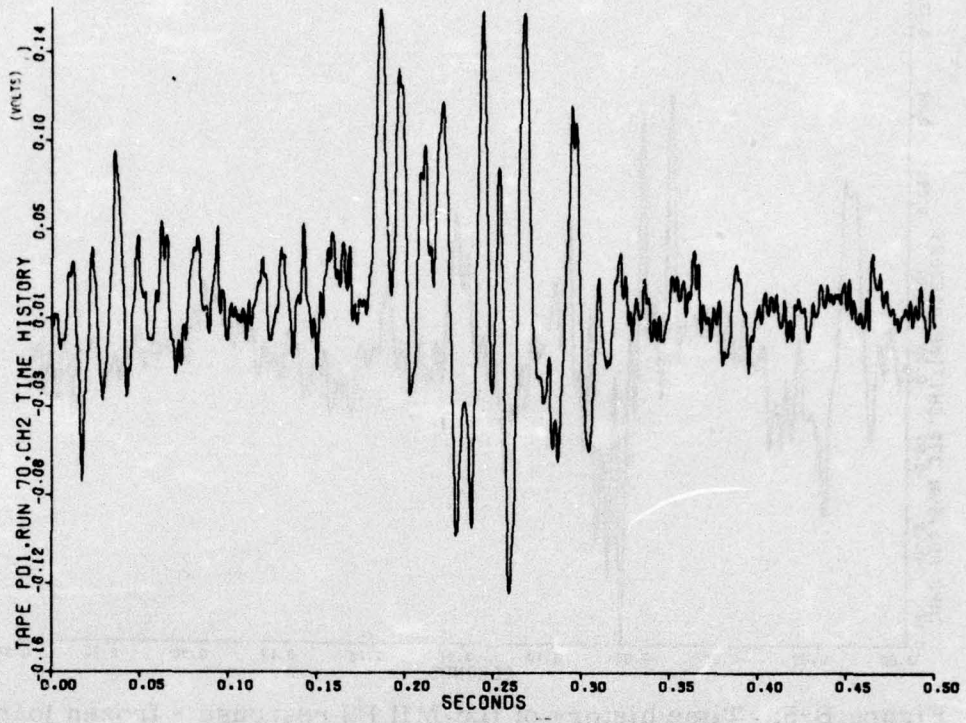


Figure B-3. Time history of round MILES response - thawed loam

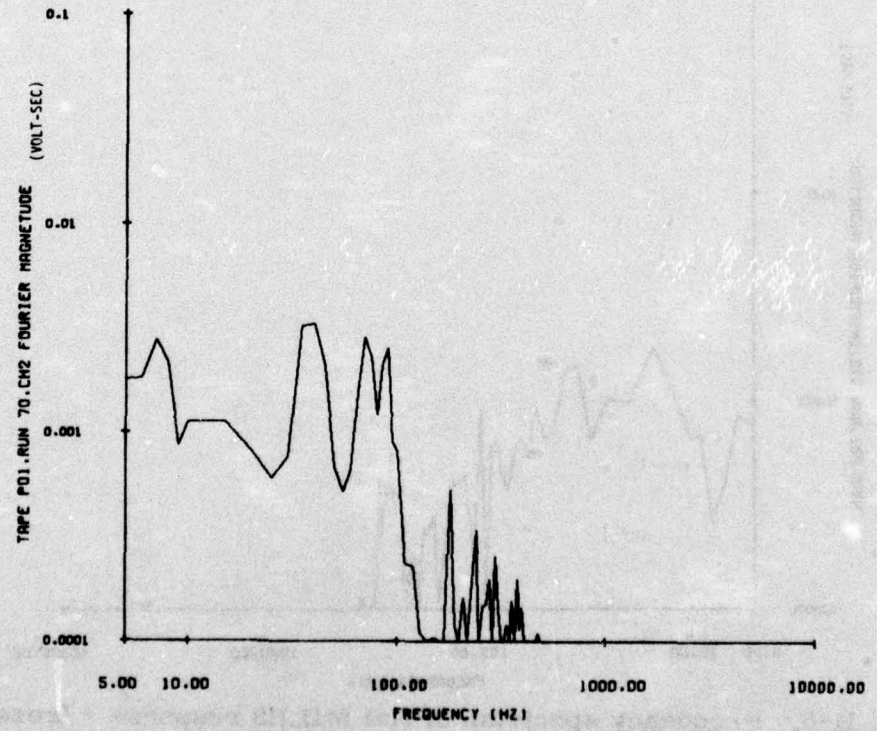


Figure B-4. Frequency spectrum of round MILES response - thawed loam

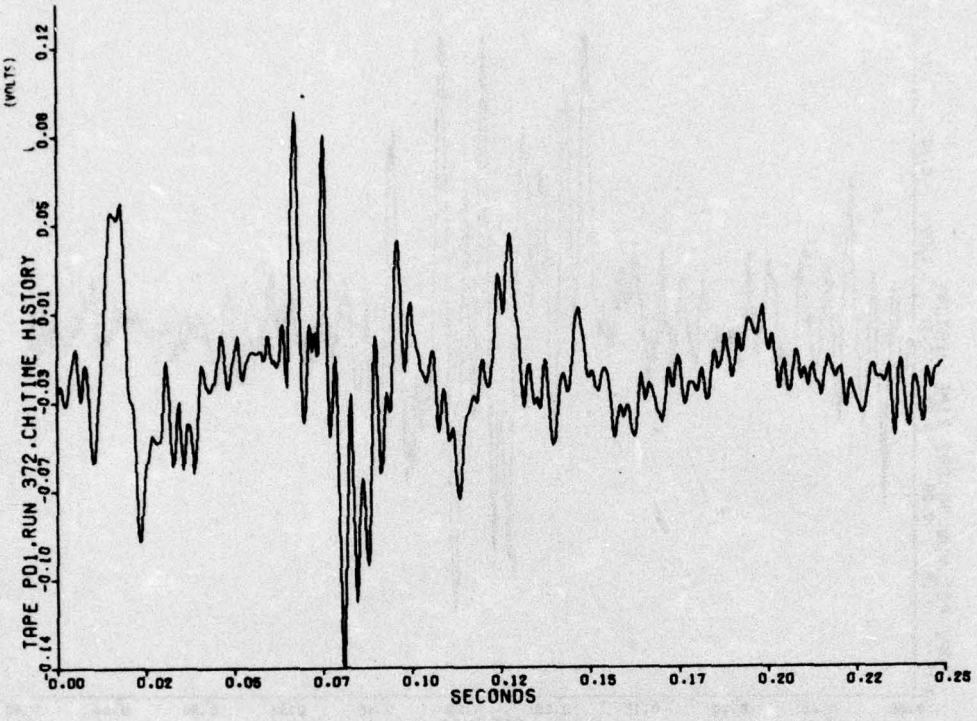


Figure B-5. Time history of flat MILES response - frozen loam

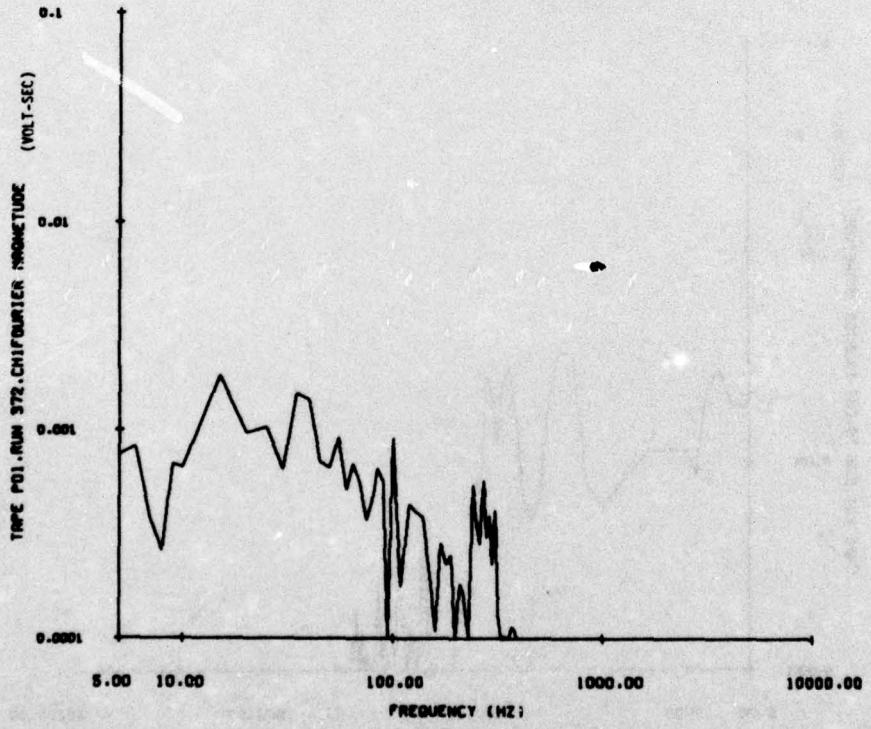


Figure B-6. Frequency spectrum of flat MILES response - frozen loam

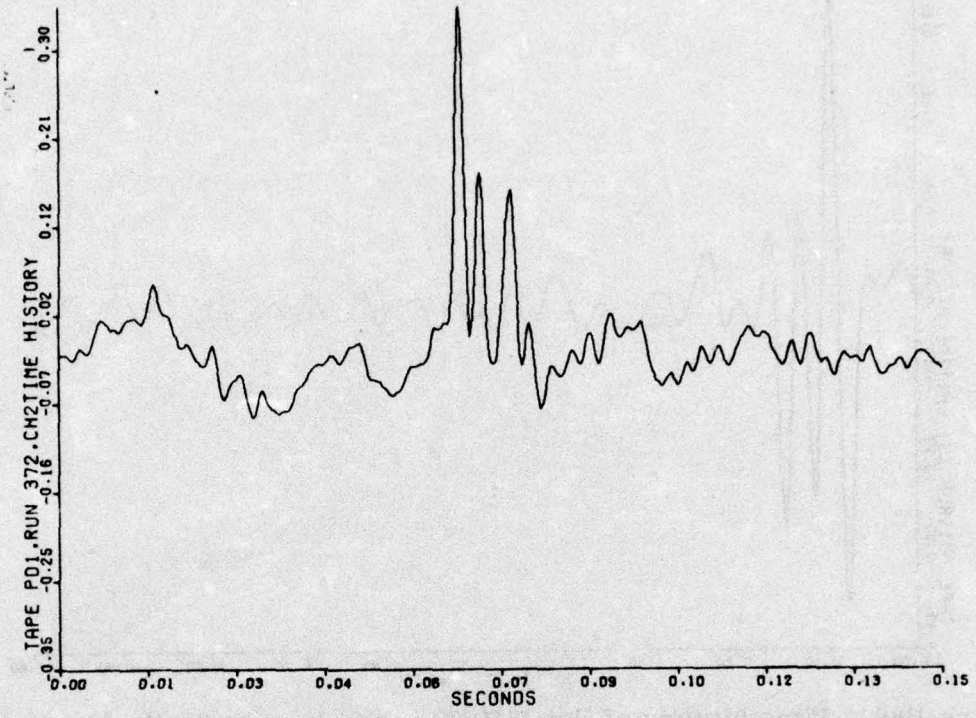


Figure B-7. Time history of round MILES response - frozen loam

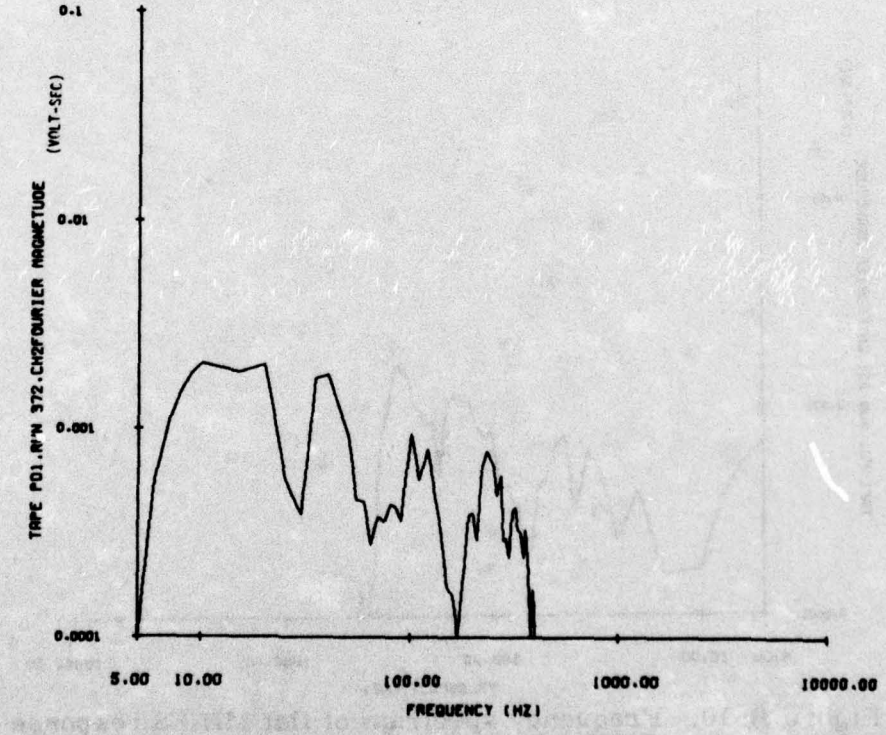


Figure B-8. Frequency spectrum of round MILES response - frozen loam

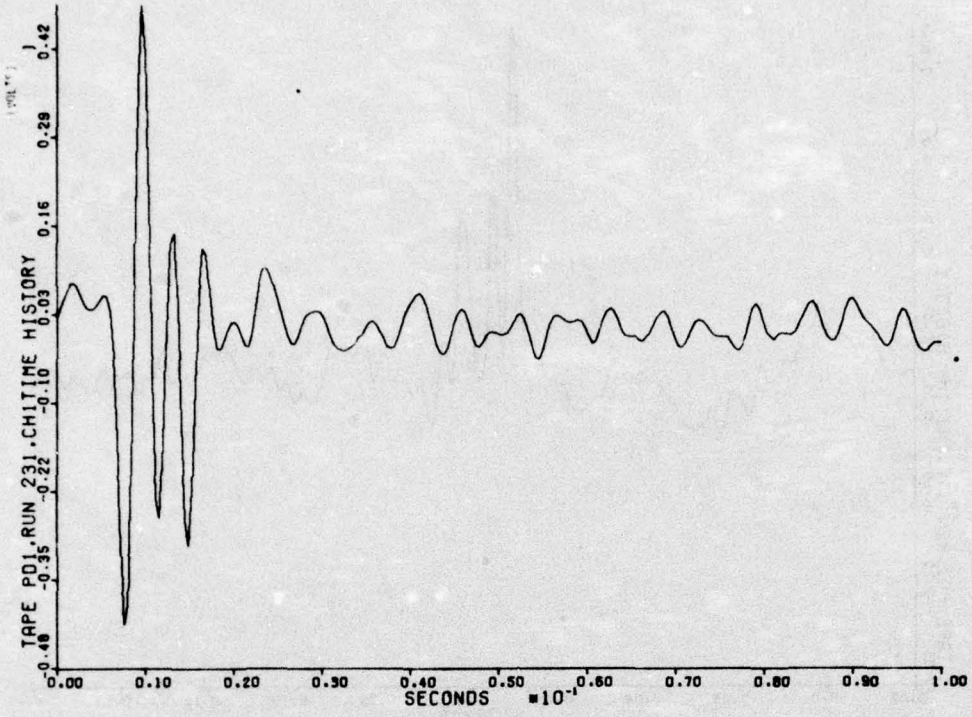


Figure B-9. Time history of flat MILES response - partially frozen loam

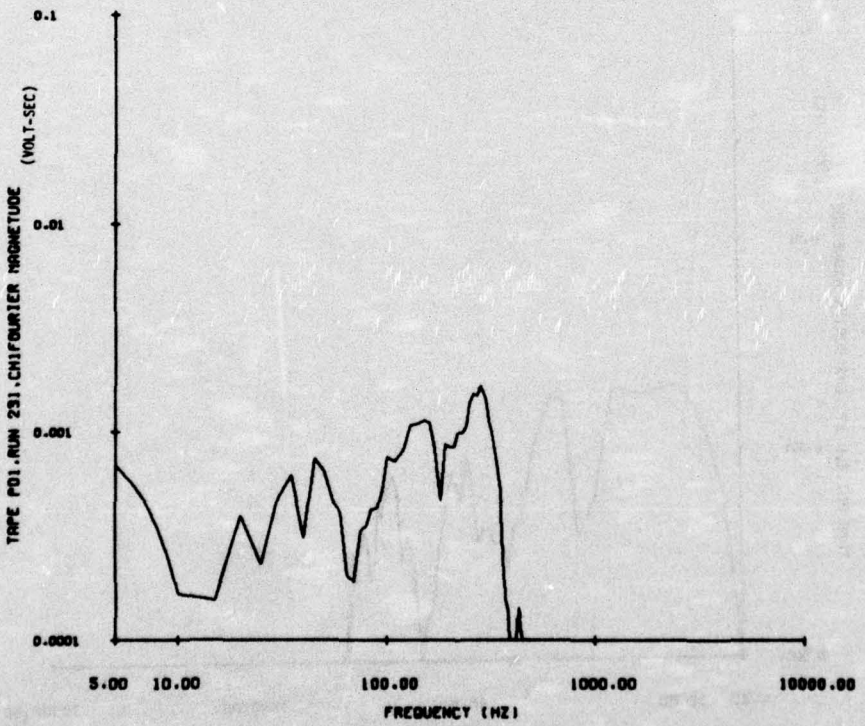


Figure B-10. Frequency spectrum of flat MILES response - partially frozen loam

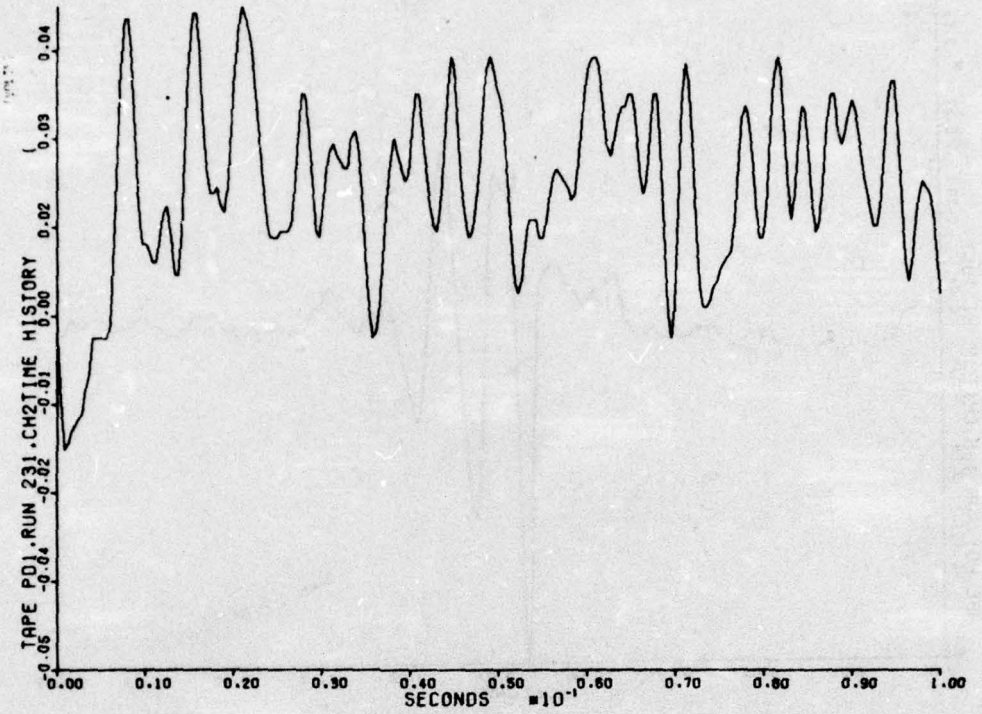


**Figure B-11. Time history of round MILES response - partially frozen loam**

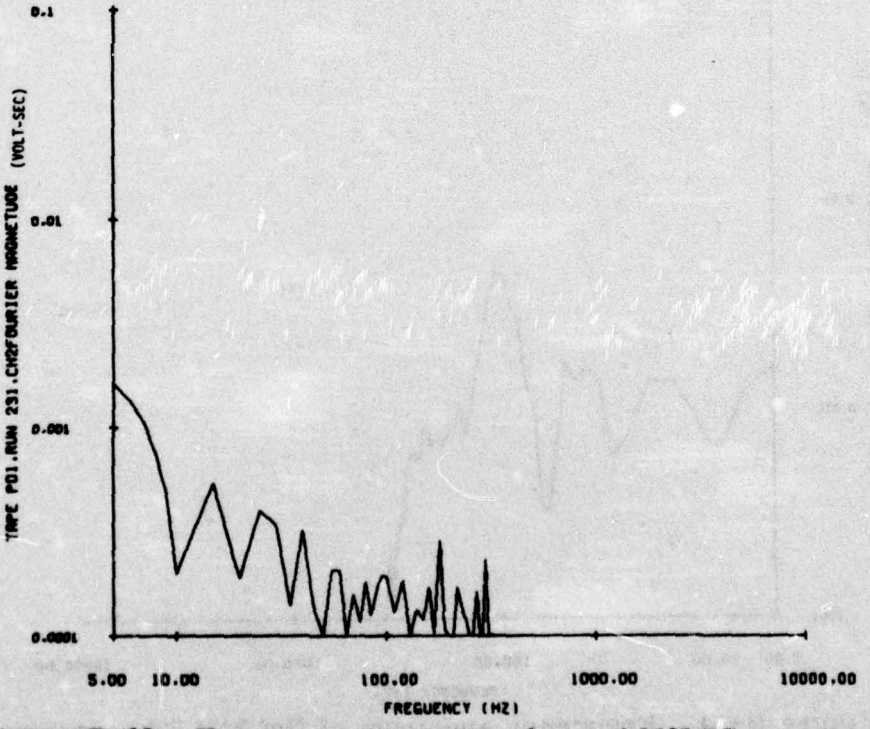


**Figure B-12. Frequency spectrum of round MILES response - partially frozen loam**

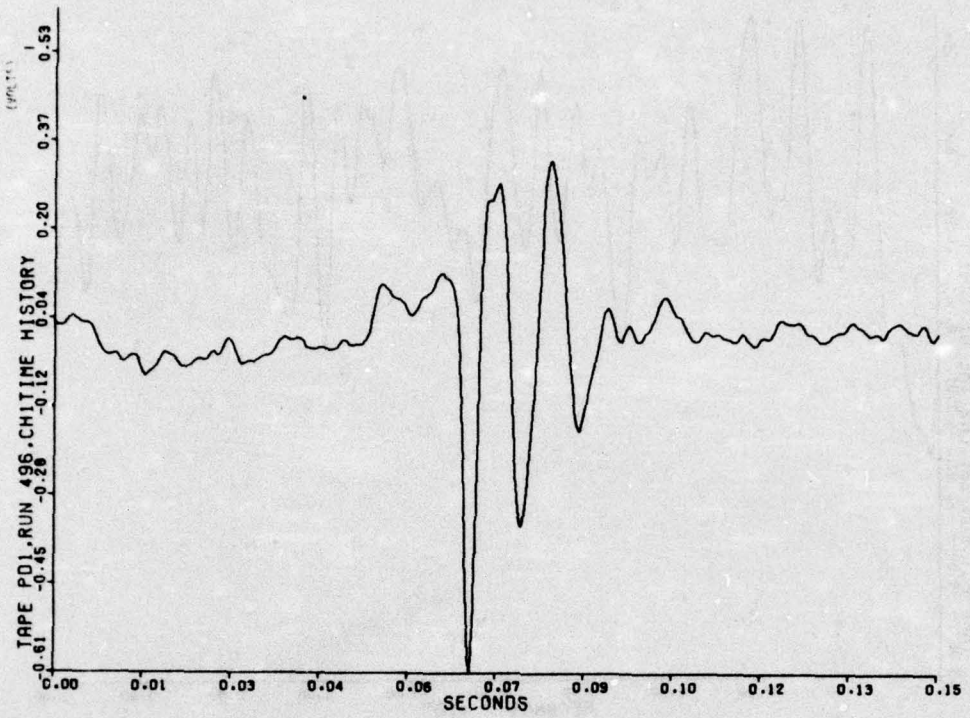


**Figure B-13. Time history of flat MILES response - frozen-layered loam**

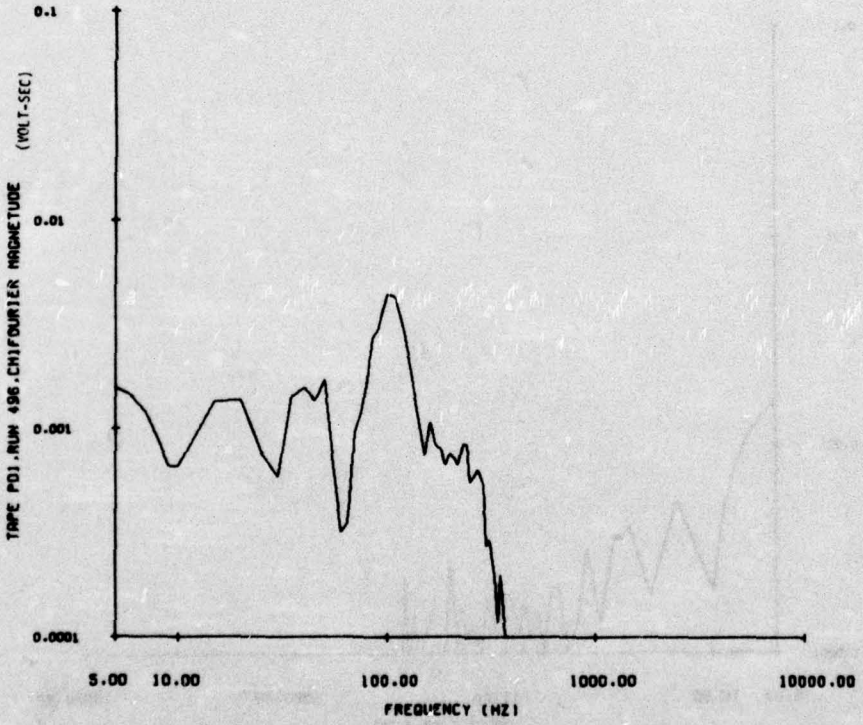


**Fiugre B-14. Frequency spectrum of flat MILES response - frozen-layered loam**

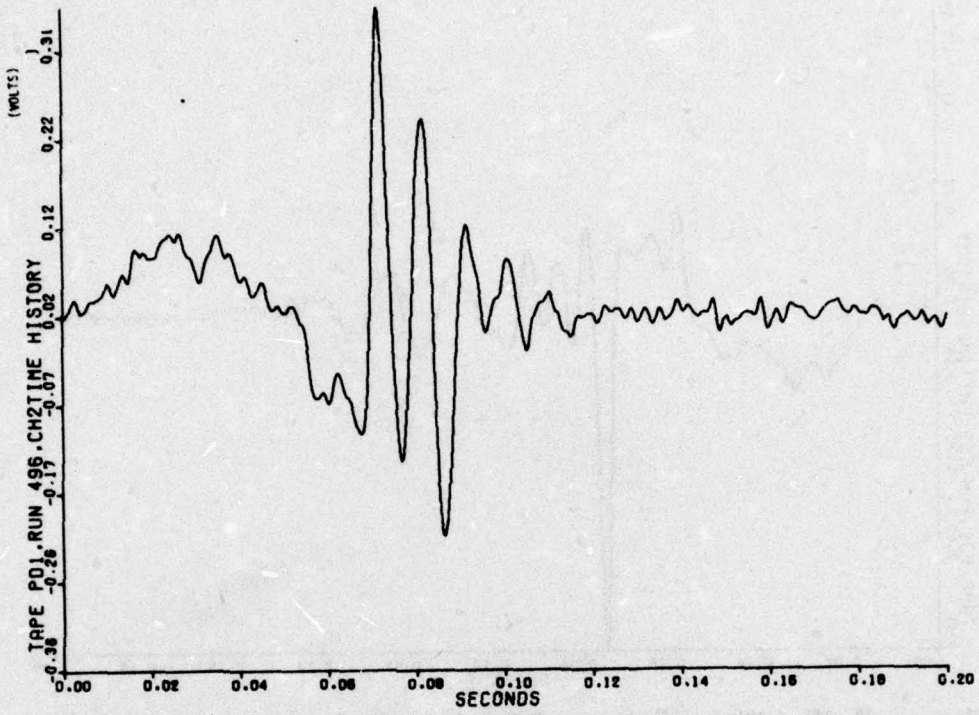


Figure B-15. Time history of round MILES response - frozen-layered loam

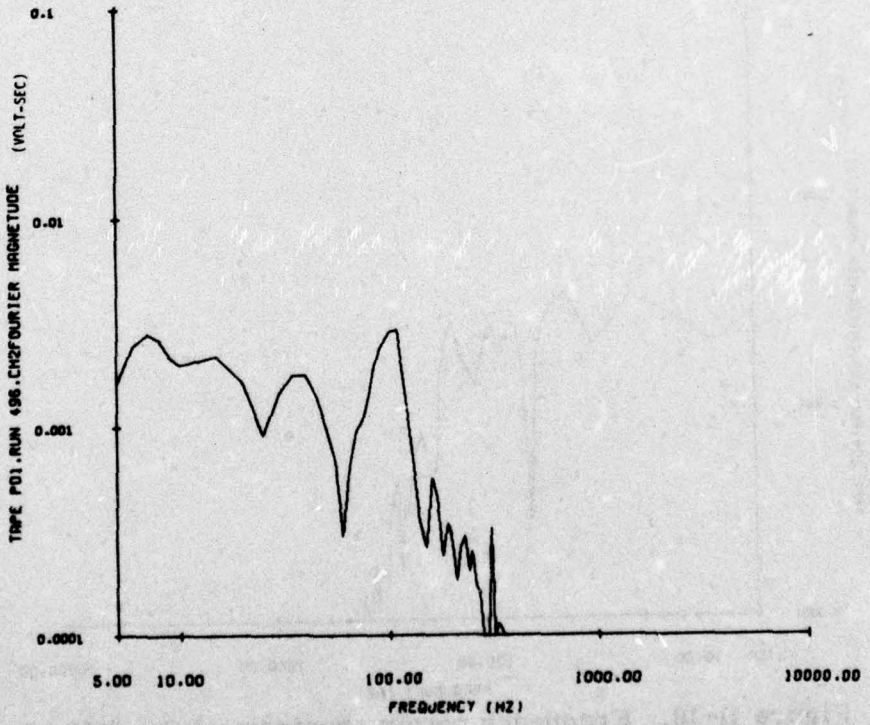


Figure B-16. Frequency spectrum of round MILES response - frozen-layered loam

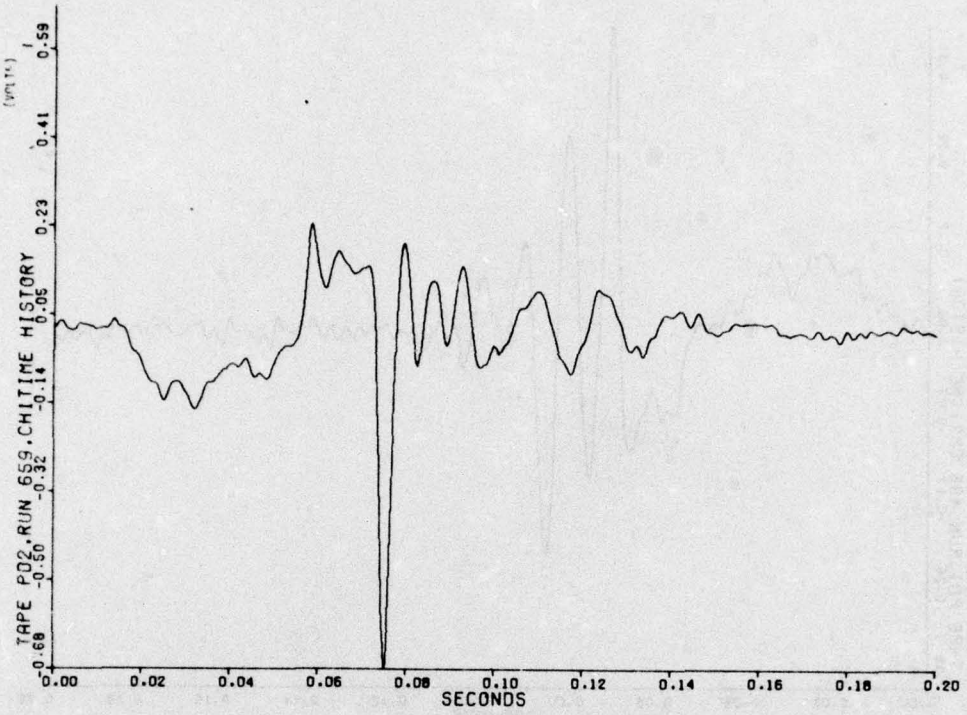


Figure B-17. Time history of flat MILES response - thawed clay

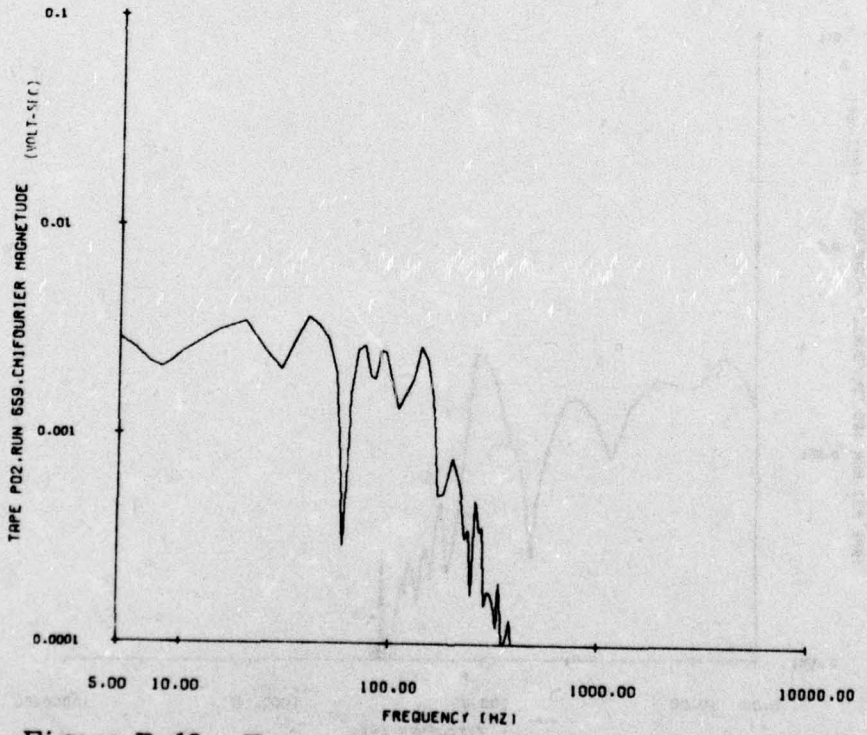


Figure B-18. Frequency power spectrum of flat MILES response - thawed clay

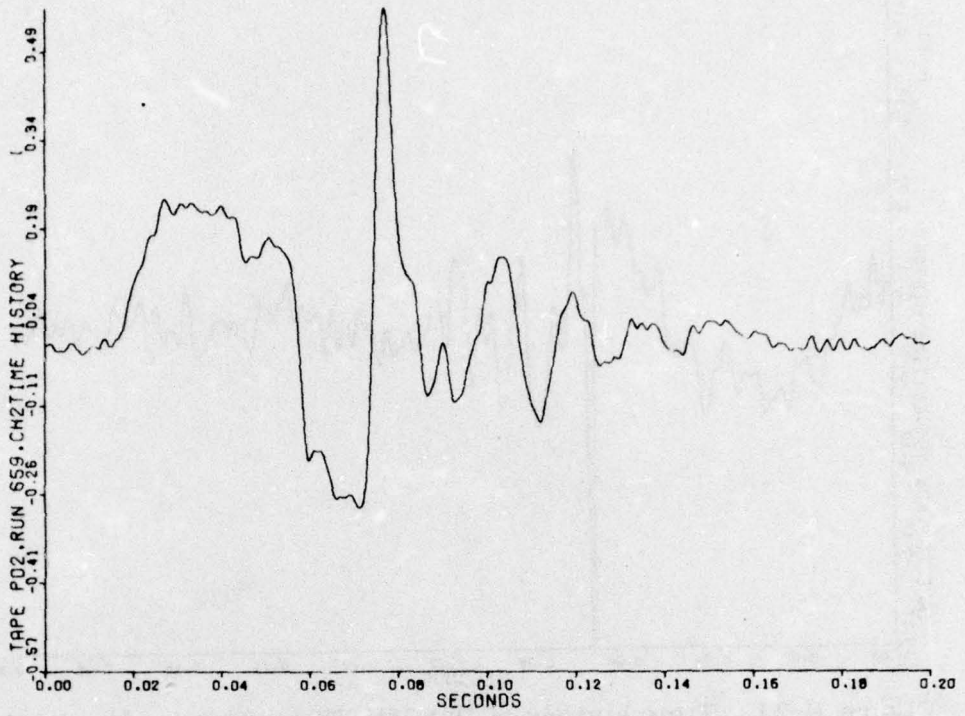


Figure B-19. Time history of round MILES response - thawed clay

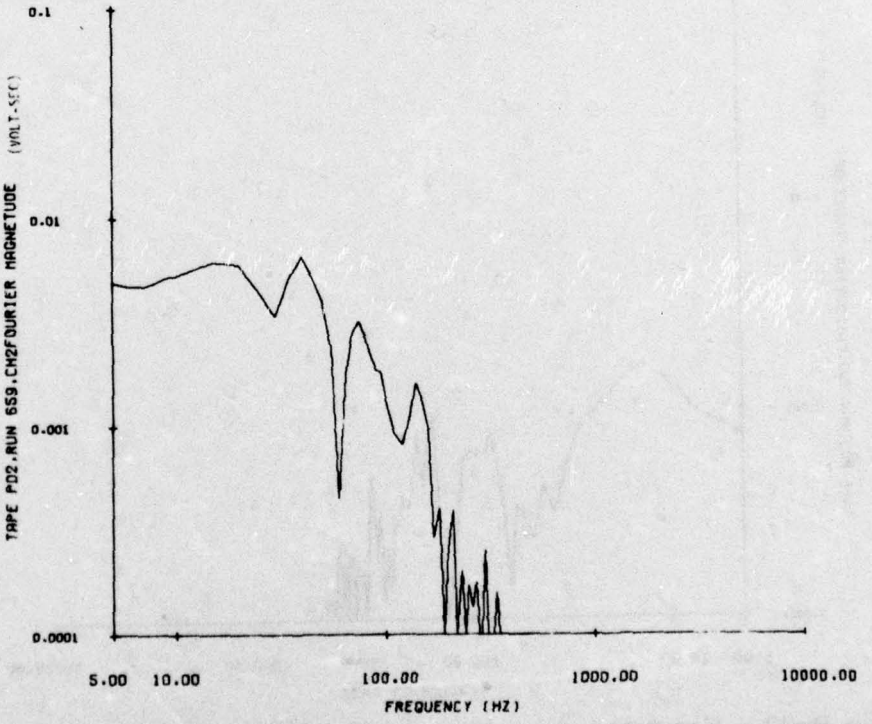


Figure B-20. Frequency power spectrum of round MILES response - thawed clay

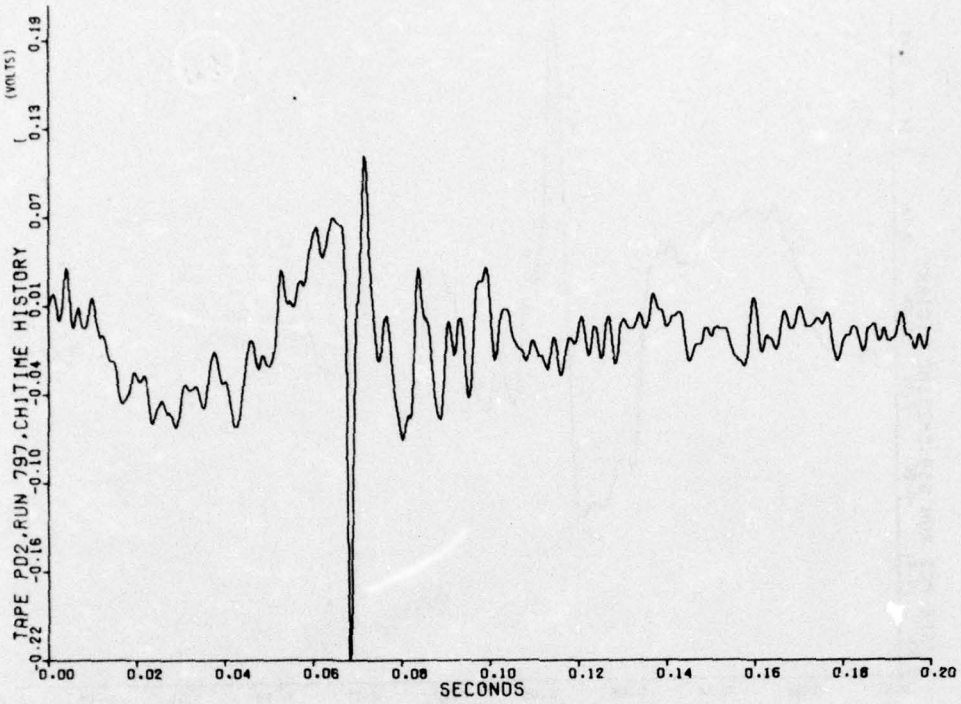


Figure B-21. Time history of flat MILES response - frozen clay

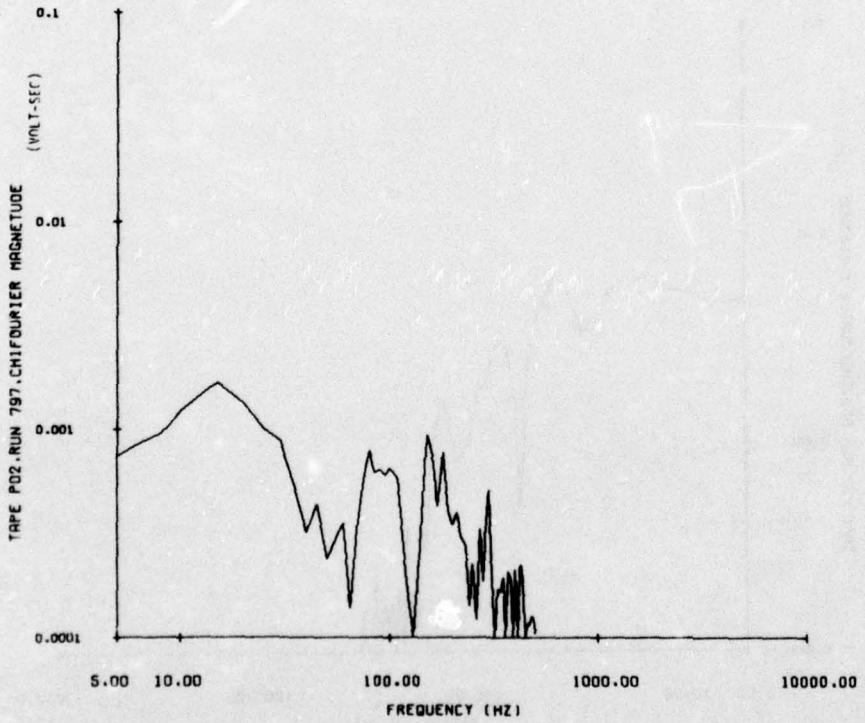


Figure B-22. Frequency spectrum of flat MILES response - frozen clay

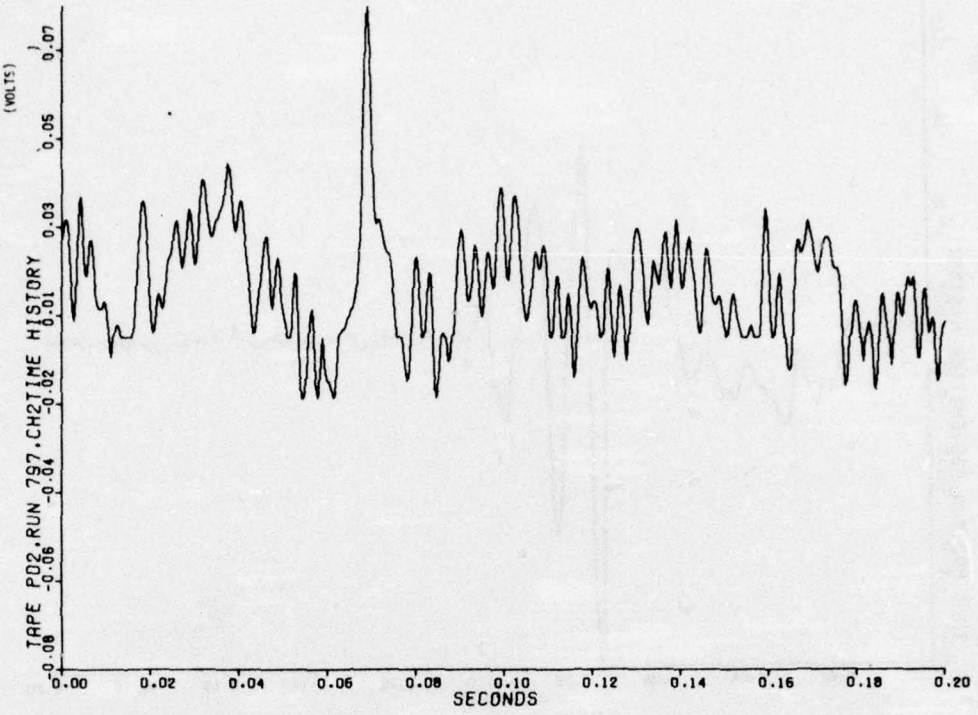


Figure B-23. Time history of round MILES response - frozen clay

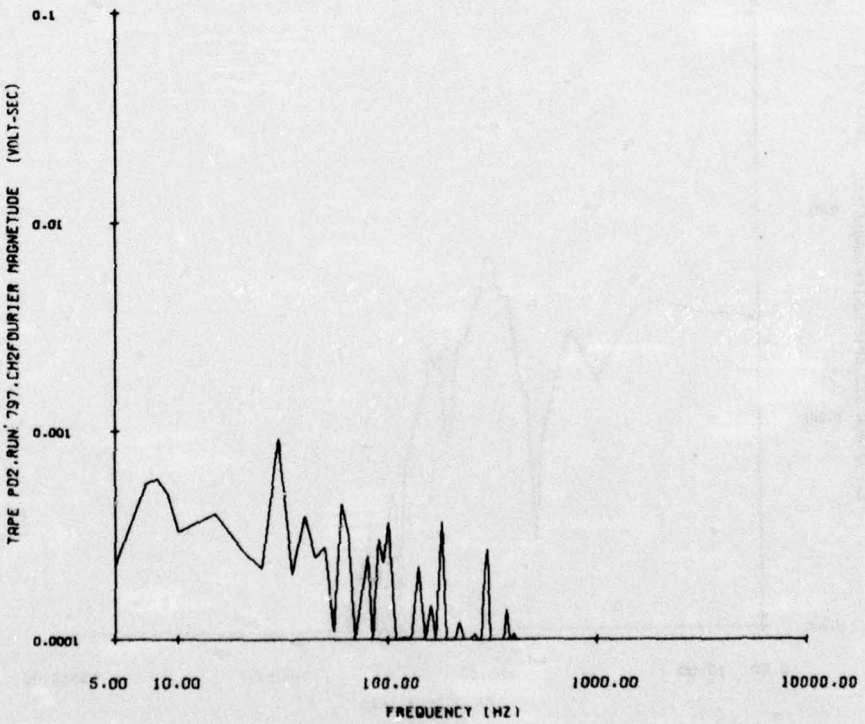


Figure B-24. Frequency spectrum of round MILES response - frozen clay

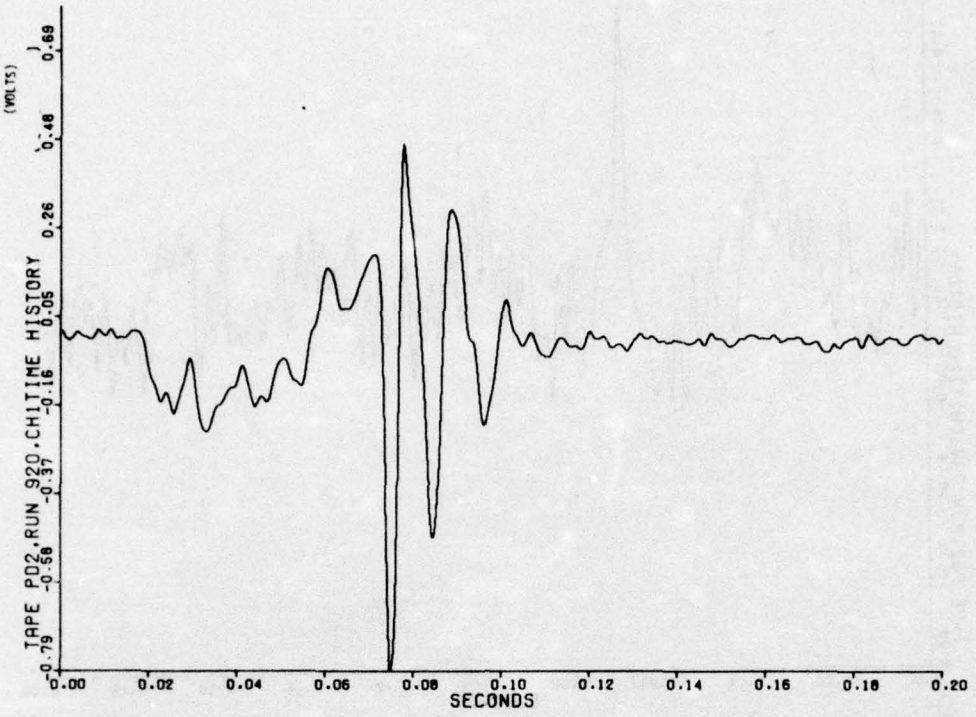


Figure B-25. Time history of flat MILES response - partially frozen clay

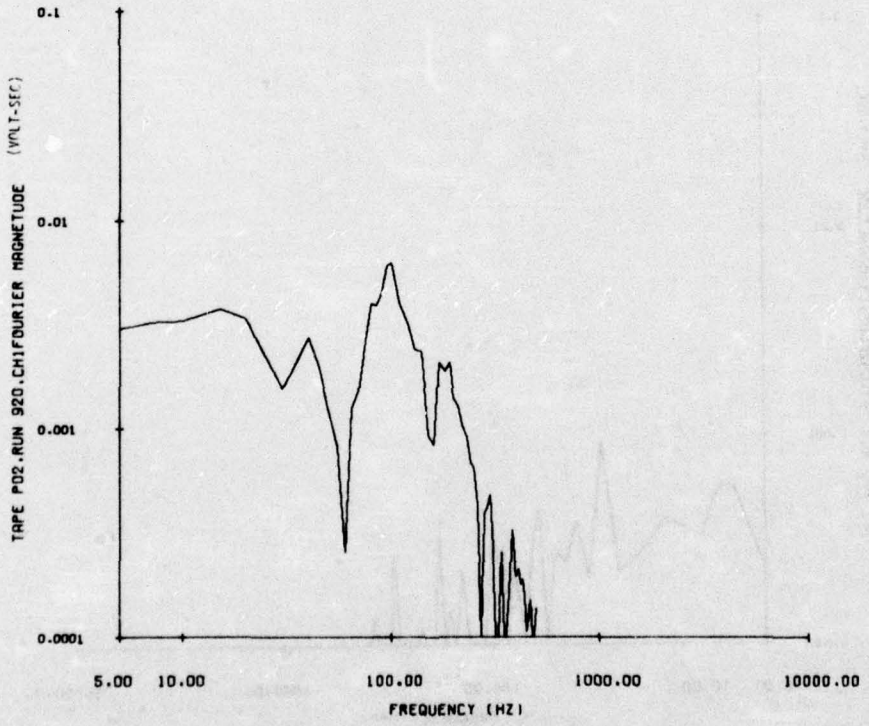


Figure B-26. Frequency spectrum of flat MILES response - partially frozen clay

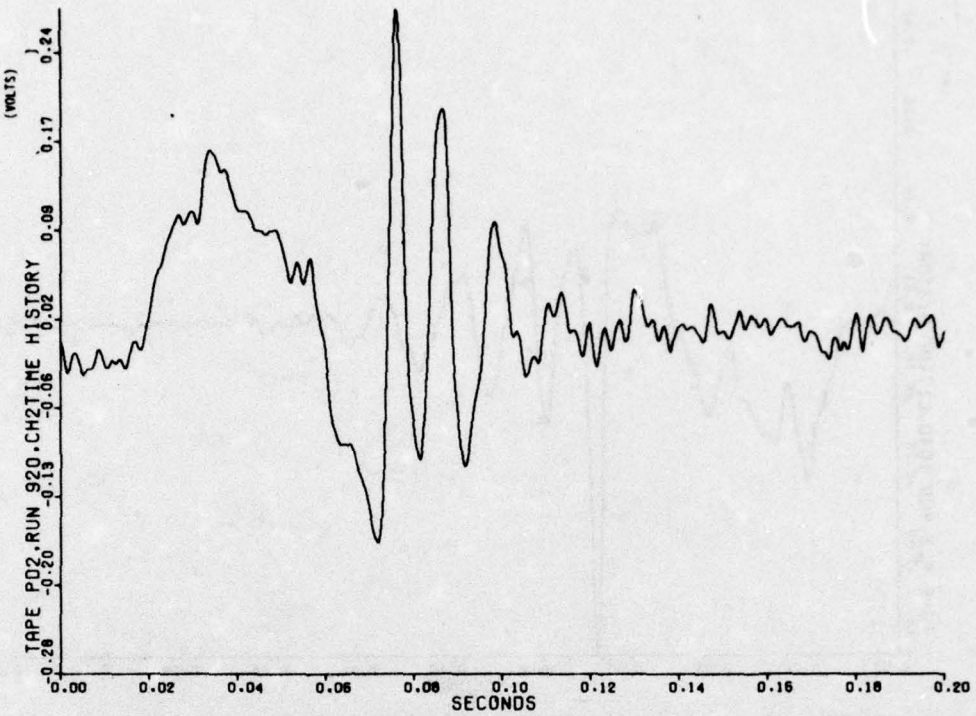


Figure B-27. Time history of round MILES response - partially frozen clay

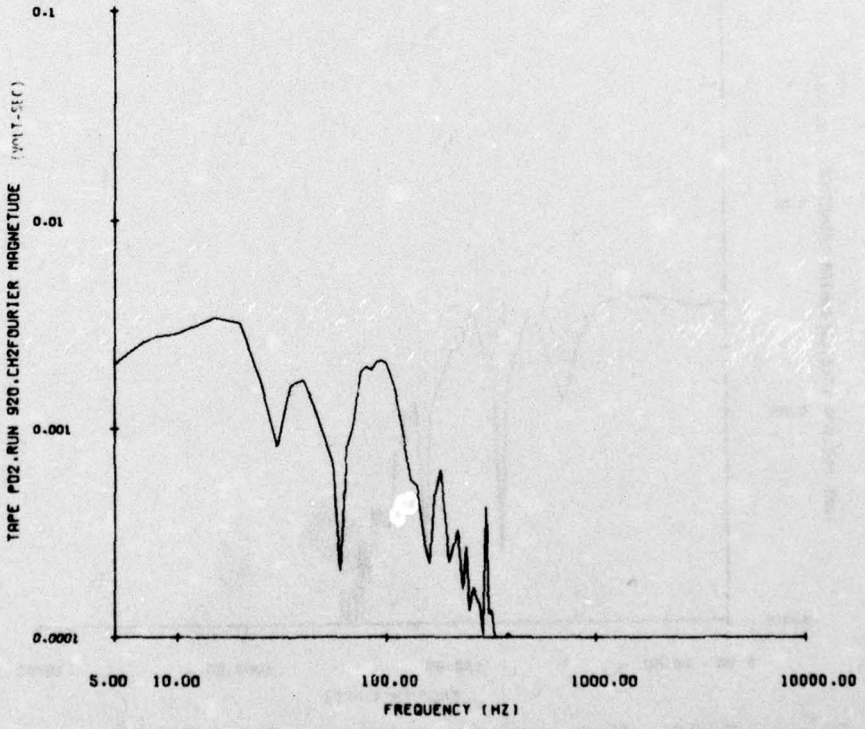


Figure B-28. Frequency spectrum of round MILES response - partially-frozen clay

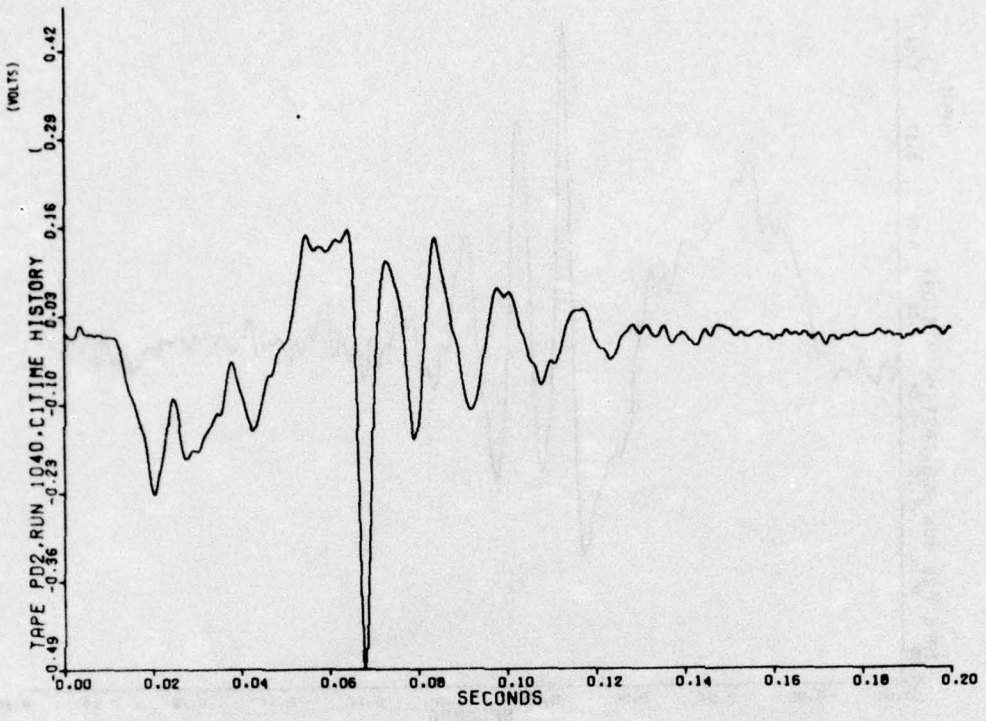


Figure B-29. Time history of flat MILES response - frozen-layered clay

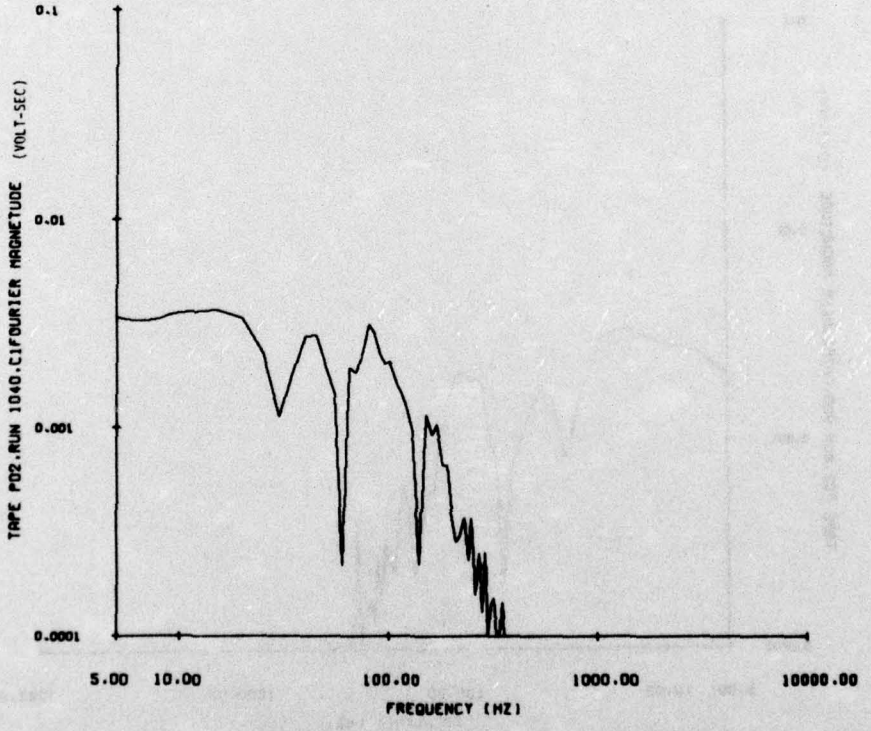


Figure B-30. Frequency spectrum of flat MILES response - frozen-layered clay

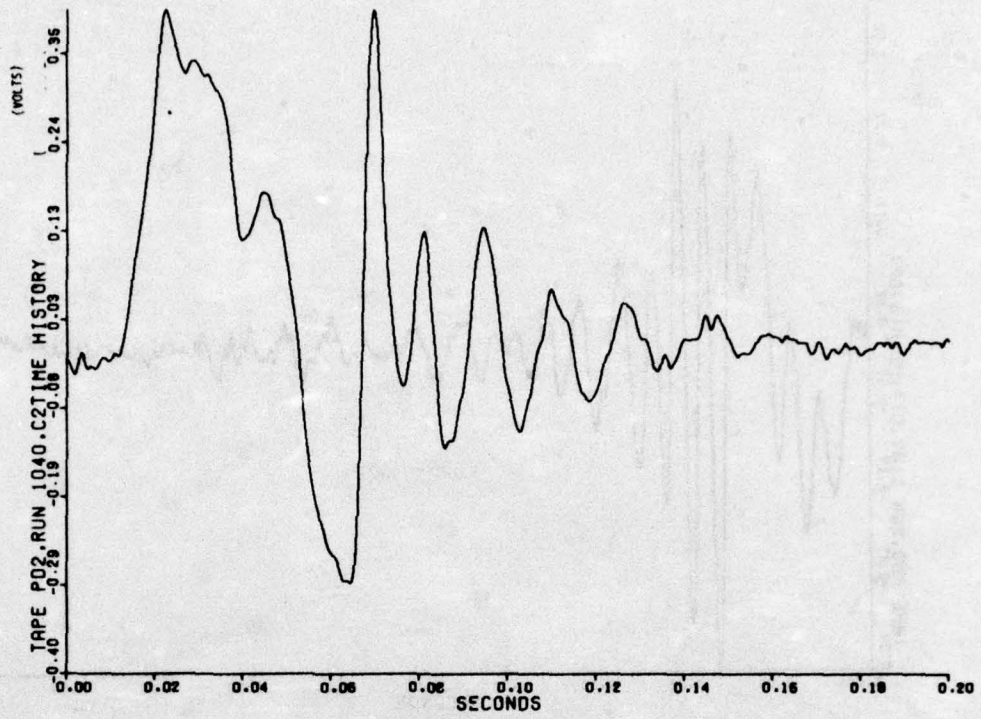


Figure B-31. Time history of round MILES response - frozen-layered clay

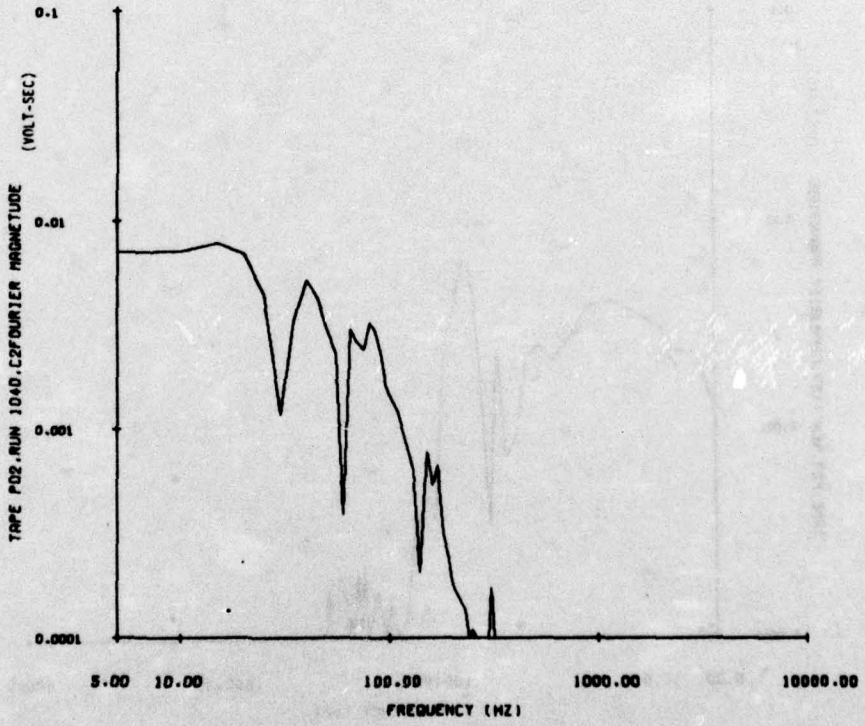


Figure B-32. Frequency spectrum of round MILES response - frozen-layered clay

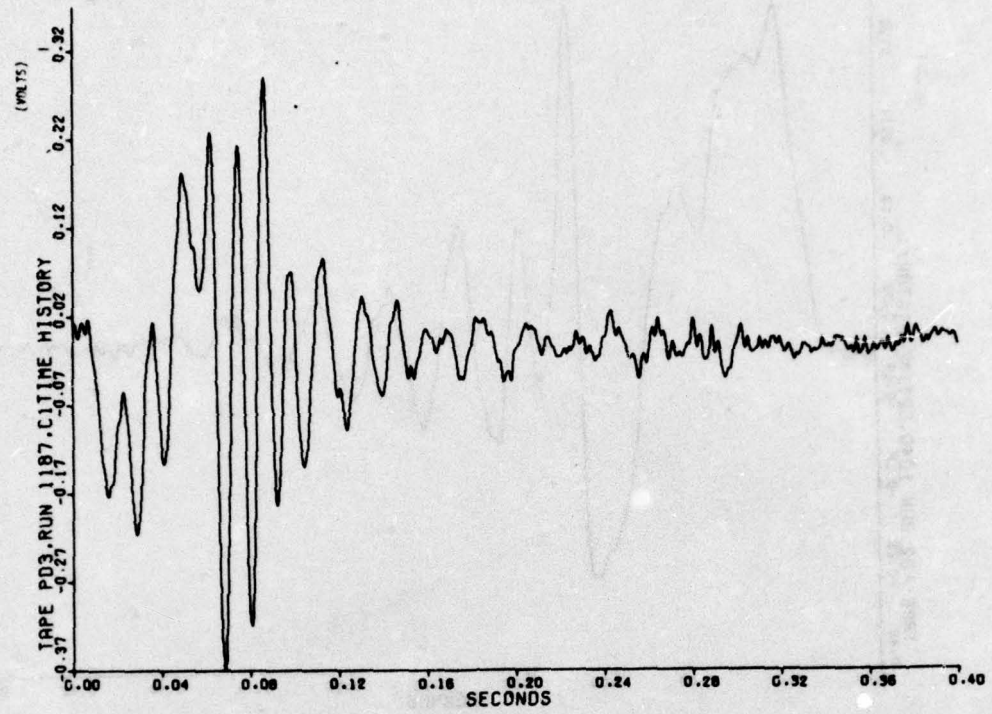


Figure B-33. Time history of flat MILES response - thawed sand

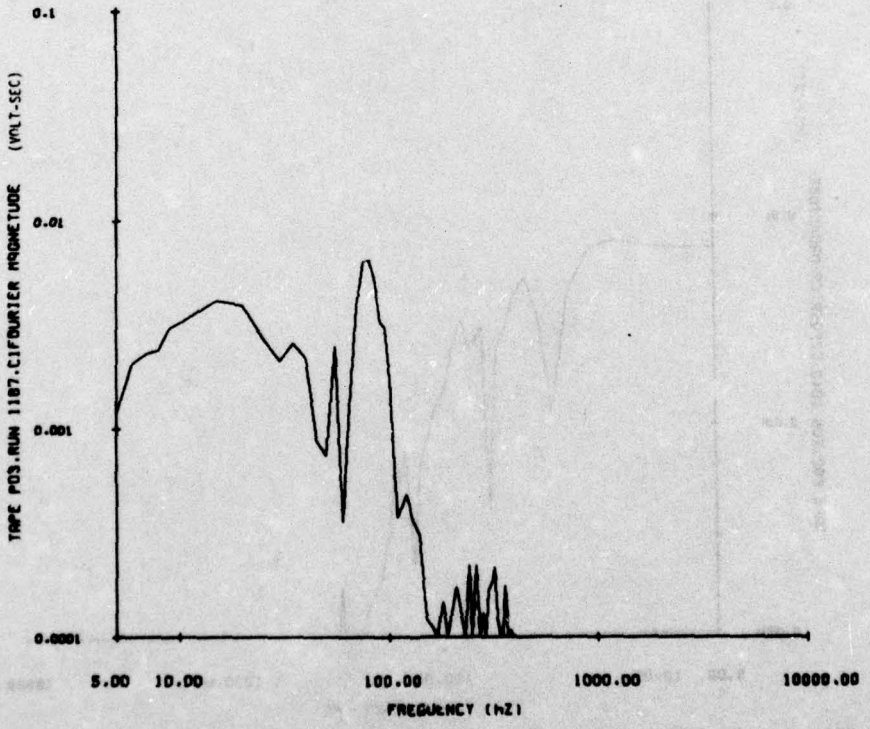


Figure B-34. Frequency spectrum of flat MILES response - thawed sand

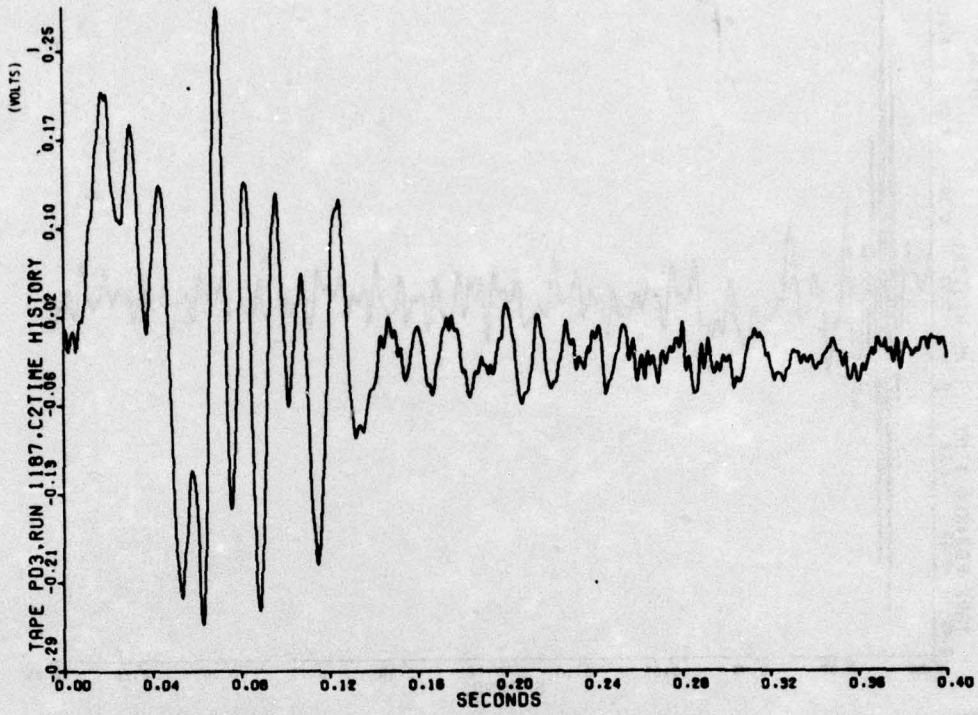


Figure B-35. Time history of round MILES response - thawed sand

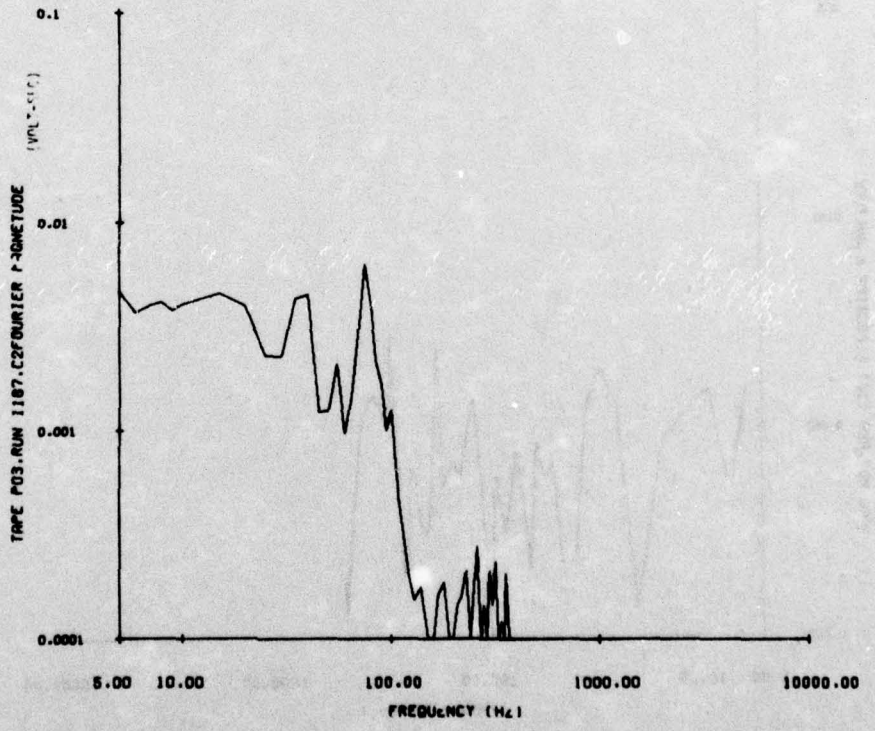


Figure B-36. Power spectrum of round MILES response - thawed sand

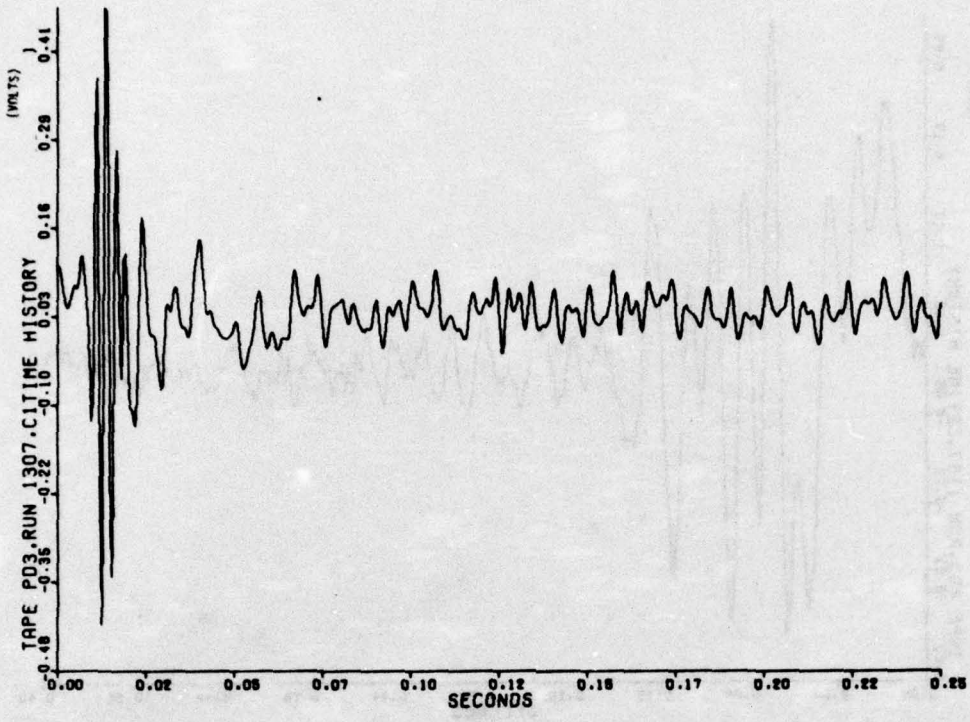


Figure B-37. Time history of flat MILES response - frozen sand

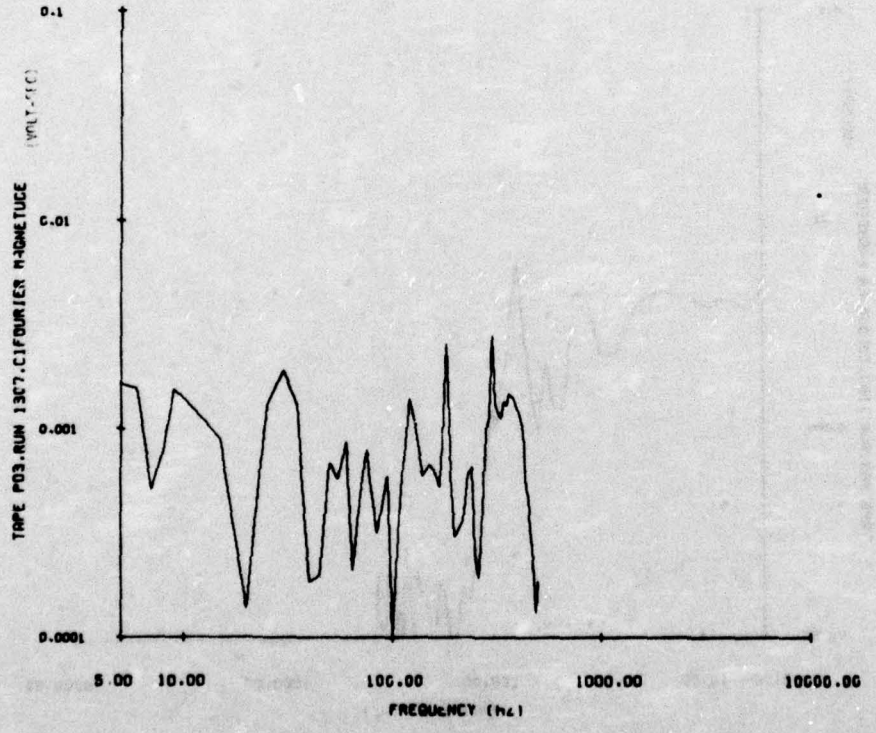


Figure B-38. Frequency spectrum of flat MILES response - frozen sand

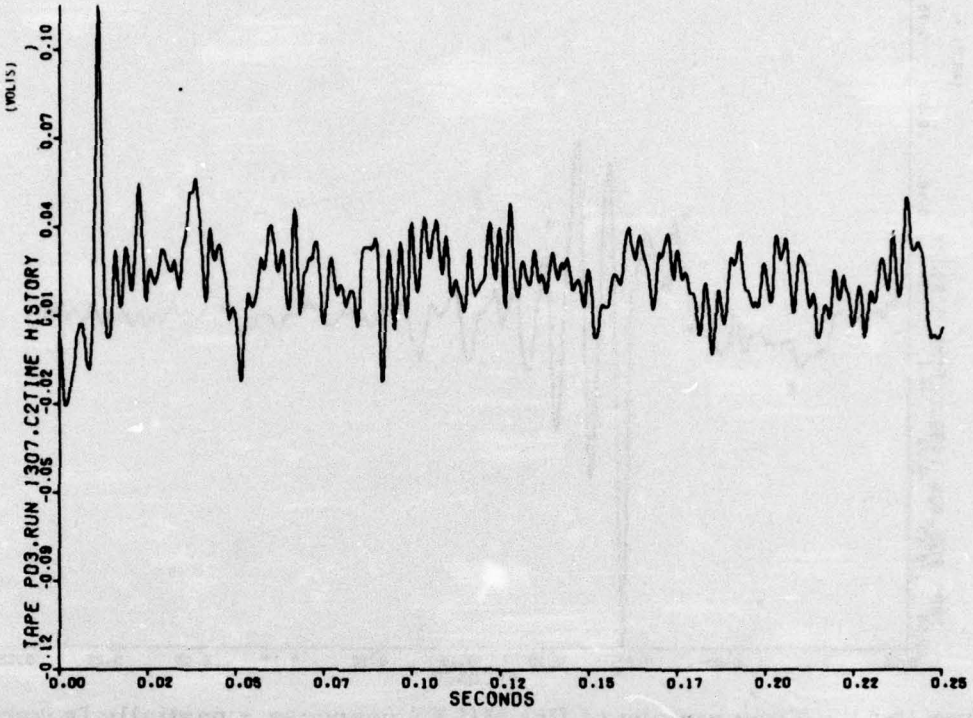


Figure B-39. Time history of round MILES response - frozen sand

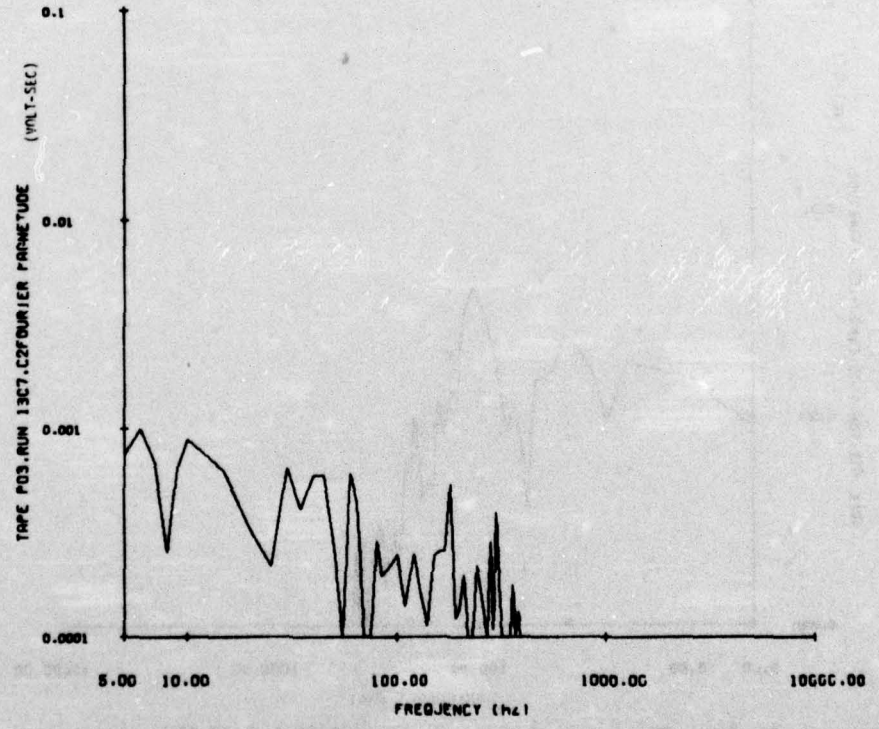


Figure B-40. Frequency spectrum of round MILES response - frozen sand

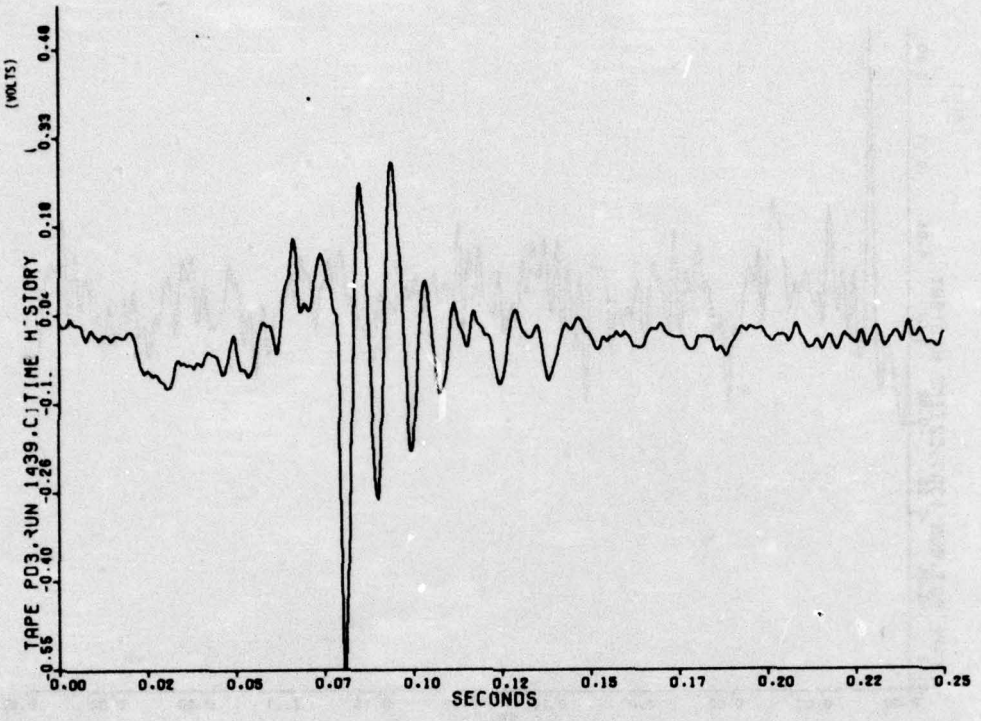


Figure B-41. Time history of flat MILES response - partially frozen sand

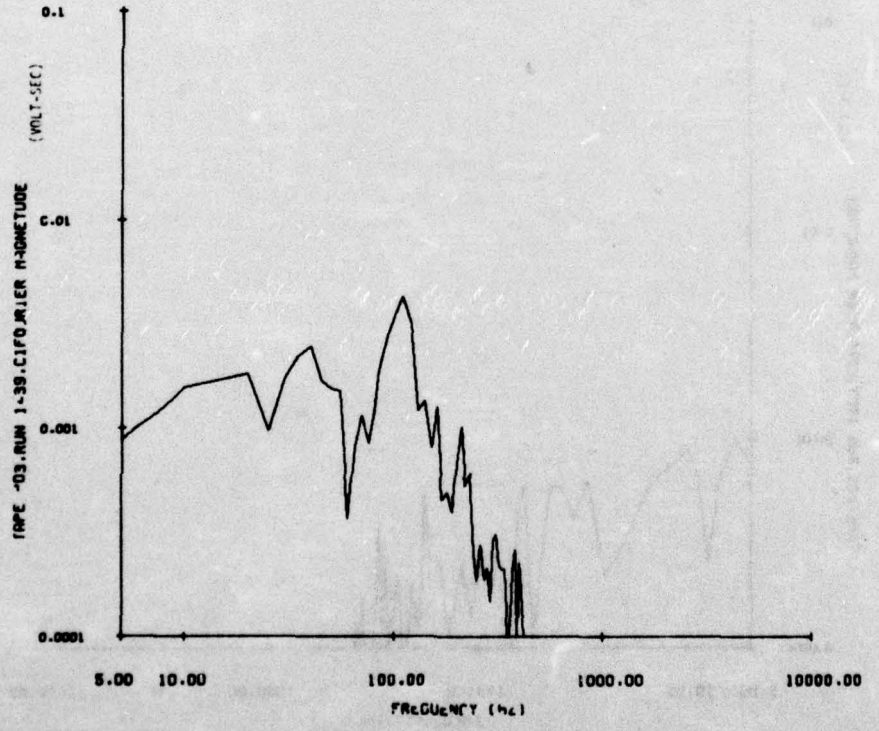


Figure B-42. Frequency spectrum of flat MILES response - partially-frozen sand

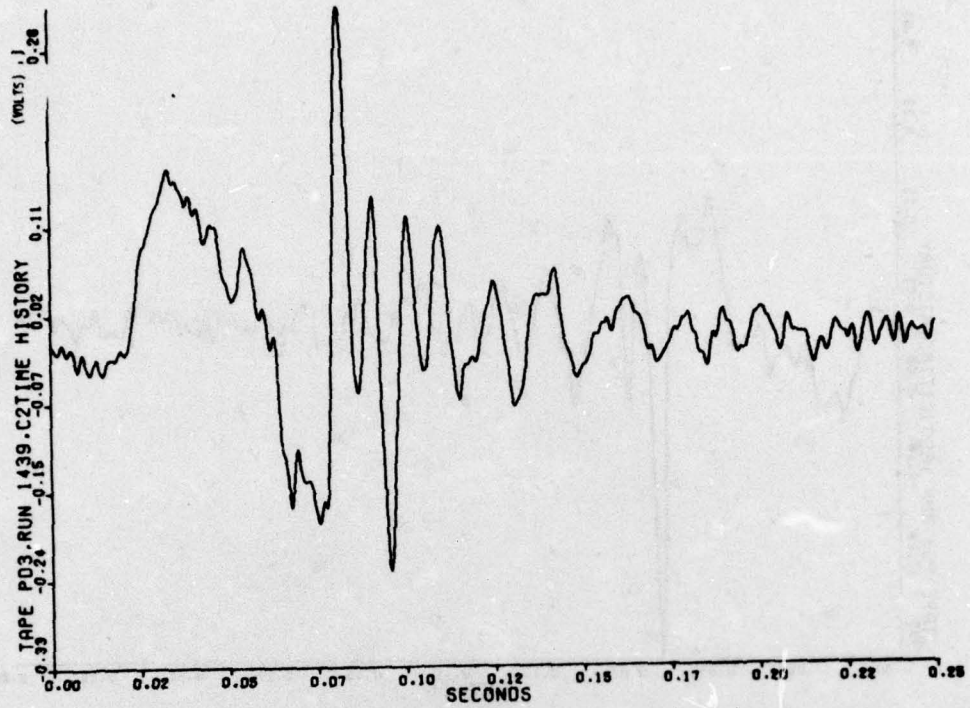


Figure B-43. Time history of round MILES response - partially-frozen sand

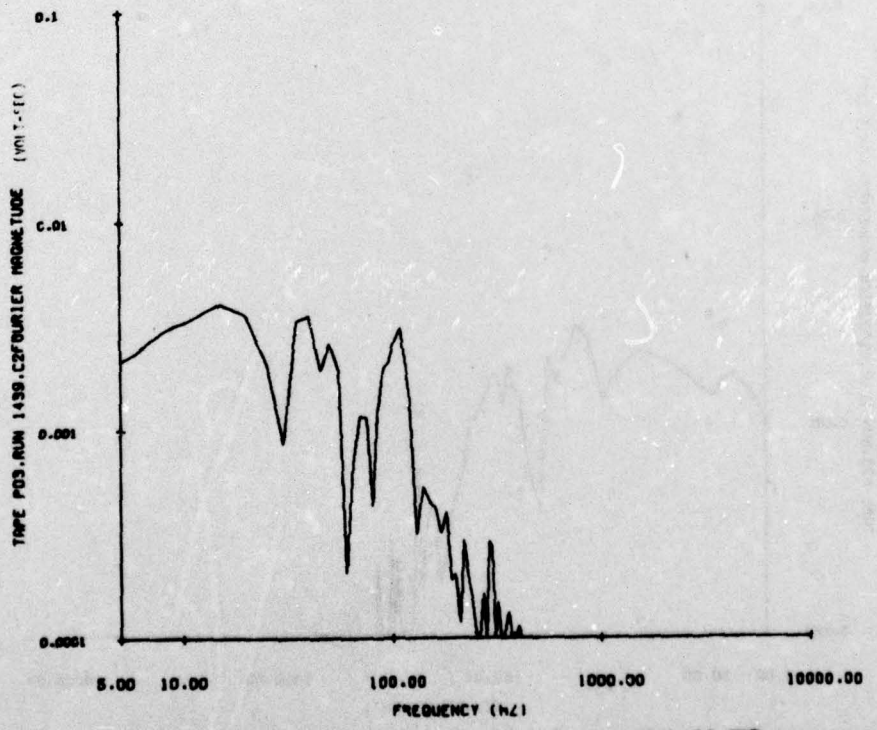


Figure B-44. Frequency spectrum of round MILES response - partially frozen sand

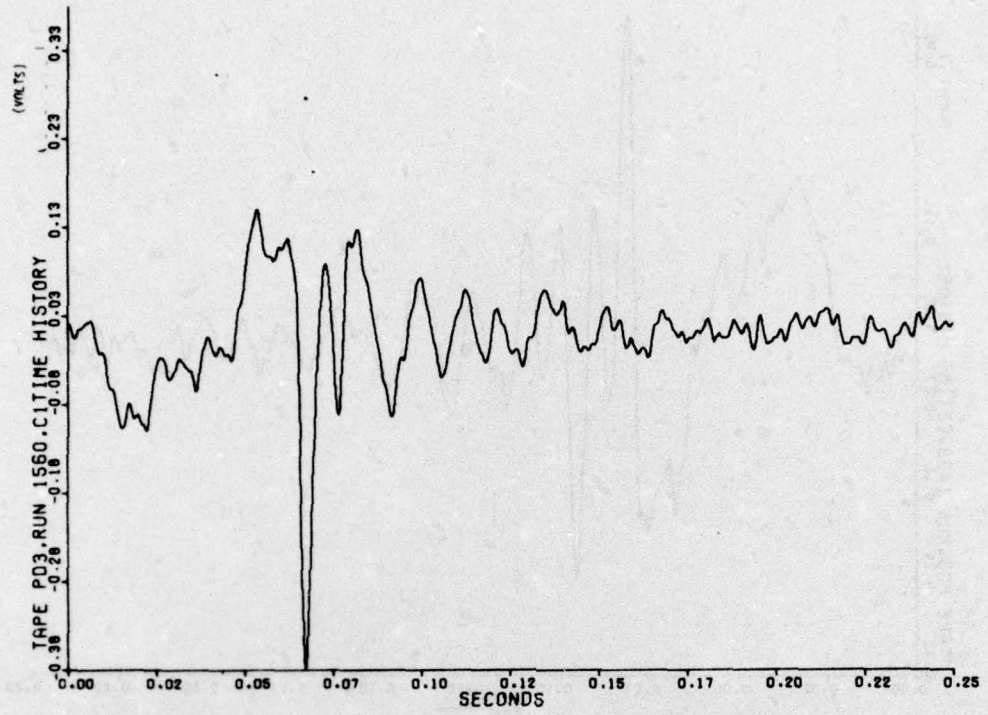


Figure B-45. Time history of flat MILES response - frozen-layered sand

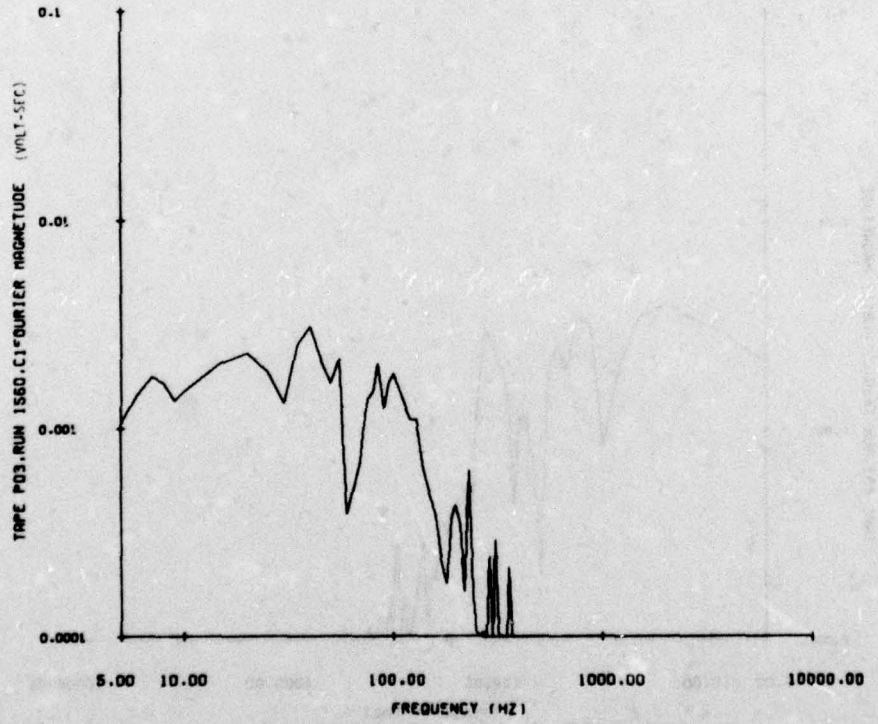


Figure B-46. Frequency spectrum of flat MILES response - frozen-layered sand

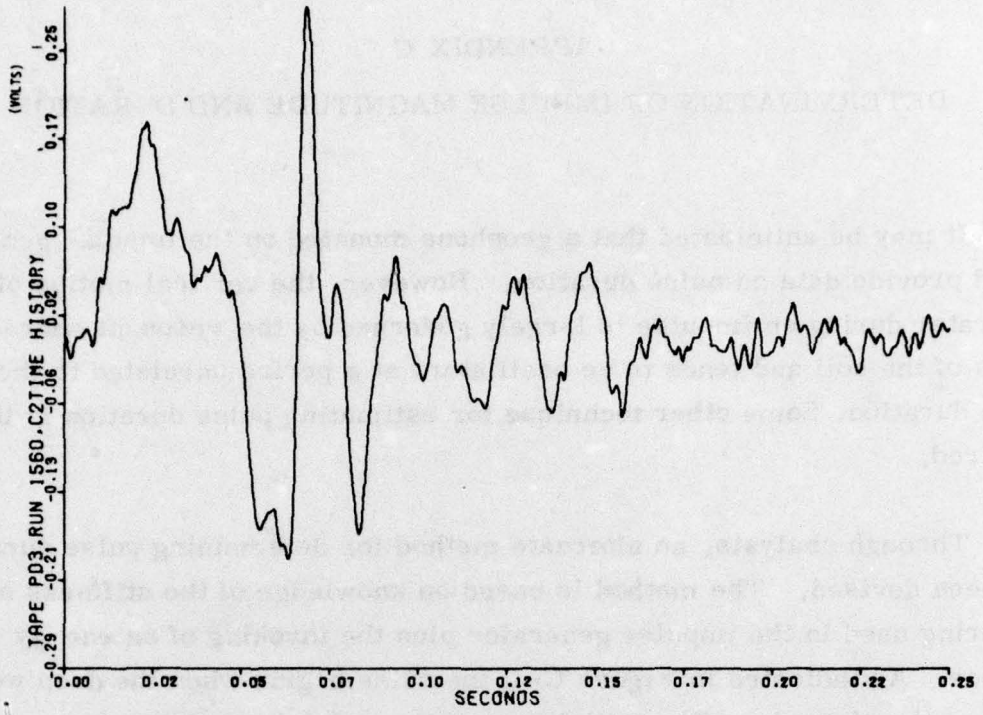


Figure B-47. Time history of round MILES response - frozen-layered sand

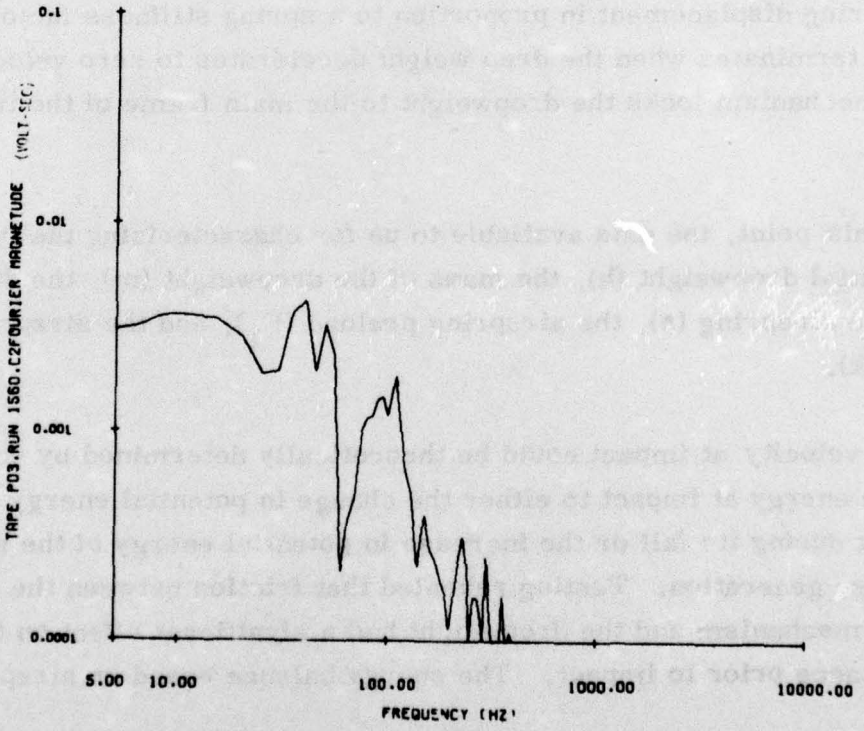


Figure B-48. Frequency spectrum of round MILES response - frozen-layered sand

## APPENDIX C

## DETERMINATION OF IMPULSE MAGNITUDE AND DURATION

It may be anticipated that a geophone mounted on the impulse generator would provide data on pulse duration. However, the vertical motion of the generator during an impulse is largely governed by the resonant characteristics of the soil and tends to be oscillatory at a period unrelated to the pulse duration. Some other technique for estimating pulse duration is thus required.

Through analysis, an alternate method for determining pulse duration has been devised. The method is based on knowledge of the stiffness of the airspring used in the impulse generator plus the invoking of an energy balance. As indicated in Figure C-1, the pulse begins when the drop weight impacts the airspring. The initial rise of the pulse is equal to the preload on the airspring $F_1$. During the pulse, the magnitude of the force increases with airspring displacement in proportion to a spring stiffness factor k. The pulse terminates when the drop weight decelerates to zero velocity when a rachet mechanism locks the dropweight to the main frame of the impulse generator.

At this point, the data available to us for characterizing the impulse are the initial dropweight (h), the mass of the dropweight (m), the displacement of the airspring ($\delta$), the airspring preload ($F_1$), and the airspring stiffness (k).

The velocity at impact could be theoretically determined by equating the kinetic energy at impact to either the change in potential energy of the dropweight during its fall or the increase in potential energy of the airspring during pulse generation. Testing revealed that friction between the center rod of the mechanism and the dropweight had a significant effect on the energy balance prior to impact. The energy balance based on airspring

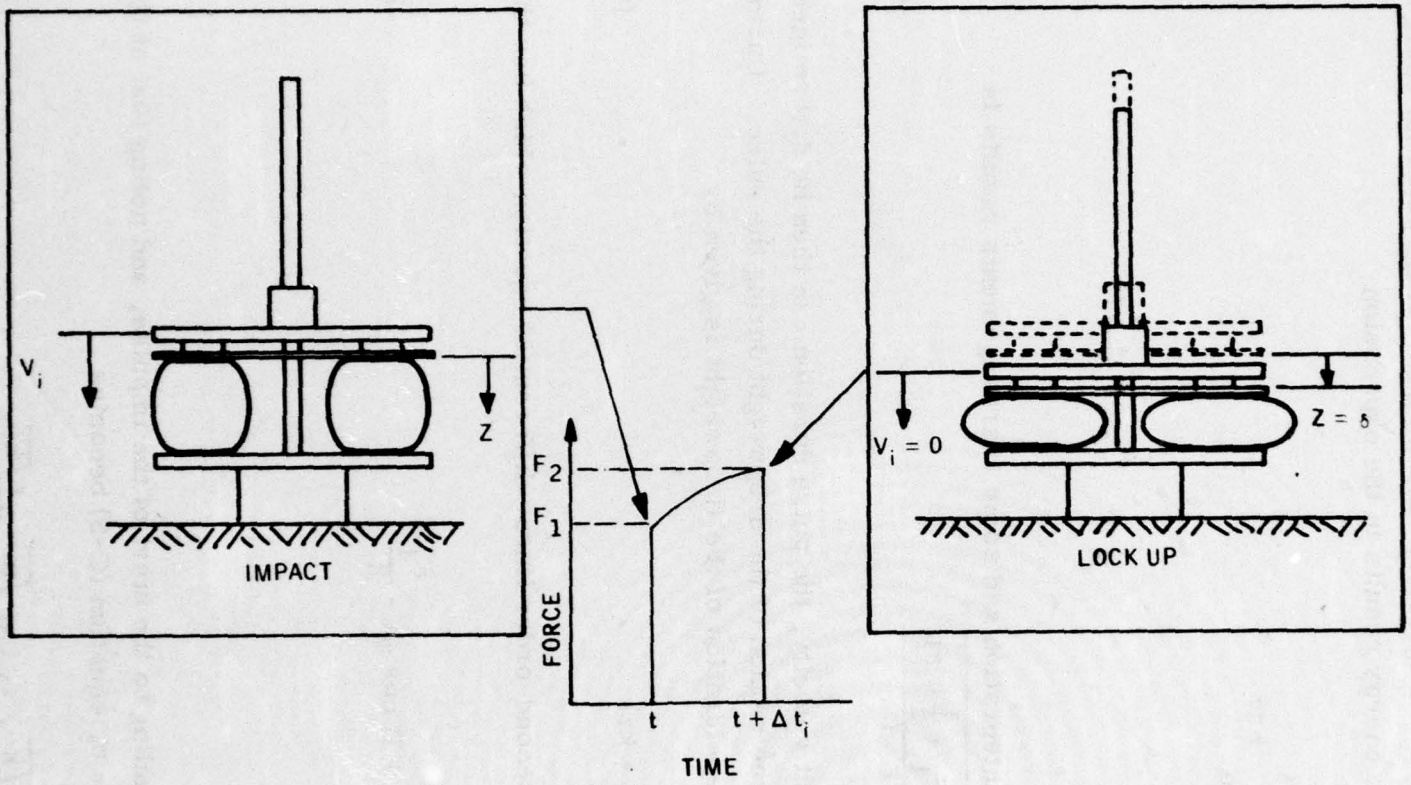


Figure C-1. Conditions at beginning and end of impulse

deflection was therefore selected. Equating airspring potential energy and dropweight kinetic energy results in the expression

$$\frac{1}{2} m V_i^2 = \int_o^\delta F dz \qquad \text{(C-1)}$$

where

$$F = F_1 + kz \qquad \text{(C-2)}$$

Carrying out the integration and some rearrangements results in

$$V_i = \sqrt{\frac{2 (F_1 + \frac{1}{2} k \delta)\delta}{m}} \qquad \text{(C-3)}$$

Knowing the impact velocity, the pulse duration can then be determined from an analysis the motion of the dropweight during the pulse. During that period, the deceleration of the dropweight is given by

$$\ddot{z} = - \frac{1}{m} (F_1 + kz) \qquad \text{(C-4)}$$

This is a simple second-order linear differential equation which has the general solution

$$\dot{z} = A \sin \omega t + B \cos \omega t - \frac{F_1}{k} \qquad \text{(C-5)}$$

where

$$\omega = \sqrt{k/m}$$

With t=0 corresponding to the start of the impulse, and noting that at that time $z = V_i$ and $z = 0$, equation (C-5) becomes

$$z = \frac{F_1}{k} (\cos \sqrt{\frac{k}{m}}\, t - 1) + V_i \sqrt{\frac{m}{k}}\, \sin \sqrt{\frac{k}{m}}\, t \qquad \text{(C-6)}$$

At the end of the impulse, $\dot{z} = 0$. Differentiating (C-6) and setting the result equal to zero thus leads to the following solution for the pulse duration:

$$\Delta t = \sqrt{\frac{m}{k}} \tan^{-1} \frac{V_i \sqrt{km}}{F_1} \qquad \text{(C-7)}$$

Equation (C-7), combined with a $V_i$ value determined from equation (C-3) provides a simple means for estimating pulse duration.